Guidelines for the Evaluation of Prosthetic Valve Function With Cardiovascular Imaging: A Report From the American Society of Echocardiography Developed in Collaboration With the Society for Cardiovascular Magnetic Resonance and the Society of Cardiovascular Computed Tomography

William A. Zoghbi, MD (Chair), Pei-Ni Jone, MD (Co-Chair), Mohammed A. Chamsi-Pasha, MD, Tiffany Chen, MD, Keith A. Collins, MS, RDCS, Milind Y. Desai, MD, MBA, Paul Grayburn, MD, Daniel W. Groves, MD, Rebecca T. Hahn, MD, Stephen H. Little, MD, Eric Kruse, RDCS, Danita Sanborn, MD, Sangeeta B. Shah, MD, Lissa Sugeng, MD, Madhav Swaminathan, MD, MBBS, Jeremy Thaden, MD, Paaladinesh Thavendiranathan, MD, SM, Wendy Tsang, MD, SM, Jonathan R. Weir-McCall, MD, MBChB, PhD, and Edward Gill, MD, *Houston and Dallas, Texas; Chicago, Illinois; Philadelphia, Pennsylvania; Cleveland, Ohio; Aurora, Colorado; New York and Manhasset, New York; Boston, Massachusetts; Richmond, Virginia; Durham, North Carolina; Rochester, Minnesota; Toronto, Ontario, Canada; and Cambridge, United Kingdom*

In patients with significant cardiac valvular disease, intervention with either valve repair or valve replacement may be inevitable. Although valve repair is frequently performed, especially for mitral and tricuspid regurgitation, valve replacement remains common, particularly in adults. Diagnostic methods are often needed to assess the function of the prosthesis. Echocardiography is the first-line method for noninvasive evaluation of prosthetic valve function. The transthoracic approach is complemented with two-dimensional and three-dimensional transesophageal echocardiography for further refinement of valve morphology and function when needed. More recently, advances in computed tomography and cardiac magnetic resonance have enhanced their roles in evaluating valvular heart disease. This document offers a review of the echocardiographic techniques used and provides recommendations and general guidelines for evaluation of prosthetic

From the Houston Methodist Hospital, DeBakey Heart & Vascular Center, Houston, Texas (W.A.Z., M.C.-P., S.H.L.); Ann & Robert H. Lurie Children's Hospital of Chicago, Northwestern University Feinberg School of Medicine, Chicago, Illinois (P.-N.J.); Hospital of the University of Pennsylvania, Perelman Center for Advanced Medicine, Philadelphia, Pennsylvania (T.C.); Northwestern Medicine Healthcare, Chicago, Illinois (K.A.C.); Heart and Vascular Institute, Cleveland Clinic, Cleveland, Ohio (M.Y.D.); Baylor Scott & White Health, University of Texas Southwestern, Dallas, Texas (P.G.); UC Health Heart and Vascular Center, University of Colorado Anschutz Medical Campus, Aurora, Colorado (D.W.G.); Columbia Structural Heart & Valve Center, Columbia University Irving Medical Center, New York, New York (R.T.H.); Heart & Vascular Imaging Services, University of Chicago Medical Center, Chicago, Illinois (E.K.); Massachusetts General Hospital, Boston, Massachusetts (D.S.); VCU Pauley Heart Center, Virginia Commonwealth University, Richmond, Virginia (S.B.S.); Northwell Health Physician Partners Cardiology, North Shore University Hospital, Manhasset, New York (L.S.); Cardiothoracic Anesthesiology and Critical Care Medicine, Duke University, Durham, North Carolina (M.S.); Department of Cardiovascular Medicine, Mayo Clinic, Rochester, Minnesota (J.T.); Toronto General Hospital, University Health Network, Toronto, Ontario, Canada (P.T.); Toronto General Hospital Research Institute, University of Toronto, Toronto, Ontario, Canada (W.T.); Department of Radiology, University of Cambridge School of Clinical Medicine, Cambridge, United Kingdom (J.R.W.-M.); and Anschutz Medical Campus, University of Colorado School of Medicine, Aurora, Colorado (E.G.).

The following authors reported no actual or potential conflicts of interest in relation to this document: William A. Zoghbi, MD, Pei-Ni Jone, MD, Mohammed A. Chamsi-Pasha, MD, Tiffany Chen, MD, Keith A. Collins, MS, RDCS, Milind Y. Desai, MD, MBA, Daniel W. Groves, MD, Stephen H. Little, MD, Eric Kruse, RDCS, Danita Sanborn, MD, Sangeeta B. Shah, MD, Madhav Swaminathan, MD, MBBS, Paaladinesh Thavendiranathan, MD, SM, Jonathan R. Weir-McCall, MD, MBChB, PhD, and Edward Gill, MD, FASE.

The following authors reported relationships with one or more commercial interests: Rebecca T. Hahn, MD, has participated on speakers bureaus for Edwards Lifesciences, Philips Healthcare, and Abbott Vascular and on advisory boards for Abbott Vascular, Boston Scientific, and Edwards Lifesciences. Lissa Sugeng, MD, has participated on speakers bureaus for Siemens Healthineers and Philips Healthcare. Paul Grayburn, MD, has participated on advisory boards for Abbott Vascular and Edwards Lifesciences. Wendy Tsang, MD, SM, has participated in equipment research for Philips Healthcare. Jeremy Thaden, MD, has participated in Medtronic trials for assessing valves.

Reprint requests: American Society of Echocardiography, Meridian Corporate Center, 2530 Meridian Parkway, Suite 450, Durham, NC 27713 (E-mail: *ase@asecho.org*).

0894-7317/$36.00

https://doi.org/10.1016/j.echo.2023.10.004

valve function on the basis of the scientific literature and consensus of a panel of experts. This guideline discusses the role of advanced imaging with transesophageal echocardiography, cardiac computed tomography, and cardiac magnetic resonance in evaluating prosthetic valve structure, function, and regurgitation. It replaces the 2009 American Society of Echocardiography guideline on prosthetic valves and complements the 2019 guideline on the evaluation of valvular regurgitation after percutaneous valve repair or replacement. (J Am Soc Echocardiogr 2024;37:2-63.)

Keywords: Echocardiography, Doppler echocardiography, Prosthetic valves, Cardiac valves, Magnetic resonance imaging, Computed tomography

This document is endorsed by the following ASE International Alliance Partners: Argentine Federation of Cardiology; Argentine Society of Cardiology; ASEAN Society of Echocardiography; Australasian Society for Ultrasound in Medicine; Australasian Sonographers Association; British Heart Valve Society; British Society of Echocardiography; Canadian Society of Echocardiography; Cardiovascular Imaging Society of the Inter-American Society of Cardiology; Chinese Society of Echocardiography; Echocardiography Section of the Venezuelan Society of Cardiology; Indian Academy of Echocardiography; Indonesian Society of Echocardiography; Interventional Imaging Group of the Saudi Arabian Cardiac Interventional Society; Iranian Society of Echocardiography; Italian Society of Cardio-Thoracic Anesthesia and Intensive Care; Japanese Society of Echocardiography; Korean Society of Echocardiography; National Association of Cardiologists of Mexico, AC; Philippine Society of Echocardiography, Inc.; Vietnamese Society of Echocardiography.

TABLE OF CONTENTS

Abbreviations

2D = Two-dimensional

3D = Three-dimensional

4D = Four-dimensional

AR = Aortic regurgitation

ASE = American Society of Echocardiography

CHD = Congenital heart disease

CMR = Cardiac magnetic resonance

CT = Computed tomography

CW = Continuous-wave

DVI = Doppler velocity index

EOA = Effective orifice area

EROA = Effective regurgitant orifice area

FDA = US Food and Drug Administration

ICE = Intracardiac echocardiography

LV = Left ventricular

LVOT = Left ventricular outflow tract

MR = Mitral regurgitation

PA = Pulmonary artery

PET = Positron emission tomography

PHT = Pressure half-time

PHV = Prosthetic heart valve

PPM = Prosthesis-patient mismatch

PR = Pulmonary regurgitation

PVL = Paravalvular leak

PVR = Pulmonary valve replacement

PW = Pulsed-wave

RA = Right atrial

RV = Right ventricular

RVOT = Right ventricular outflow tract

SAVR = Surgical aortic valve replacement

SSFP = Steady-state free precession

SVD = Structural valve dysfunction

TAVI = Transcatheter aortic valve implantation

TEE = Transesophageal echocardiography

TTE = Transthoracic echocardiography

TR = Tricuspid regurgitation

TV = Tricuspid valve

TVR = Tricuspid valve replacement

VC = Vena contracta

ViV = Valve-in-valve

VTI = Velocity-time integral

VTI_{PrMV} = Prosthetic mitral valve velocity-time integral

In patients with significant valvular disease, intervention with either valve repair or replacement is often required. Despite advances in valve repair, valve replacement remains common, particularly in adults. The first American Society of Echocardiography (ASE) guideline for the evaluation of prosthetic heart valves (PHVs) was published in 2009.[1] Subsequently, there has been a European Association of Cardiovascular Imaging guideline on prosthetic valves in 2016[2] and an ASE guideline in 2019 on the evaluation of valvular regurgitation after percutaneous valve repair or replacement.[3] Although many principles and recommendations detailed in the 2009 ASE guideline are still current and valid, it lacks several important developments: function of percutaneous valves, the use of three-dimensional (3D) echocardiography, and the role of computed tomography (CT) and cardiac magnetic resonance (CMR) in the evaluation of PHVs. With the evolution of structural heart disease interventions and imaging of valvular heart disease, a comprehensive update is necessary. The present document replaces the 2009 ASE guideline and complements the 2019 guideline on valvular regurgitation after percutaneous valve repair or replacement.[1,3]

I. GENERAL CONSIDERATIONS WITH PROSTHETIC VALVES

A. Types of Prosthetic Valves

A wide variety of PHV types and sizes are available, with selection dependent upon implantation location, underlying valvular pathology, implantation technique, and patient-specific factors. Although percutaneous valves are bioprosthetic, surgically implanted prosthetic valves can be either bioprosthetic or mechanical, with the latter associated with greater durability[4] but necessitating chronic anticoagulation. The shared decision-making surrounding valve choice and implantation technique must integrate patient anatomy, procedural risk, expected patient longevity, the expected PHV durability, and patient preferences and lifestyle.[5]

The prevalence of mechanical valve implantation has declined over the past 10 years for several reasons, including patient preference. Transcatheter valve repair and replacement have changed the demographics and clinical characteristics of patients undergoing surgical valve replacements.[6,7] The need for concurrent procedures such as aortic root and ascending aorta modification, as well as left ventricular outflow tract (LVOT) or right ventricular outflow tract (RVOT) alteration may also affect PHV choice. The most common type of mechanical valve is the bileaflet tilting disk valve (e.g., St. Jude Medical, Carbomedics, On-X), which offers the best hemodynamics of currently available mechanical valves.[8] Single tilting disk valves with low thrombogenicity (e.g., Medtronic-Hall) are infrequently used in contemporary practice. Last, the Starr-Edwards ball-in-cage valve is no longer implanted; however, given its durability, some of these valves continue to function satisfactorily and may be encountered in clinical practice. Examples of

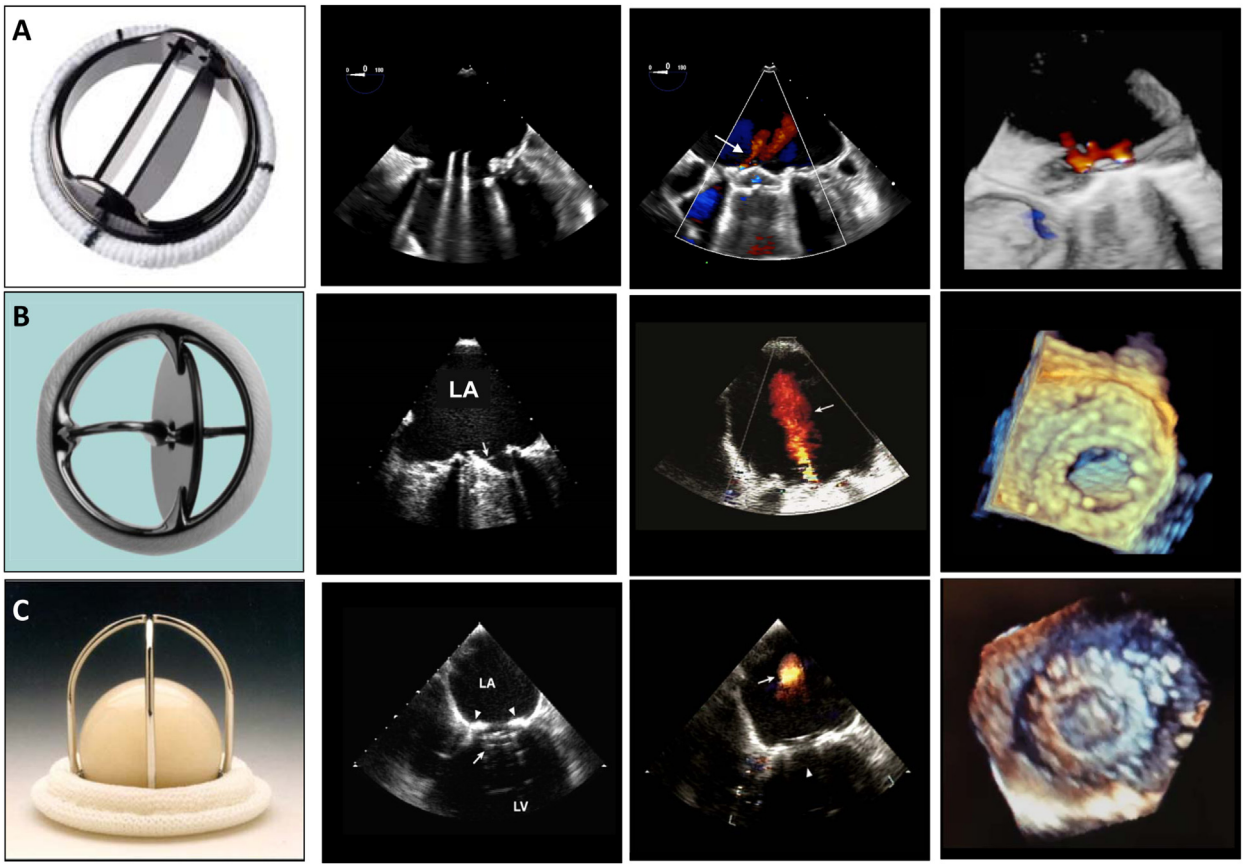

Figure 1 Mechanical valves: **(A)** bileaflet, **(B)** single-leaflet, and **(C)** caged-ball valves and their 2D and 3D transesophageal echocardiographic characteristics taken in the mitral position in diastole and systole (*second and third panels from left*). The *arrows* in diastole point to the open occluder mechanism of the valve and in systole to the characteristic physiologic regurgitation observed with each valve. Three-dimensional transesophageal echocardiography images (*fourth panel*) from a midesophageal window are displayed from a left atrial view. *LA*, Left atrium; *LV*, left ventricle.

mechanical prosthetic valves are depicted in Figure 1 and examples of stented and percutaneous bioprosthetic valves in Figure 2.

Surgical bioprosthetic valves may be xenografts comprising porcine or bovine pericardial tissue, homografts from cadaveric donors, or autografts (such as in the Ross procedure). Stented xenografts are most frequently used; the pericardial leaflets are mounted onto either the inside or outside of a stent frame. Externally mounted leaflets and stentless bioprostheses have the advantage of larger valve areas and lower transvalvular gradients but recent studies show high rates of early structural valve dysfunction (SVD), particularly in younger patients.[9] In the setting of SVD, transcatheter valve-in-valve (ViV) procedures offer patients an alternative to surgical reoperation.[10] Although the risk for coronary obstruction with externally mounted leaflets as well as stentless valves following a ViV procedure is greater than for internally mounted bioprosthetic valves, percutaneous leaflet laceration procedures may mitigate this risk. Different bioprosthetic valves can often be identified by the fluoroscopic and computed tomographic appearance of the stent posts' configuration and sewing ring.

Transcatheter heart valve technology has continued to evolve with expanding indications.[5] Transcatheter aortic valve implantation (TAVI) prostheses in commercial use include balloon-expandable intra-annular devices (e.g., SAPIEN valves; Edwards Lifesciences), self-expanding supra-annular valves (e.g., Evolut valves; Medtronic), and intra-annular valves (Navitor valves; Abbott Structural Heart). Other TAVI prostheses are in trials or early human use. On the other hand, several mitral and tricuspid transcatheter valves are currently under clinical investigation. These feature a wide variety of designs and anchoring mechanisms, including radial force, leaflet capture, annular engagement, and apical tethering. In addition, a ViV transcatheter mitral valve implantation with a balloon-expandable TAVI prosthesis is feasible and has US Food and Drug Administration (FDA) approval. The SAPIEN valve has also been approved for implantation in the pulmonary position. Last, the self-expanding Harmony valve (Medtronic) recently received breakthrough device designation from the FDA and is also available for treatment of pediatric or adult patients with severe pulmonary regurgitation (PR).

From an imaging standpoint, the type, position, and size of a prosthetic valve influence its hemodynamic profile and rate of complications. Normal transvalvular velocities and gradients are flow dependent but can vary depending on the particular valve size and type.[11,12] The valve type also affects the amount of artifact seen with echocardiography, CT, and CMR, which may affect the evaluation of PHV function. Normal echocardiographic parameters of valve function for various prosthetic valve types and sizes in the aortic, mitral, pulmonary, and tricuspid positions are detailed in Appendix Tables A1-A9.

B. PHV Dysfunction

Prosthetic valve dysfunction can be divided into the following categories: SVD, nonstructural valve dysfunction, endocarditis, and thrombus.[13] Regardless of etiology, the hemodynamic consequences

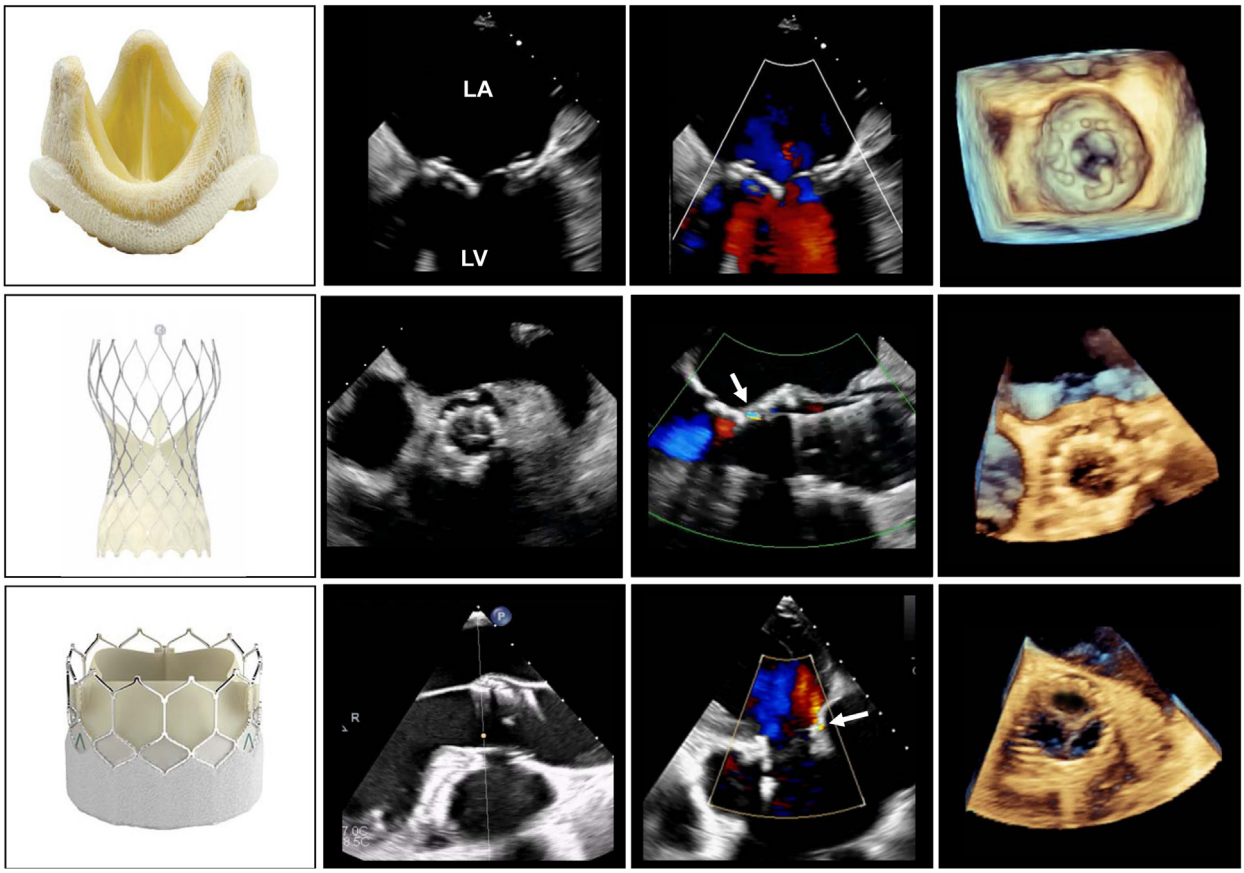

Figure 2 Biological valves: stented (*top row*) and percutaneous valves with their echocardiographic features and 3D transesophageal echocardiographic images. The self-expanding percutaneous valve is in the *middle row*, and the balloon-expandable valve is in the *bottom row*. Mild paravalvular regurgitation is highlighted by the *arrows* in the *middle panels*. *LA*, Left atrium; *LV*, left ventricle.

of dysfunction must be quantified. The following definitions are derived from the Valve Academic Research Consortium 3[13]:

i. **SVD:** intrinsic permanent changes to the prosthetic valve. Examples include wear and tear, leaflet disruption, leaflet fibrosis or calcification, and stent or strut fracture or deformation. Structural failure is more common in bioprosthetic than mechanical prostheses. Valve calcification is the most common cause of bioprosthesis degeneration, seen in 50% of porcine valves at 5 years and in 75% at 8 years.[14] Failure rates at 10 to 15 years are 10% to 20% in homografts and 30% in heterografts.[15] The leaflets and stents are the primary sites with calcification and leaflet tear or rupture.

ii. **Nonstructural valve dysfunction:** any abnormality of the prosthesis not related to the valve itself but still resulting in valve dysfunction.
   a. Prosthesis-patient mismatch (PPM) occurs when a normally functioning PHV is small relative to the patient's size, causing a high gradient and functional stenosis. Outcomes have been related to the severity of PPM.
   b. Paravalvular leak (PVL) may occur in surgical valves from dehiscence of the sewing ring and for transcatheter valves from malapposition of the stent frame with native tissue. Dehiscence is a serious complication, with 4.9% of aortic PHVs requiring reoperation or catheter-based intervention compared with 2.0% of mitral PHVs. Risk factors for dehiscence include bacterial endocarditis, surgical technique, ascending aortic aneurysm, degenerative regurgitation, and severe calcification of the native valve. Transcatheter PVL is related to multiple factors, including missizing of the device, bulky calcification of leaflet or annulus, underdeployment of the transcatheter valve, or improper implantation depth.[13]
   c. Other nonstructural causes of dysfunction: Other causes of dysfunction include leaflet entrapment or dysfunction from pannus, inappropriate position or sizing, dilatation of the cardiac chambers after implantation (e.g., aortic root dilatation, mitral annular or left atrial) dilatation), and valve embolization. Pannus is fibrous tissue that grows in the periannular region and can cause PHV dysfunction.[16] Pannus has a prevalence of 0.2% to 4.5% and occurs equally in mechanical and bioprosthetic valves, with three times higher risk in the mitral position.[17] Pannus may coexist with thrombus formation in PHVs.

iii. **Endocarditis** has a prevalence of 1% to 6% and can occur any time after surgery. In mechanical valves, the infection almost always spreads from the sewing ring and results in complications such as PVL, abscess, and extension to adjacent structures. Bioprosthetic valve infections originate in the leaflet cusps and may involve the sewing ring or paravalvular region. Paravalvular abscess is more common in PHVs (56%-100%) than in native valves (10%-40%), especially in the aortic position.[18,19] Pseudoaneurysms are commonly seen in the aortic position, with a prevalence of 7% to 25% of prosthetic valve endocarditis.[18-20] An infected pseudoaneurysm in relation to a PHV refers to drainage of a paravalvular abscess into an adjacent cardiac chamber. An abnormal communication such as a fistula can occur between two neighboring cavities through a perforation from the infection that extends beyond the valve.[18,19] Last, endocarditis after TAVI is an increasingly important consideration in the appropriate clinical setting, given the increasing number of TAVI prostheses implanted.[21]

iv. **Thrombus** is seen in 0.3% to 8% of PHVs.[2] Mechanical valves are more thrombogenic than bioprosthetic valves, although the risk for thrombus for a mechanical valve with appropriate anticoagulation therapy is similar to that of a bioprosthetic valve. Right-sided valves are more vulnerable to thrombosis than left-sided valves, with the tricuspid valve (TV) affected 12 to 20 times more frequently than left-sided valves.[22] Thrombus is seen on echocardiography as a mass on the valve with a soft echodensity that can be associated with intracardiac thrombus[16]; in bioprosthetic valves, it may appear as valve thickening.[23] On CT, thrombus on bioprosthetic valves may manifest as hypoattenuated leaflet thickening, characterized by thickened and hypoattenuating

Table 1 Essential clinical and echocardiographic parameters in the comprehensive evaluation of prosthetic valve function

	Parameters
Clinical information	Date of valve replacement
	Type and size of the prosthetic valve
	Height/weight/body surface area
	Symptoms and related clinical findings
	Blood pressure and heart rate
Echocardiography	Opening and closing of leaflets or occluder
	Presence of leaflet thickening, calcifications, or abnormal echo density(ies) on the various components of the prosthesis or adjacent to prosthesis
	Valve sewing ring or stent integrity and stability
	Position of sewing ring or stent frame
Doppler echocardiography of the valve	Contour of the jet velocity signal
	Peak velocity and gradient
	Mean pressure gradient
	VTI of the jet
	DVI
	Acceleration time, acceleration time/ejection time for AV
	PHT in MV and TV
	EOA*
	Presence, location, and severity of regurgitation†
Other echocardiographic data	LV and RV size, function, and hypertrophy
	Left atrial and RA size and function
	Concomitant valvular disease
	Estimation of PA pressure
	Venous inflow pattern (i.e., pulmonary vein for MV and hepatic vein for TV)
Previous postoperative study(ies), when available	Comparison of above parameters is particularly helpful in suspected prosthetic valvular dysfunction

AV, Aortic valve; *MV*, mitral valve.

*EOA using the continuity equation; must be compared with normal Doppler values of the valve type and size.

†Transthoracic Doppler is less sensitive for detection of valvular regurgitation in mitral and tricuspid prosthesis; TEE is frequently needed for a more definitive assessment.

PHV leaflets and reduced valve motion (hypoattenuation affecting motion). The reported prevalence is 3.6% to 40%.[24]

C. Evaluation of Prosthetic Valves

A comprehensive assessment of prosthetic valve function includes clinical information, echocardiography, and Doppler evaluation. Comparison with a baseline study or serial postoperative studies is key to determining whether valve function has changed (Table 1).

i. **Clinical information:** Study indications, patient symptoms, size and type of valve replacement, and date of surgery should be included in the report when available. This allows comparison of the study measurements with the expected normal PHV hemodynamics. Similarly, blood pressure, heart rate, height, weight, and body surface area should be included. Heart rate affects the duration of diastolic filling and therefore mean gradients in the mitral valve and TV; body surface area is helpful in assessing the presence of PPM and chamber size.

ii. **Echocardiographic imaging:** Standardized measurements of cardiac chambers, systolic and diastolic function, aortic root, and ascending aorta per ASE guidelines are recommended in patients with PHVs. Zoom imaging with multiple views should be used to evaluate all components of the prosthetic valve (Table 1). Because of acoustic reverberation by prosthetic material, visualizing the central occluder or leaflets may require off-axis imaging. Biplane imaging allows simultaneous assessment of the valve structure in real time and localization of paravalvular regurgitation with color Doppler. Mild thickening is often the first sign of primary failure of a biologic valve and is a signal to reduce the interval between follow-up studies. Independent or rocking motion of a replacement valve is a sign of dehiscence and may be more diagnostic for valves in the aortic position.[25] In the mitral position, normal increased mobility of a valve may be due to annular motion, atrial or annular reconstruction, or location of the sewing ring (i.e., within the left atrium); it needs to be differentiated from dehiscence by the absence of a PVL. Thickening of the aortic root due to hematoma and edema after insertion of a stentless valve usually resolves in 3 to 6 months but can be mistaken for an aortic root abscess. Reviewing the postoperative or intraoperative study is useful to corroborate this finding. Note that careful attention to the possibility of abscess formation is needed at the level of the annulus or sewing ring.[25]

When using 3D echocardiography, the prosthesis should be assessed via 3D volume data sets, with and without color Doppler, from the imaging view that best visualizes the valve or paravalvular structures. The en face view of prosthetic valves allows easier localization of PVL and guidance of percutaneous interventions. When acquiring 3D data sets, the two-dimensional (2D) multiplanar images should be used to optimize line density and frame rate, allowing an accurate assessment of spatial and temporal changes. This may be achieved with single-beat narrow volumes using live 3D modes or multibeat acquisition using live 3D, zoom, or full-volume modes, preferably with volume rates surpassing 20 Hz. If measurements are performed using 3D volumes, high–volume rate single-beat acquisitions are preferred. However, if 3D color Doppler is required to quantify the vena contracta (VC) area, then a multibeat acquisition may be necessary to improve line density and volume rate. Optimal 3D acquisitions will include surrounding tissue and valvular landmarks so that the location of the lesion may be referenced and displayed in accordance with the ASE and European Association of Echocardiography guidelines.[26]

iii. **Doppler echocardiography:** The principles of interrogation and recording flow velocity through prosthetic valves using pulsed-wave (PW), continuous-wave (CW), and color Doppler are similar to those used in assessing native valve function.

a. Determination of gradients across prosthetic valves: Velocity across a prosthetic valve is dependent on flow, valve size, and valve type. The simplified Bernoulli equation ($\Delta P = 4V^2$) is key to the noninvasive calculation of pressure gradients. In patients with aortic prostheses and high cardiac output or narrow LVOT in whom the proximal velocity (V_1) is >1.5 m/sec, the proximal velocity can no longer be ignored, and estimation of the pressure gradient is $\Delta P = 4(V_2^2 - V_1^2)$. In bileaflet prostheses and caged-ball valves, however, overestimation of the gradient may occur more than in bioprosthetic valves, particularly with smaller valves and high cardiac output (see "Pressure Recovery: Hemodynamic Conditions and Clinical Implications"; Figure 3).[27,28]

b. Effective orifice area (EOA): The prosthetic valve EOA derived using the continuity equation is a better index of valve function than gradient alone as it is less dependent on flow through the valve:

EOA = stroke volume/prosthetic valve velocity-time integral (VTI).

For stroke volume calculation using the LVOT, the LVOT diameter measurement and the corresponding position of the PW Doppler sample volume introduce the largest errors in estimating EOA.[1,2] The diameter used should always be the largest diameter measured perpendicular to the LVOT direction, not an average determination, as the error is in

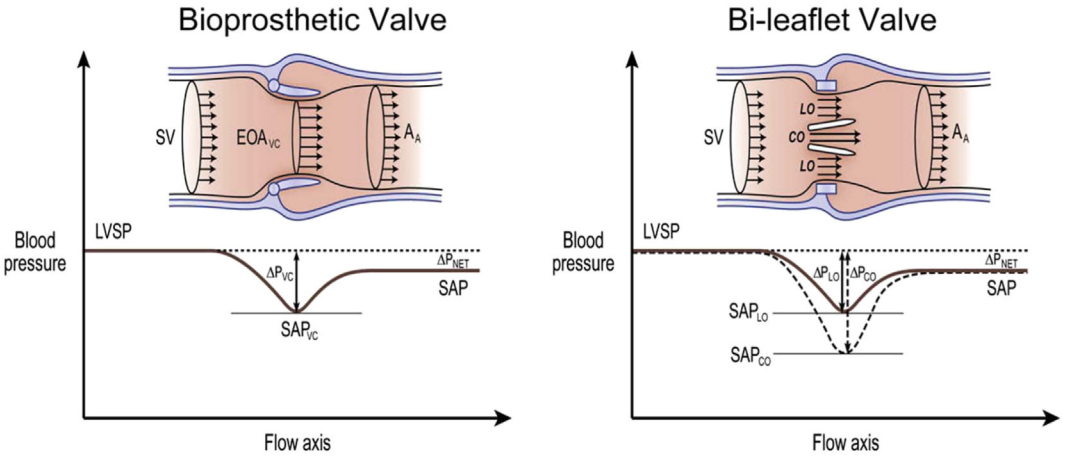

Figure 3 Pressure recovery in prosthetic valves. Schematics of changes in velocity and pressure in prosthetic aortic valves. Velocities are lower and systolic arterial pressure (SAP) is higher at the distal aorta than at the level of the VC. The *left figure* represents changes in velocity and pressure from the LV outflow to the ascending aorta (A_A) in a stented bioprosthetic valve. As flow expands into the wider lumen beyond a valve, velocity and kinetic energy decrease and pressure recovers. The magnitude of this phenomenon is small, except in patients with aortas <3 cm in diameter. On the *right*, in mechanical bileaflet prostheses, the velocity is higher in the central orifice (CO) compared with the lateral orifices (LOs); hence the pressure drop is higher at this level. This is not seen in a single tilting disk or bioprosthetic valve. The smaller CO gives rise to a higher velocity jet that corresponds to a localized pressure drop that then recovers once the central flow reunites with flows from the two LOs. Doppler-estimated velocity and gradients usually cannot differentiate between the lower and maximal velocities, leading to overestimation compared with the invasive standard. *LVSP*, LV systolic pressure; *SV*, stroke volume in LV outflow.

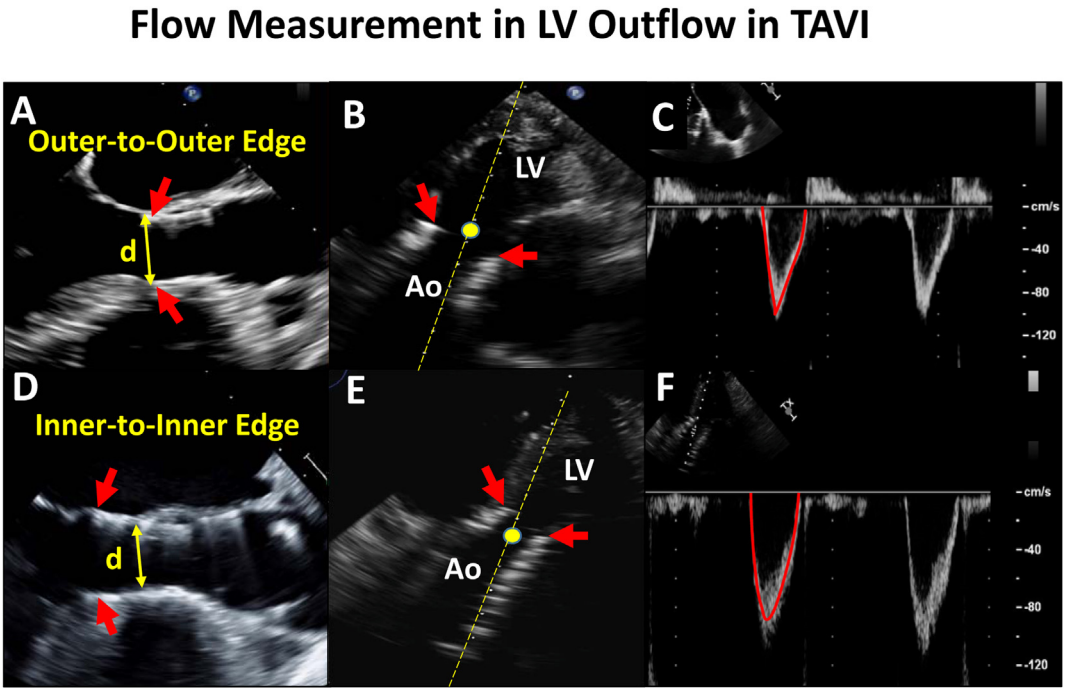

Figure 4 Calculation of flow in the left ventricular outflow in transcatheter aortic valves. The default approach is to measure LVOT diameter using the outer edge–to–outer edge diameter at the lower (ventricular) end of the valve stent (**A**, *arrow*). The PW sample volume from the apical view is placed immediately proximal to the site of flow acceleration at the inlet to the stent **(B)**. Stroke volume is then calculated as usual, assuming a circular LVOT geometry as $0.785 \times d^2 \times$ VTI. In instances in which a self-expanding valve is placed low in the left ventricular outflow, particularly if the lower end of the stent is not in close proximity to the anterior mitral leaflet and interventricular septum, an alternative approach is to measure the inner edge–to–inner edge diameter of the valve stent immediately proximal to the cusps **(D)**. Then, the Doppler sample volume should be placed just inside the stent but proximal to the site of flow acceleration at the valve cusps **(E)**. Velocity and VTI would be larger if the PW Doppler sample volume is placed just inside the stent (**F** vs **C**). Note that with transcatheter valves, there is flow acceleration at the inlet to the stent and again at the valve cusps. *Red arrows* point to the lower end of the stent. *Ao*, Aorta; *LV*, left ventricle.

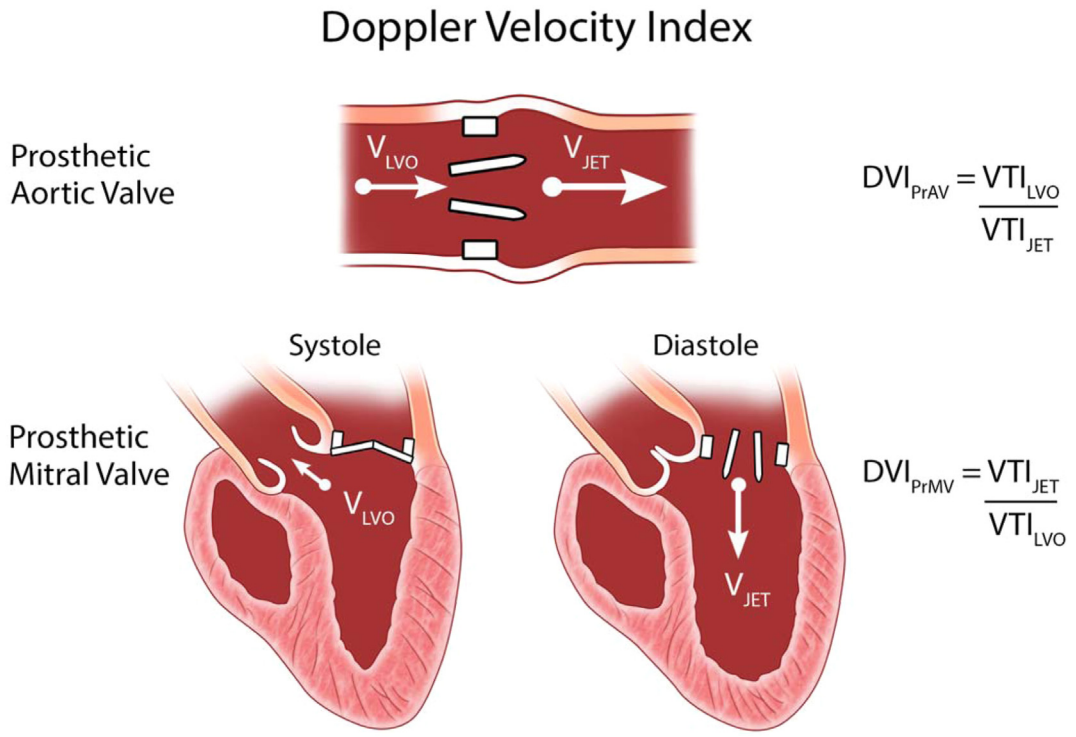

Figure 5 DVI, an index of valve performance, is derived for the prosthetic aortic valve (PrAV) and for the prosthetic mitral valve (PrMV). The VTI in the LV outflow (LVO) is by PW Doppler, and that of the jet is by CW Doppler. The same concept can also be applied to the pulmonary valve and TV. DVI use in prosthetic mitral, tricuspid and pulmonary valves is valid in the absence of significant AR.

underestimating LVOT diameter. In surgical aortic valve replacement (SAVR), the diameter is measured just below the valve plane. For TAVI, the LVOT diameter preferentially is the outer-to-outer diameter of the stented valve.[3,11] The PW Doppler sample volume should also be placed apical to the stent frame at peak systole. The inner-to-inner stent diameter may be used, but the matched PW Doppler sample volume within the stent may record flow acceleration, overestimating stroke volume (Figure 4). Using the label size of the prosthetic valve to calculate the annular cross-sectional area is not recommended.[29] The biplane method of disks for left ventricular (LV) volume calculation (modified Simpson method) and 3D LV volumes are alternative methods to calculate total LV stroke volume and EOA, particularly in the presence of flow acceleration in the LVOT. However, avoidance of LV foreshortening and the use of ultrasound-enhancing agents are strongly recommended to prevent underestimation of LV stroke volume, which is known to occur with echocardiography compared with CMR.[30,31] In prosthetic mitral valves, stroke volume calculated at the aortic annulus or pulmonary annulus may be used, provided no significant mitral, aortic, or PR exists.

c. Doppler velocity index (DVI): In prosthetic aortic valves, DVI—the ratio of VTI proximal to the valve to that through the valve—can be used to assess aortic valve function.[29,32] A DVI $\leq$0.35 is associated with adverse outcomes for SAVR but not TAVI.[32] The inverse of this ratio is used for prosthetic mitral valves (Figure 5).[33] For mitral valves, this ratio is also helpful in detecting significant mitral regurgitation (MR), as flow velocity increases through the mitral valve and decreases in the LVOT with significant MR. The DVI parameter may also be applied to prosthetic pulmonary valves and TV, but more validation is needed.

D. Pressure Recovery: Hemodynamic Conditions and Clinical Implications

In prosthetic valves, the phenomenon of pressure recovery can occur in two regions (Figure 3): (1) downstream from a prosthetic valve and (2) within some prosthetic valves, typically bileaflet or caged-ball valves.[27,34-36]

In the first scenario (Figure 3, *left*), as flow expands into the wider lumen beyond a valve, velocity and kinetic energy decrease and pressure recovers. Several factors influence the magnitude of pressure recovery and the accuracy of Doppler-derived gradients, including flow profile, flow rate, size of the downstream chamber, and simplification of the Bernoulli equation, which may lead to higher gradients with Doppler compared with invasive measurements.[37] The magnitude of this discordance is usually small, except in patients with aortas <3 cm in diameter.

In the second scenario (Figure 3, *right*), the design of the mechanical bileaflet and caged-ball prosthetic valves creates a separate pressure recovery at the level of the valve not seen in monoleaflet or bioprosthetic valves.[38] In bileaflet valves, the smaller central orifice gives rise to a high-velocity jet that corresponds to a localized pressure drop that normalizes once the central flow reunites with flows originating from the two larger lateral orifices.[34,38] CW Doppler recording often includes this high-velocity jet, which leads to overestimation of gradients and underestimation of EOA compared with the invasive hemodynamic measures, particularly in small prostheses and high-flow states. Differentiation of central from lateral orifice jets is possible in prosthetic mitral valves with transesophageal echocardiography (TEE; in the near field) but not with transthoracic echocardiography (TTE). The effect of pressure recovery usually does not interfere with assessment of PHV function, as it is already incorporated in the normal values of Doppler velocities, gradients, and DVIs of various valves (Appendix Tables A1-A9). However, in patients with small bileaflet aortic valves (e.g., 19 mm) accompanied by high flow, differentiation of abnormal function may require further evaluation of valve motion and structure with fluoroscopy, CT, or TEE. Last and most important, as

the valve (bioprosthetic or mechanical) becomes stenotic, the echocardiographic and invasive measures of valvular hemodynamics become concordant and associated with outcomes.[27,28,37]

E. Prosthesis-Patient Mismatch

PPM occurs when the prosthetic EOA is too small relative to the body size and resting blood flow needs of the patient.[39] EOA as well as leaflet morphology and mobility are all normal; however, the indexed EOA is small for body size.[40] Although PPM may be one cause for high transvalvular gradients, gradients may be normal in the setting of PPM with low flow, an entity that is associated with poor outcomes.[41]

The diagnosis of aortic PPM relies on measurement of EOA using the continuity equation indexed to the patient's body surface area. CT may provide additional diagnostic information, including confirmation of normal leaflet mobility, prosthesis size, and stent frame inlet area. It also allows the identification of valve obstruction (reduced mobility from thrombus, calcifications, or pannus).[2] Gradients have been shown to increase exponentially when the indexed EOA is <0.8 to 0.9 cm^2/m^2.[39,42] Importantly, indexed EOA can overestimate PPM severity in the setting of obesity (body mass index > 30 kg/m^2), and thus different PPM thresholds are suggested for these patients.

The impact of aortic PPM on clinical outcomes increases with severity.[43,44] The reported incidence of moderate aortic PPM in SAVR varies between 20% and 70%, whereas that of severe PPM is between 2% and 20%.[40] The incidence of severe PPM in TAVI is lower than that for SAVR.[45,46] It should be emphasized that the indexed EOA (rather than the size or geometric specifications of the prosthesis) is the only parameter that is consistently related to postoperative gradients and/or adverse clinical outcomes. SAVR PPM is associated with decreased exercise capacity and lower functional class. The main adverse clinical outcome of PPM is reduced short-term and long-term survival but higher rates of heart failure and hospitalization, less regression of LV hypertrophy, and faster development of SVD have also been reported.[40] Worse outcomes have also been described in specific patient subsets, such as in individuals <65 to 70 years old and those with coexisting LV dysfunction, significant hypertrophy, low-flow, low-gradient aortic stenosis, and MR.[47,48] Aortic PPM can usually be avoided[47,49,50] with calculation of the projected indexed EOA of the prosthesis before implantation. If PPM is anticipated, choosing an alternative prosthesis, opting for TAVI, or considering aortic root enlargement surgery is recommended.[40]

PPM can also occur with mitral prostheses, but the correlation between indexed EOA and transvalvular gradients is not as strong as in aortic prostheses.[51] Calculation of indexed EOA for mitral prostheses is best done using the continuity equation; it should be emphasized that calculation of EOA using the pressure half-time (PHT) method is frequently inaccurate and leads to overestimation of EOA, particularly in normal valves.[52,53] The threshold values for mitral PPM are higher than for aortic valves, with an ideal indexed EOA of >1.2 cm^2/m^2 to avoid abnormally high postoperative gradients.[53] Moderate mitral PPM is defined as <1.2 cm^2/m^2, and severe mitral PPM is defined as ≤0.9 cm^2/m^2.[2,54] The reported prevalence of mitral PPM varies between 39% and 71%. It is associated with persistent pulmonary hypertension and decreased perioperative and long-term survival.[55,56] Mitral PPM can be prevented or minimized by implanting a prosthesis with a larger projected EOA when possible.[54]

F. Physiologic Regurgitation

Mechanical valves typically have minor regurgitant jets. Two types of "physiologic" regurgitation may be seen: a closing volume (retrograde displacement of blood caused by the motion of the occluder) and true trivial or mild regurgitation at the hinges of the occluder. For the Starr-Edwards valve, there is typically a small closing volume and little or no true transvalvular regurgitation (Figure 1). The single tilting disk valves have both types of regurgitation, but the pattern may vary: the Bjork-Shiley valve has small jets located just inside the sewing ring where the closed disk meets the housing, while the Medtronic-Hall valve has these same jets plus a single large jet through a central hole in the disk where it pivots (Figure 1). The now commonly used bileaflet valves typically have multiple jets located just inside the sewing ring where the closed leaflets meet the housing and centrally where the closed leaflets meet each other (Figure 1). These "washing jets" are thought to prevent the formation of thrombi at sites of stasis within the sewing ring. The regurgitant fraction is usually no larger than 10% to 15%; the associated color jet can appear large, up to 5 cm long (especially in Medtronic-Hall valves) but narrow at its origin. In the case of bileaflet valves, the washing jets are usually found in formation, two from each pivot point; sometimes these single pivotal washing jets divide into two or three separate "plumes" (Figure 1). The jets are invariably low in momentum so that they are homogeneous in color, with aliasing confined mostly to the base of the jet. Regurgitation is increasingly reported in normal biologic valves, mainly because of improved Doppler sensitivity of current ultrasound machines. Stentless valves, including homografts and autografts, are more likely than stented valves to have minor regurgitant jets. Percutaneous aortic valves rarely have small central regurgitation. More often, the regurgitation is paravalvular at the apposition of the valve stent to the calcified native valve (Figure 2).[3] The incidence of paravalvular regurgitation has significantly decreased with improvements in valve skirt design.

G. Pathologic Prosthetic Regurgitation

Pathologic regurgitation can be either central or paravalvular. Pathologic central valvular regurgitation is most often seen with biologic valves, whereas paravalvular regurgitation can be seen with either valve type but is more frequent in mechanical and percutaneous valves (Figure 2). Localization of paravalvular regurgitation may be challenging but is possible if the jet can be visualized originating and traveling outside the sewing ring. This may require the use of multiple transducer positions and off-axis views.[3] Multiplanar and/or 3D TEE may be helpful, particularly in the mitral valve and TV. Although paravalvular regurgitation is abnormal, small jets are not uncommon, especially during perioperative examination early after surgery. Immediately following implantation, the prevalence of paravalvular regurgitation ranges between 5% and 20%[57]; the majority of these leaks, however, are clinically and hemodynamically insignificant and, in the absence of endocarditis, have a benign course.

In general, the same methods used for quantitation of native valvular regurgitation[58] can be used for prosthetic valves, but application of these methods can be more challenging. Because of acoustic reverberation and shadowing from the prosthesis, detection of regurgitation with TTE is more difficult for valves in the mitral and tricuspid positions, particularly in mechanical valves (Figure 6). Indirect clues from various Doppler parameters can suggest the presence of significant regurgitation. However, TEE is frequently needed for the diagnosis of prosthetic MR. The frequent eccentricity of regurgitant jets, particularly in mechanical valves, renders the quantitation and assessment of regurgitation in general more difficult or limited. Multiple small normal transprosthetic jets cannot be quantified accurately, but these are typically not clinically relevant. For paravalvular jets, the proportion of the

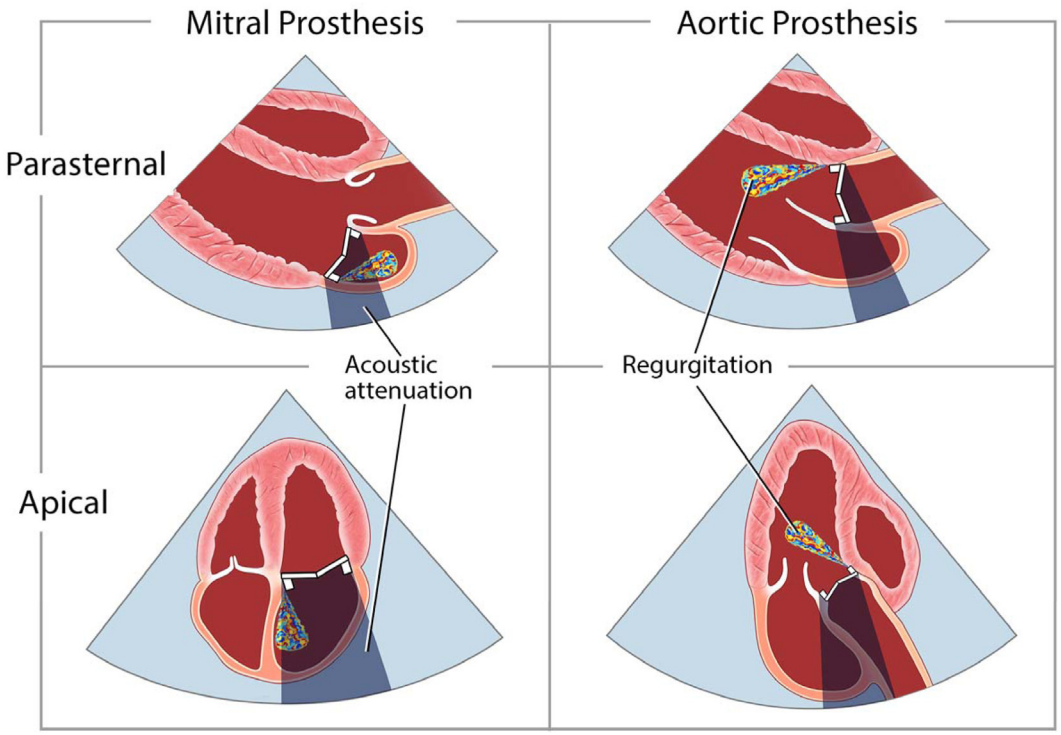

Figure 6 Effect of mechanical prosthetic valve position and echocardiographic imaging view on ultrasound attenuation and masking of a color Doppler regurgitant jet. A higher effect from transthoracic imaging is seen on prostheses in the mitral position compared with the aortic position.

circumference of the sewing ring occupied by the jet gives an approximate guide to severity.[3] Comparative flow measurements for the determination of regurgitant volume or fraction, which frequently rely on the determination of stroke volume at annular sites, can be used for prosthetic aortic regurgitation (AR) and PR but not for prosthetic MR, as mitral inflow cannot be measured using Doppler because of the mitral prosthesis. The use of 3D TEE with Doppler improves the assessment and quantitation of prosthetic regurgitation.[59]

H. Changes During Stress

Stress echocardiography can be useful to evaluate symptoms in patients with prosthetic valves,[60] especially when there is discrepancy between the resting valve hemodynamics and the patient's symptoms. Normally and abnormally functioning prosthetic valves can have similar transvalvular gradients at rest.[61] Symptoms can develop from prosthetic stenosis or regurgitation, PPM, coronary stenoses, or pulmonary diseases, and these can be assessed during stress echocardiography. As hemodynamics can return rapidly to baseline following treadmill stress, supine bicycle and pharmacologic stress with dobutamine are preferable modalities; both allow the assessment of valvular hemodynamics during stress and at peak stress. Exercise is generally preferred over pharmacologic stress because of its physiologic response, important in these clinical circumstances. In general, the assessment for valve obstruction should be similar to that of native valve stenosis, and details regarding stress protocols have been previously described.[60]

I. Considerations for Intraoperative and Intraprocedural Guidance

TEE with the use of both 2D and 3D imaging remains the mainstay for intraoperative and intraprocedural guidance for PHV deployment. In addition, intracardiac echocardiography (ICE), including 3D ICE and image fusion, is becoming more important for image guidance during structural procedures. Other approaches such as epicardial and epiaortic echocardiography, are used infrequently in the operating room, according to local expertise.[62]

i. **Intraoperative echocardiography during prosthetic valve placement:** Apart from evaluating dysfunctional prosthetic valves or newly seated prostheses, TEE can identify previously undetected pathology for appropriate surgical planning and guide placement of cannulas to facilitate cardiopulmonary bypass, especially in minimally invasive and robotic valve surgery. A fundamental goal of intraoperative evaluation of newly seated valves is to diagnose any pathology that requires resumption of cardiopulmonary bypass and immediate surgical correction. These include significant paravalvular regurgitation, dehisced prostheses, and complications in adjacent structures, such as coronary ostial obstruction or stuck prosthetic valve leaflets. Three-dimensional TEE has had a major impact in assessing PHVs in the mitral position compared with other positions because of the proximity of the mitral valve to the left atrium and the en face view of the entire mitral valve. Three-dimensional TEE is particularly helpful for detecting and characterizing paravalvular regurgitation. A more comprehensive approach to intraoperative imaging of prosthetic valves is discussed in the ASE guidelines on the use of TEE to assist surgical decision-making.[62]

ii. **Image guidance during percutaneous prosthetic valve replacement**
   a. Two-dimensional and 3D TEE: TEE is an important tool for image guidance for percutaneous PHV replacement, particularly for prosthetic mitral valves, and for repair of paravalvular regurgitation.[63] TEE for TAVI has also been extensively reviewed. Pulmonary valve replacement (PVR) is often guided by ICE. TV intervention is still experimental but is guided using TEE, supplemented with ICE when needed.
   b. TAVI: Image guidance during TAVI is performed using both transthoracic and transesophageal echocardiographic approaches.[3,64] The key focus is detecting paravalvular regurgitation while remaining cognizant

Table 2 Multimodality imaging of prosthetic valves after initial transthoracic echocardiographic evaluation: advantages and limitations

	Advantages	Limitations
TEE	• High spatial and temporal resolution in real time of valvular structure and function • Doppler quantitative hemodynamic assessment of valve function • Best visualization and assessment for mitral valves (en face) followed by aortic, tricuspid, and pulmonary valves: Valve and occluder/leaflet motion, etiology of dysfunction, gradient; localization and severity assessment of regurgitation (trans- or paravalvular) • 3D TEE, using en face views and/or MPR, may offer more definitive assessment of valve structure, leaflet/occluder motion, localization of PVL, and baseline assessment prior to structural intervention. • Detection of valvular vegetations (small, mobile) • Identification of paravalvular complications (dehiscence, abscess, pseudoaneurysm) • Portable, feasible to use in ICU/emergency department setting and intubated patients • No contraindications in renal dysfunction	• Optimal valve visualization and assessment depends on valve and probe position • Reverberation/shadowing from near field prosthetic valve structures prevent visualization of far-field structures; changing acoustic windows may allow imaging of previously shadowed structures. • Less able to assess pulmonary valve structure and function; special views needed
ICE	• Best modality to evaluate the pulmonary valve and TV and anterior structures of the heart • 3D ICE can show en face views of the pulmonary valve and TV as well as the mitral valve (when performed from the left atrium) • Simultaneous biplane imaging using 3D ICE has higher temporal and spatial resolution compared with 3D volume-rendered images	• Narrow sector width of 3D ICE volume-rendered images with limited temporal and spatial resolution • Color Doppler in 3D ICE has low spatial and temporal resolution with current systems
CT	• Excellent spatial resolution • Good visualization of occluder/leaflet motion, pannus, and leaflet calcification/thickening irrespective of valve position • Identification of paravalvular complications (dehiscence, abscess, pseudoaneurysm) • Useful in the context of multiple prosthetic valves where artifact may affect TEE quality	• Lack of hemodynamic evaluation • Valve regurgitation severity is inferred from anatomic defect; mild regurgitation or shunt may not be detected. • Beam-hardening artifact, particularly in mechanical valves, may interfere with identifying vegetations, thrombus, pannus, small dehiscence • Nephrotoxic contrast agents needed for angiography (noncontrast CT can be used for mechanical valve motion) • Full R-R acquisitions contribute to higher radiation doses • Temporal resolution may be limited
CMR	• Quantitation of peak velocity and gradients (in bioprosthetic valves), irrespective of valve position • Quantitation of regurgitant volume and fraction in regurgitant valves • Identification of anatomic valve area and leaflet pathologies in bioprosthetic valves (thickening, flail) • Identification of large paravalvular complications (e.g., dehiscence, pseudoaneurysm)	• Limited spatial and temporal resolution • Artifact from prosthesis interferes with evaluation of mechanical valves and some bioprosthetic valves • Inability to detect small, highly mobile vegetations • Irregular rhythm and atrial fibrillation effect on valve visualization (potential to overcome with real-time cines) and flow quantitation

ICU, Intensive care unit; *MPR*, multiplanar reconstruction.

of major complications that can occur after TAVI, such as aortic annular rupture, ventricular septal defect, periaortic hematoma, LVOT obstruction, and interference with mitral valve function.[64,65] Most laboratories apply a semiquantitative approach using color Doppler only in this setting and corroborate with invasive hemodynamics and aortography when needed.

c. Mitral valve repair or replacement. Three-dimensional TEE has been revolutionary with regard to guidance of transcatheter edge-to-edge

mitral valve repair and device deployment.[66,67] Three-dimensional TEE is similarly important for the placement of ViV in the mitral position for a degenerated bioprosthetic valve, a failed mitral valve repair with surgical ring, or for a valve–in–mitral annular calcification procedure.[63]

d. Tricuspid valve repair or replacement for native tricuspid regurgitation (TR): TV repair or replacement is typically guided by 2D and 3D TEE. In this more challenging and relatively new procedure, additional imaging from a deep esophageal position is recommended to avoid acoustic noise from the left heart. From this level, the inflow-outflow view with orthogonal 140° and 40° to 60° deep esophageal views are the most helpful.[68] The 140° TEE view is helpful because of the lack of adjacent structures to impede the ultrasound beam.[68-70]

J. Other Techniques for Assessing PHVs

i. **Cine fluoroscopy:** Cine fluoroscopy was the initial noninvasive modality to evaluate mechanical valves.[71] Because of the radiopaque base and disk occluder, abnormal tilting of the base ring and impaired disk occluder mobility can be assessed. Abnormal tilting of the base ring is representative of significant valve dehiscence and paravalvular regurgitation. Impaired disk occluder mobility can be evaluated by calculating the opening and closing angles and is suggestive of prosthetic valve dysfunction.[71] Cine fluoroscopy has limited value in bioprosthetic valves. Calcifications on bioprosthetic tissue valve leaflets are suggestive of valvular degeneration, although its hemodynamic impact cannot be assessed. With TEE and the increasing use of cardiac CT, cine fluoroscopy is now primarily a complementary tool in evaluating mechanical valve mobility.

ii. **Cardiac catheterization:** The widespread availability of echocardiography limits the need for invasive hemodynamic evaluation for prosthetic valve dysfunction. The Gorlin formula is used to calculate EOA of a valve invasively.[72] Ideally, a dual-catheter approach should be used to measure the pressures upstream and downstream from the valve simultaneously. Catheter crossing of a mechanical valve for pressure gradient measurement should be avoided because of potential complications.[73] In prosthetic mitral stenosis, the pulmonary artery (PA) wedge pressure for measurement of transmitral pressure gradient frequently results in an overestimation of the true gradient resulting in underestimation of valve area; direct measurement of the left atrial pressure with a transseptal technique is recommended in circumstances where invasive mitral stenosis assessment is required.[74,75] Contrast injection may be used to evaluate prosthetic transvalvular or paravalvular regurgitation and other complications including fistulas and pseudoaneurysm.

iii. **CT:** Electrocardiographically gated CT provides high–spatial resolution volumetric imaging of the prosthetic valve and cardiac chambers that can be combined with full cardiac cycle imaging to provide functional and anatomic assessment. In patients with arrhythmias, retrospective gating is often beneficial, further aided by the use of absolute delay (in milliseconds) reconstructions rather than relative delay (as a percentage) reconstructions.[76] CT is of greatest utility when dysfunction of a valve is detected on TTE but its etiology is not clear or structural intervention is planned. Advantages and limitations of advanced imaging modalities after an initial transthoracic echocardiographic examination of prosthetic valves are detailed in Table 2. The relative strengths of TTE, TEE, CT, and CMR in assessing prosthetic valve structure, function, and complications are shown in Table 3. CT has a limited role in the routine surveillance or quantification of hemodynamic severity. Noncontrast images can be used to assess mechanical valve mobility where the degree of leaflet opening can be accurately measured. The addition of intravenous contrast allows the detection and potential differentiation between thrombus and pannus as the underlying cause of any restricted motion (Figure 7).[77] The accuracy of CT with contrast is on par with 3D TEE for PHV and may be superior in aortic mechanical valves and pulmonary valves.[77] In bioprosthetic valves, routine use of intravenous contrast is beneficial, as it allows the assessment of leaflet thickening and restricted motion, as well as the detection and localization of significant PVLs.[78,79] Of note is that felt or pledgets may have slightly higher or similar Hounsfield units as contrast and thus can be mistaken for small PVLs. Comparison of noncontrast images and correlation with echocardiography is essential for accurate identification of PVLs. On the other hand, small PVLs can be obscured by metallic artifacts from the prosthetic ring or disk occluders. Calcification of bioprosthetic valve leaflets is a marker of degeneration; however, there is currently no quantitation or scoring strategy to allow its use in a diagnostic capacity.[80] CT may also play a complementary role in the workup of prosthetic valve endocarditis, with TEE providing a more accurate assessment of leaflet vegetations and perforations, while CT provides a more accurate assessment for the presence of root abscess.[81]

Table 3 Comparative strength of imaging modalities in evaluating prosthetic valve structure, function, and complications

	TTE	TEE	CT	CMR
Valve function/stenosis				
Valve structure, anatomic area (bioprosthetic)	++	++++	++++	+++
Valve structure, motion (mechanical)	+	++ (MV 4+)	++++	+
Gradient, EOA*	+++	++ (MV 3+)		++
Thrombus, pannus (mechanical)	+	+++	++++	+
Valve regurgitation				
Localization	++	++++	++	+
Valve dehiscence	++	++++	++++	++
Endocarditis†	++	+++	++	+
Quantitation	++	++++	++	++++

MV, Mitral valve.
On a scale of none to 4+.
*Gradients may be higher in prosthetic valves, particularly in mechanical bileaflet valves.
†For abscess detection, computed tomographic angiography is +++.

iv. **CMR:** CMR has a complementary role in the assessment of PHV function (Table 2). PHVs can be safely imaged using 1.5- and 3-T magnets, which are the most common field strengths used in clinical practice.[82-84] The various techniques used in CMR and their applications in the assessment of prosthetic valves are detailed in Figure 8. The presence of prosthetic valve stenosis or regurgitation may first be recognized on cine images. However, steady-state free precession (SSFP) cines are susceptible to artifacts and are less sensitive to flow. Fast-gradient echo sequences can help reduce flow-related artifacts,[85,86] and spin-echo sequences can be used to reduce prosthetic valve artifacts.[83] The degree of artifact is related to the type of valve (i.e., mechanical vs bioprosthetic, bileaflet vs single leaflet, stented vs nonstented) and can be minor or severe, the latter precluding diagnostic assessment. When there are minimal artifacts, cine images may help visualize excursion of bioprosthetic valve leaflets or mechanical PHV occluders, allow planimetry of bioprosthetic valve area,[85,86] and enable the identification of exaggerated motion of the prosthesis in the context of valve dehiscence. Phase-contrast acquisitions using in-plane phase encoding can help improve visualization of flow turbulence through stenotic prosthetic valves or both valvular and paravalvular regurgitation. For assessment of PHV stenosis, phase-contrast images using through-plane phase encoding enables direct quantification of peak velocities/gradients through PHVs.[87] However, this is usually not feasible for mechanical prostheses in the mitral and tricuspid positions because of artifact and is often challenging with bioprosthetic valves because of annular translation. For assessment of valvular or paravalvular regurgitation, through-plane phase-contrast images can provide quantification of total stroke volume, regurgitant volume, and regurgitant fraction for PHVs at

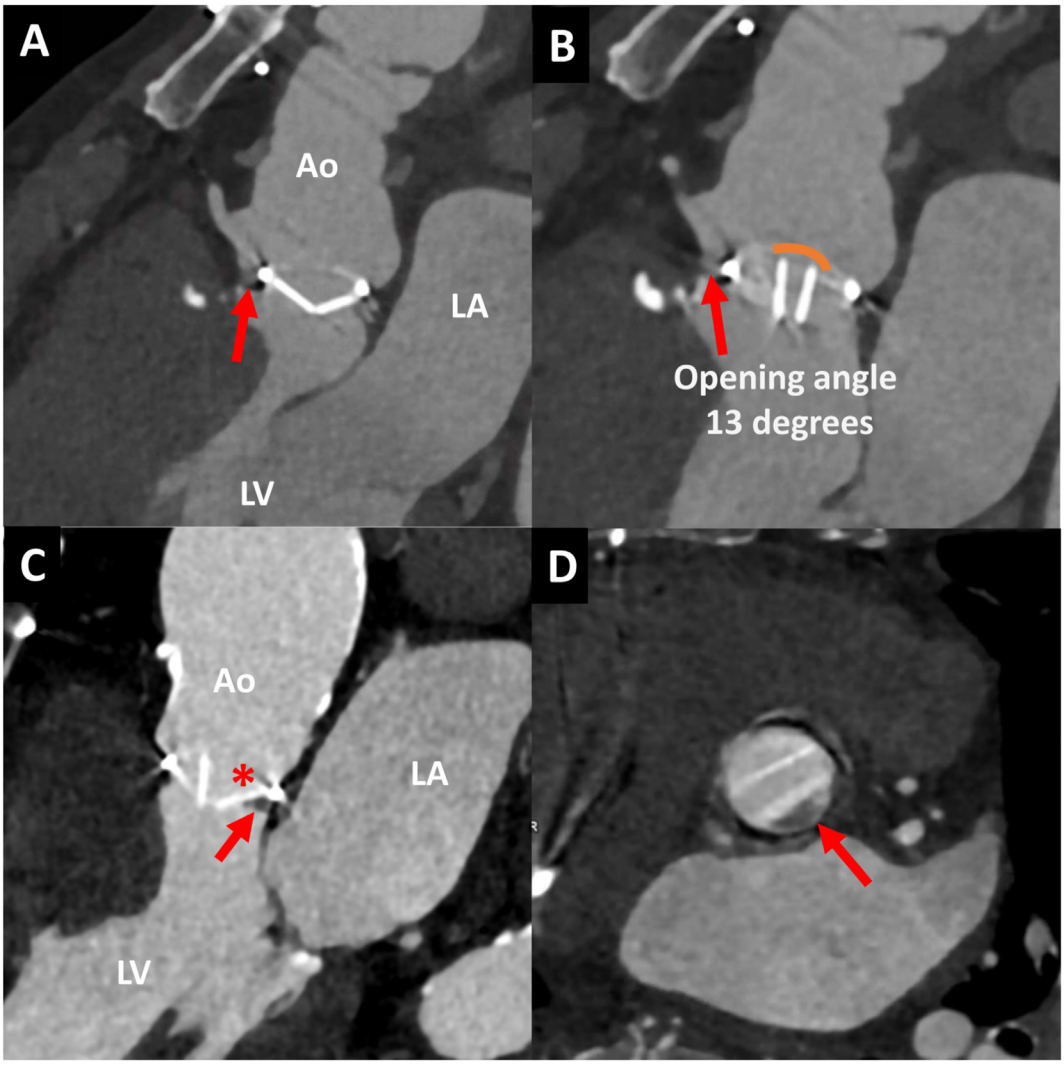

Figure 7 Two cases of bileaflet mechanical aortic valves imaged with cardiac computed tomographic angiography. Case 1 of a patient after the Bentall procedure (*top panels*) shows the aortic valve in diastole **(A)** and systole **(B)** with normal closure and opening angles. However, there is an anterior paravalvular dehiscence (*red arrows*). In case 2 (*bottom panels*), three-chamber and short-axis views show a frozen disk of the mechanical aortic valve (*asterisk*) imaged in systole **(C)**. Pannus is seen over the left coronary cusp (*arrow*) in long-axis **(C)** and short-axis **(D)** views, with Hounsfield units of 150. *Ao*, Aorta; *LA*, left atrium; *LV*, left ventricle.

the aortic and pulmonary positions (Figure 9, Table 2).[58,88] For the mitral valve and TV, an indirect approach using a combination of ventricular stroke volume and through-plane phase-contrast images at the aortic or pulmonary valve position is required.[58,88] Specific techniques are described in the respective valvular sections below and in previous ASE guidelines.[3,58]

v. **Cardiac positron emission tomography (PET):** The principal role of cardiac PET is in the workup of suspected prosthetic valve endocarditis. Fluorodeoxyglucose PET will show an intense increase in uptake in the adjacent annular tissue in the presence of prosthetic valve endocarditis (Figure 10),[89] although this should be interpreted with caution as low to intermediate paravalvular uptake is a normal finding even up to 1 year postoperatively.[90,91] Fluorine-18 fluoride may be of benefit in identifying valves at risk for structural degeneration; however, results in this field are limited, and further work is required.[80]

Key Points for Assessing PHVs

1. The different types of PHVs must be understood before assessing the hemodynamics of PHV function. Knowledge of the type and size of the valve in a particular patient is important.
2. Bioprosthetic valve dysfunction can be divided into the following categories: SVD, nonstructural valve dysfunction, thrombosis, and endocarditis.
3. A comprehensive assessment of prosthetic valve function includes echocardiographic imaging (2D and 3D), Doppler evaluation, and pertinent clinical information.
4. Stress echocardiography can be useful to evaluate symptoms in patients with prosthetic valves.
5. Two-dimensional TEE and 3D TEE remain the mainstay for intraoperative and intraprocedural guidance for PHV deployment.
6. CT and CMR provide complementary and valuable information to a transthoracic echocardiographic evaluation of PHV. CT is particularly helpful in assessing valvular anatomy, while CMR can provide hemodynamic evaluation.

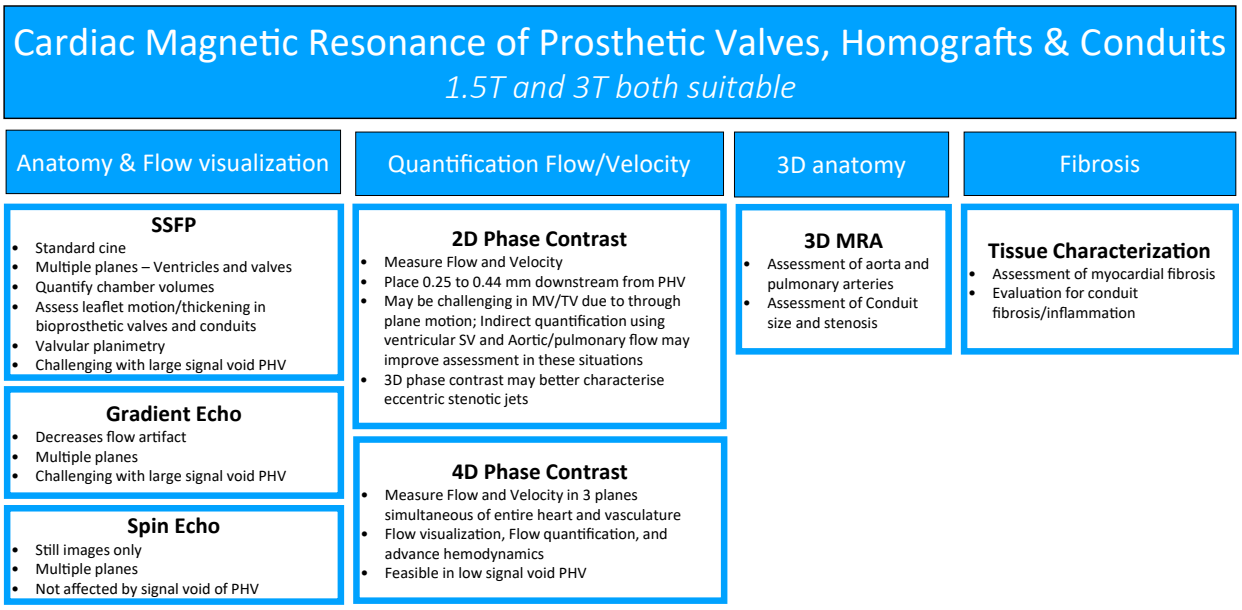

Figure 8 Cardiac magnetic resonance methodology and respective applications in the evaluation of prosthetic aortic valves, homografts, and conduits. *MRA*, Magnetic resonance angiography; *MV*, mitral valve; *SSFP*, steady-state free precession; *SV*, stroke volume.

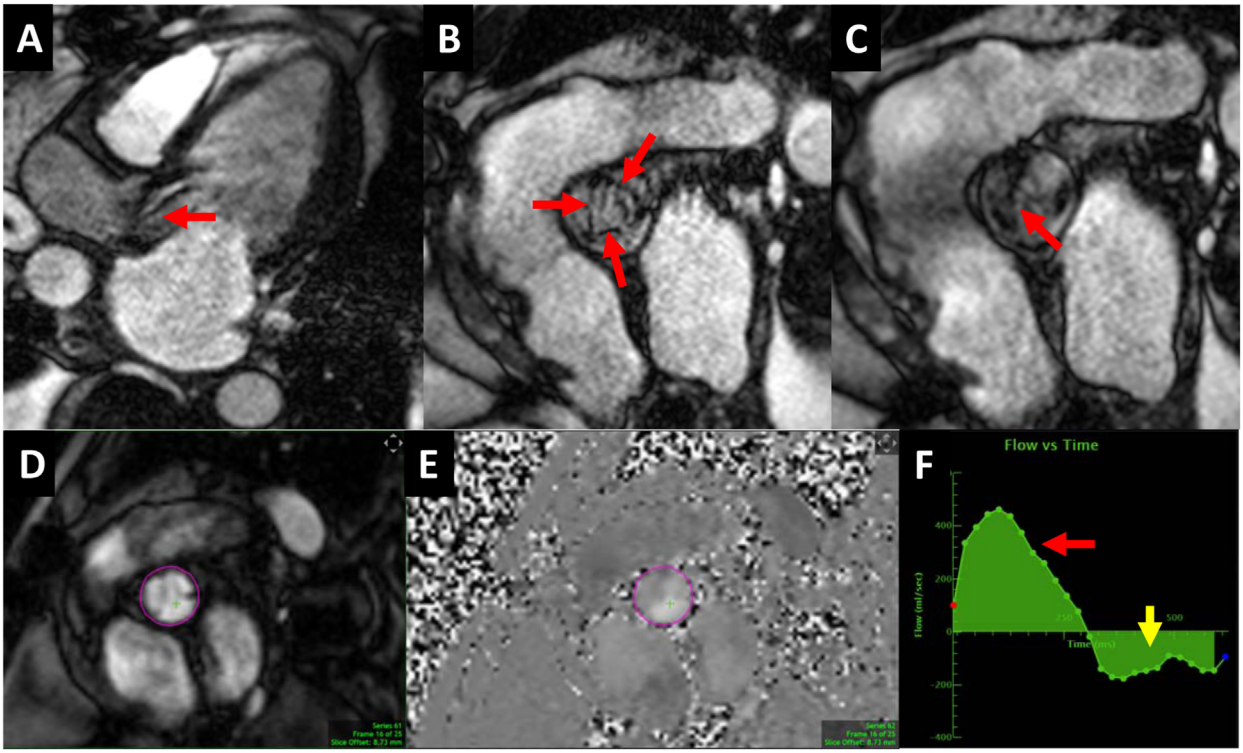

Figure 9 Cardiac magnetic resonance imaging of a case with severe bioprosthetic AR. **(A)** Three-chamber long-axis view on steady-state free precession cine CMR showing spin dephasing in diastole across the valve, suggestive of turbulence from AR (*red arrow*). **(B, C)** Short-axis views of the bioprosthetic valve in systole showing normal systolic excursion (**B**, *three arrows*) and leaflet malcoaptation in diastole (**C**, *arrow*). **(D-F)** Magnitude and phase-contrast CMR sequence with region of interest at the level of sinotubular junction. Flow-vs-time curve **(F)** shows forward (*red arrow*) and backward (*yellow arrow*) flow for direct assessment of AR (regurgitant volume = 55 mL).

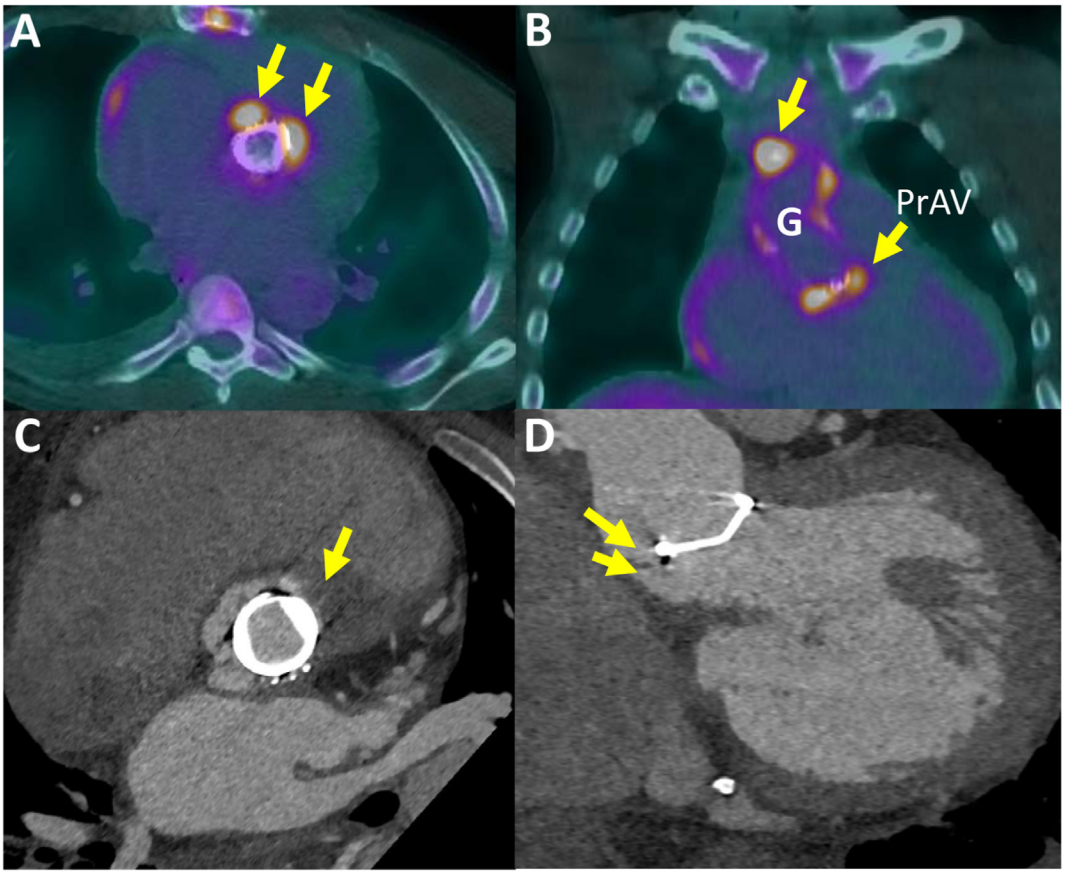

Figure 10 Example of endocarditis affecting a mechanical aortic valve and ascending aortic graft (G), detected on fluorodeoxyglucose (FDG) PET. The patient presented with malaise and dyspnea. Dehiscence of the bileaflet valve and severe AR were detected by TTE. FDG PET performed after prolonged fasting showed intense uptake around the aortic valve in the area of suggested abscess (**A**, *arrows*) and, importantly, also in the aortic graft (**B**, *upper arrow*). Computed tomographic angiography confirmed the possible abscess anterior to the aortic valve (**C**, *arrow*) and dehiscence of the aortic valve prosthesis (PrAV) with a 10-mm PVL (**D**, *arrows*).

II. EVALUATION OF PROSTHETIC AORTIC VALVES

A. Echocardiographic and Doppler Evaluation of Prosthetic Aortic Valve Function

The application of imaging tools to evaluate prosthetic aortic valve function should begin with the identification of the implanted prosthetic valve size and type, followed by a comprehensive echocardiographic study (Table 4). Although surgical valve types and techniques have remained stable over the years, the introduction of sutureless valves along with TAVI in native valves and in degenerated bioprostheses has increased the scope and complexity of evaluating prosthetic valves.

i. **TTE:** TTE is the initial imaging modality used to assess patients with SAVR or TAVI. The parameters for evaluation of PHVs in the aortic position are detailed in Table 4. Standard views required to evaluate valve function have been summarized previously (Figure 11).[1,3] Although TTE assessments of bioprosthetic SAVR and TAVI are similar, special consideration should be given to percutaneous valves. A full assessment of percutaneous valves

Table 4 Echocardiographic evaluation of prosthetic aortic valves

	Parameter
Doppler echocardiography of the aortic valve	Peak velocity/gradient
	Mean gradient
	Contour of the jet velocity; acceleration time
	DVI (DVI = VTI_{LVOT}/VTI_{PrAV})
	EOA
	Presence, location, and severity of regurgitation
Pertinent cardiac chambers	LV size, function, and hypertrophy
Previous postoperative study(ies), when available	Comparison of above parameters is particularly helpful in suspected prosthetic valvular dysfunction

VTI_{PrAV}, VTI through the prosthetic aortic valve.

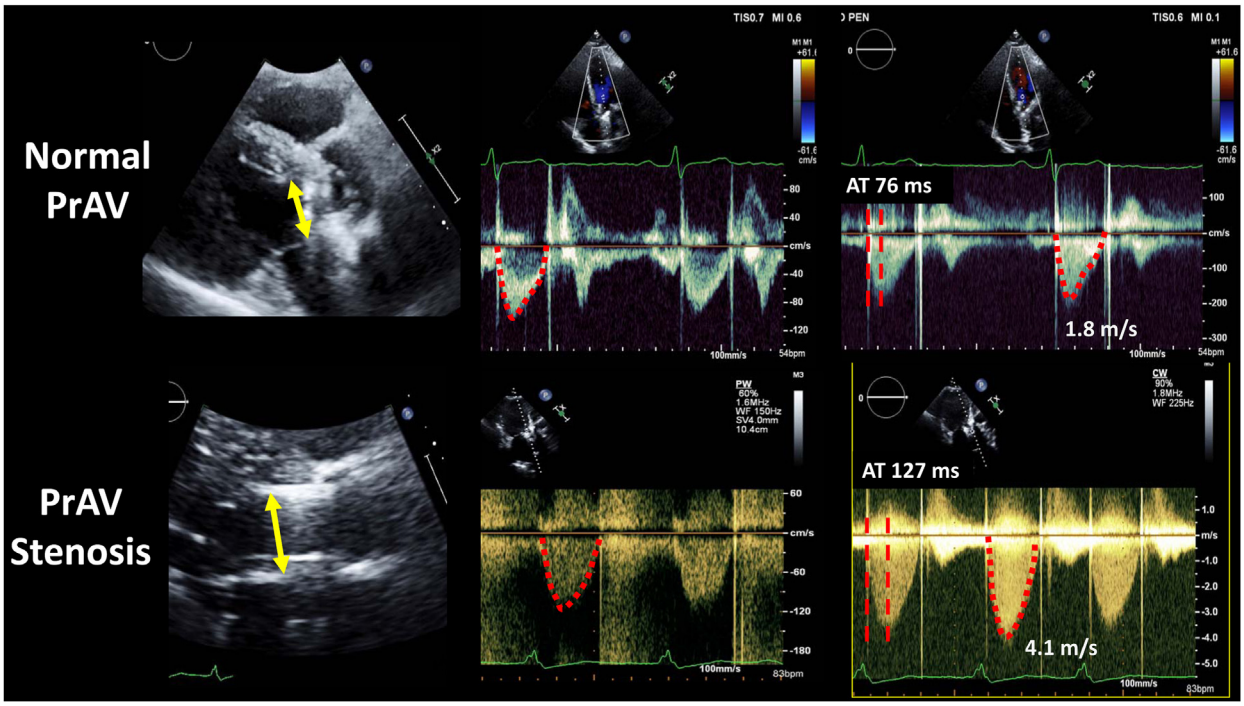

Figure 11 Doppler echocardiographic findings in a normal and a stenotic mechanical aortic valve showing the difference in velocity and its contour, and acceleration time (AT). Normal valve: LVOT diameter 2 cm, VTI_{LVOT} 19 cm, VTI_{PrAV} 31 cm, DVI 0.6, and EOA 1.92 cm^2. The calculated ratio of AT to ejection time (ET) is normal at 0.24. Stenotic valve: LVOT diameter 2 cm, VTI_{LVOT} 24 cm, VTI_{PrAV} 98 cm, DVI 0.24, EOA 0.77 cm^2, and calculated AT/ET ratio 0.4. *PrAV*, Prosthetic aortic valve.

should include valve position in the aortic root, the short-axis valve shape, apposition of the valve stent to native aortic tissue, and the presence of aortic annular injury or ventricular septal defects. Furthermore, sweeping the imaging plane through the valve is necessary to detect valve regurgitation as regurgitant jets may not be seen adequately in a single valve plane (refer to the recent guideline for further details[3]). Low deployment of a TAVI prosthesis can limit anchoring and result in protrusion of the native valve leaflets above the aortic edge of the frame. This increases the risk for delayed migration of the valve into the LVOT or left ventricle. In addition to valve regurgitation, low deployment can affect mitral valve function, causing MR. Incomplete expansion of the TAVI valve because of calcium can result in paravalvular and valvular regurgitation and higher valve gradient.[3]

ii. **TEE:** TEE plays an important role in the assessment of prosthetic aortic valve function.[3,92] One limitation of the transthoracic echocardiographic assessment of a prosthetic aortic valve is aortic prosthesis–related reverberation and shadowing, precluding complete interrogation of the posterior annulus and root (Figure 12). Conversely, although TEE allows excellent visualization of the posterior aortic root, its assessment of the anterior root may be limited because of the same artifact. This may be addressed by adjusting the imaging angle or the depth of the transesophageal probe to "shift" the artifact and allow partial visualization of other prosthetic valve segments. The presence of a mechanical mitral valve will also affect assessment of the LVOT using TEE. Thus, transgastric images play a valuable role in patients with prosthetic aortic valves, allowing assessment of prosthetic valve leaflet motion, gradient, and regurgitation. However, one must be cognizant that Doppler angulation from the transgastric approach may not be optimal. Three-dimensional TEE imaging of prosthetic aortic valve cusps or a mechanical occluder can be challenging. The orientation of the prosthetic aortic valve coaxial to the insonation beam can result in leaflet body dropout with tissue prosthetic valves, especially if the leaflets are thin and noncalcified. Conversely, mechanical valves and tissue valves that are heavily calcified also pose a challenge because of artifacts caused by attenuation and/or reverberation from the leaflet calcium, disks, valve struts, or annulus. For these reasons, the precise motion and excursion of metallic leaflets may not be well delineated; if this is clinically needed, such as when there is a question of valve obstruction or PPM, radiologic imaging (CT or fluoroscopy; Tables 2 and 3) is advised. Details regarding the acquisition and presentation of a 3D rendering of the aortic valve are provided in previous European Association of Echocardiography and ASE recommendations.[26]

iii. **Doppler echocardiography:** The assessment of prosthetic aortic valve function includes peak velocity through the valve, mean gradient, and the EOA, in addition to other criteria such as DVI, the contour of the jet and acceleration time (Tables 4 and 5, Figures 11 and 12). A Doppler algorithm that helps facilitate assessment of prosthetic aortic valve function in patients with elevated maximal velocity through the prosthesis is shown in Figure 13. Similar to native aortic valve disease, Doppler insonation should be acquired from all possible windows. A small nonimaging probe should also be used for better access between rib spaces and for optimal suprasternal notch angulation. Normal Doppler echocardiographic parameters for various types and sizes of percutaneous and surgical valves in the aortic position are detailed in Appendix Tables A1-A4.[1,11,93] Recommended criteria for assessing possible or significant stenosis, SVD, and PPM are provided in Tables 5-7, respectively. The recommendations for SVD differ slightly from other published criteria.[13,94,95]

The diagnosis of prosthetic valve stenosis should not rely on the measurement of a single parameter, as fluctuations in blood flow can affect Doppler measurements.[13] Diagnosis should incorporate assessments from two or more serial echocardiograms when available. Baseline postprocedural echocardiograms are crucial to establish if PPM is present after implantation and to permit comparison of valve performance over time. Other causes of elevated Doppler gradients such as high-flow states, supra- or subvalvular obstruction, and pressure recovery should be excluded. Integration of Doppler hemodynamic data with dedicated imaging to visualize the prosthetic leaflets, often by TEE or CT (especially in mechanical valves [Table 3], as discussed below), is important as it improves diagnostic

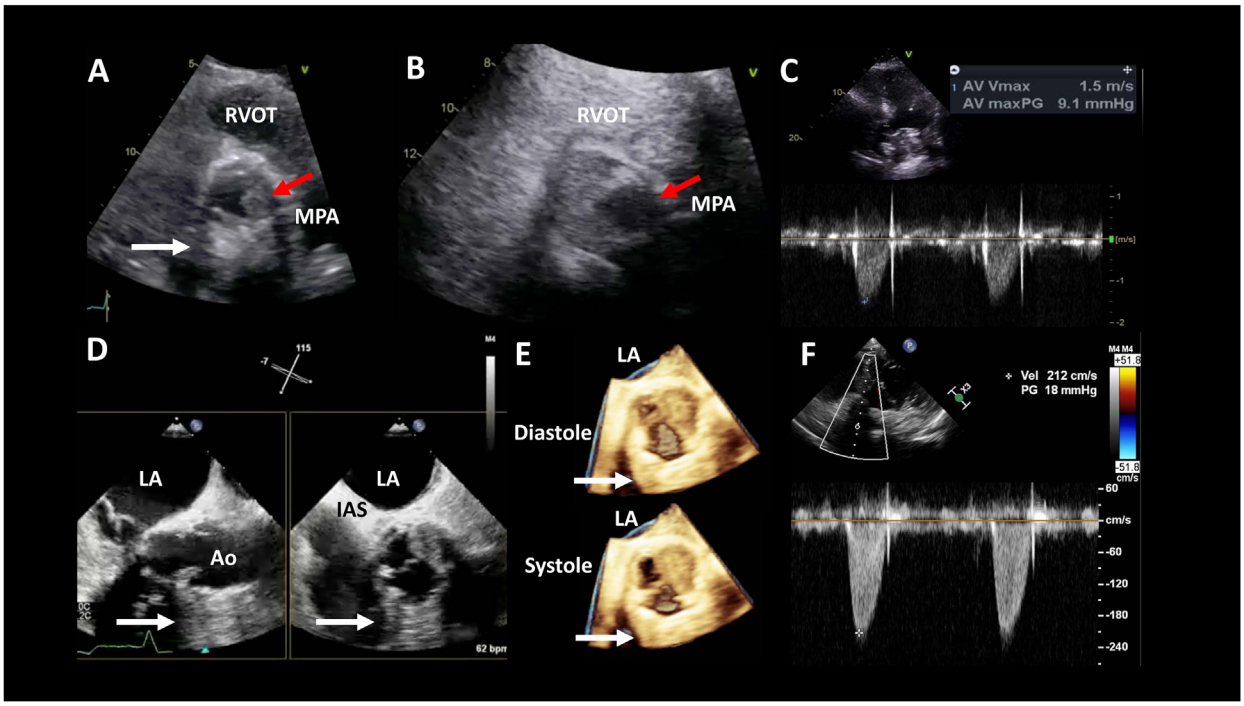

Figure 12 A case of bioprosthetic aortic valve thrombus. **(A)** Transthoracic echocardiographic parasternal short-axis image of the aortic valve during systole demonstrates shadowing of the posterior structure (*white arrow*). Note that there is failure of the left coronary cusp to open because of a mass (*red arrow*). **(B)** The administration of ultrasound-enhancing agent reveals that this mass is likely a thrombus. **(C)** CW Doppler in the apical five-chamber view demonstrating a normal peak systolic gradient of 9 mm Hg. **(D)** TEE performed a few days later allows clear visualization of the posterior annulus. However, there is artifact obscuring the anterior annulus (*white arrow*). It also shows in the long-axis view that the right coronary cusp is now thickened (*left*), and in the short-axis view obtained through biplane, it does not open fully during systole (*right*). **(E)** Three-dimensional transesophageal echocardiographic rendering of the aortic valve in the short-axis view during diastole (*top*) and systole (*bottom*) demonstrating prosthesis-related shadowing (*white arrow*) and fixation of the left and right coronary cusps. **(F)** CW Doppler in the transgastric view demonstrates a higher peak systolic gradient of 18 mm Hg. *Ao*, Aorta; *AV*, aortic valve; *IAS*, interatrial septum; *LA*, left atrium; *maxPG*, maximal pressure gradient; *MPA*, main PA; *PG*, pressure gradient; *Vel*, velocity; *Vmax*, maximal velocity.

performance and frequently identifies a specific etiology for elevated transvalvular gradient.[96] Note that in patients with poor LV function or elevated systemic blood pressures, high gradients may not be present despite significant valve stenosis.

iv. **Considerations for TAVI and ViV:** For TAVI in native valves, in-stent flow acceleration occurs at two locations, below the valve and at the level of the cusps.[97] Thus, LVOT diameter and flow measurements should be obtained immediately proximal to the stent to prevent overestimation of the EOA by flow acceleration within the stent (Figure 4). It is recommended that one highly flow-dependent (e.g., peak velocity, mean gradient) and one less flow-dependent (e.g., EOA) measurement be used to assess prosthetic aortic valve stenosis.[13] Studies have demonstrated that compared with patients with SAVR patients, TAVI patients have similar or lower valve gradients, higher indexed EOA, and lower rates of PPM.[98,99] However, although the percentage of patients with moderate or severe AR was similar between SAVR and third-generation TAVI valves, the prevalence of postprocedural mild AR is higher in TAVI patients.[99]

For TAVI ViV, echocardiographic parameters are affected by the type and size of both the original implanted surgical or TAVI valve and the second implanted valve.[100,101] Appendix Table A3 summarizes echocardiographic findings after ViV at 1 year. Echocardiographic findings on the basis of the original implanted valve and the secondary TAVI valve are limited in the literature. Overall, supra-annular valves compared with intra-annular valves tend to have larger EOAs, lower mean gradients, and lower incidence of moderate or greater AR. Elevated echocardiographic ViV gradients (mean gradient $>$ 20 mm Hg) are found in 28% of patients after ViV. Clinically significant elevated gradients should be confirmed with cardiac catheterization as echocardiographic gradients may be higher compared with invasive measurements because of the pressure recovery phenomenon and limitations of the simplified Bernoulli equation.[102-104] The degree of discordance is greater with self-expandable valves than with balloon-expandable valves.[104-106] Significant PPM has also been observed after ViV, with moderate or greater PPM in 60% of patients and severe PPM in 25%.[102] However, the presence of moderate or greater PPM does not affect 1- or 3-year mortality or clinical outcomes.[102,107,108] Finally, long-term follow-up studies have reported that echocardiographic findings remain stable up to 5 years after the procedure, and rates of valve deterioration are approximately 6.6% at 5 years.[109]

B. Echocardiographic and Doppler Evaluation of Prosthetic Aortic Valve Regurgitation

i. **TTE and TEE:** TTE is used to identify both prosthetic aortic intravalvular and paravalvular regurgitation. In addition to assessing the location and mechanism of AR, TTE can identify associated complications such as endocarditis, abscess formation, masses, and thrombus (Figure 14). Sweeps in both the parasternal long- and short-axis views are often needed to ensure that all jets are identified. Off-axis views may be needed to determine jet origin. Because of reverberation and shadowing from the prosthesis, posterior paravalvular AR may be obscured with TTE, while anterior regurgitation can be masked during TEE.[3] Thus, TTE and TEE are complementary in this

Table 5 Doppler parameters of prosthetic valves in the aortic valve position

	Normal	Possible stenosis	Suggests significant stenosis
Appropriate for all prosthetic aortic valves			
Jet velocity contour*	Triangular, early peaking	Triangular to intermediate	Rounded, symmetric
Acceleration time, msec*	<80	80-100	>100
Acceleration time/LV ejection time ratio	<0.32	0.32-0.37	>0.37
Peak velocity, m/sec†‡	<3	3-4	≥4
Specific AVR considerations			
SAVR			
Mean gradient, mm Hg†	<20	20-34	≥35
DVI§¶	>0.35	0.25-0.35	<0.25
EOA§	Reference EOA ± 1 SD	1 SD smaller than reference EOA	2 SDs smaller than reference EOA
TAVI (change from baseline)			
Mean gradient†	Change <10 mm Hg from baseline†	Increase of 10-19 mm Hg from baseline	Increase ≥20 mm Hg from baseline
DVI§¶	Change <0.1 or 20% from baseline‖	Decrease 0.1-0.19 or 20%-39% from baseline‖	Decrease ≥0.2 or ≥40% from baseline‖
EOA§	Change <0.3 cm^2 or 25% from baseline‖	Decrease of 0.3-0.59 cm^2 or 25%-49% from baseline‖	Decrease ≥0.6 cm^2 or ≥50% from baseline‖

AVR, Aortic valve replacement.
Significant stenosis should meet at least one flow-dependent (i.e., velocity and mean gradient) and one flow-independent (i.e., EOA or DVI) parameter.
*This can be affected by LV function and heart rate.
†Flow dependent.
‡Valid with normal stroke volume (50-90 mL) and flow rates (200-300 mL).
§Flow independent.
¶DVI calculated using VTI as in Table 4.
‖Baseline defined as TTE performed under stable hemodynamic conditions.

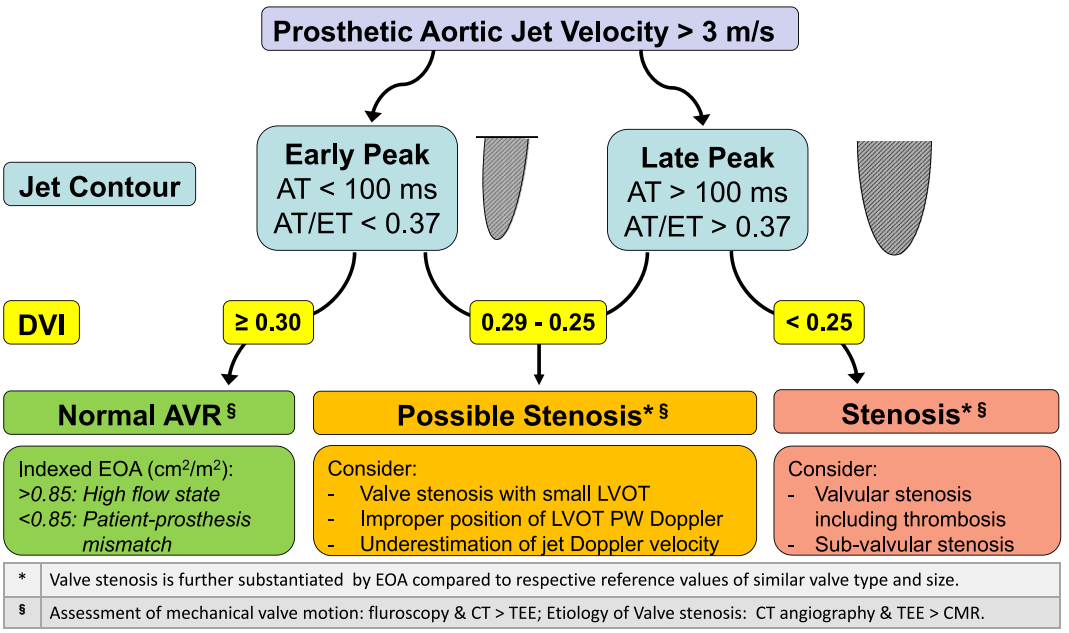

Figure 13 Algorithm for initial evaluation of elevated peak prosthetic aortic jet velocity incorporating DVI, jet contour, and measures of acceleration time (AT) and the ratio of AT to ejection time (ET). Improper PW Doppler sample volume influences both DVI and EOA calculations: too close to the valve will increase DVI and EOA, while too far (apical) will decrease them. *AVR*, Aortic valve replacement.

Table 6 Hemodynamic criteria for structural valve deterioration*†

Possible structural valve deterioration	Significant structural valve deterioration
• Increase in mean transvalvular gradient ≥10 mm Hg resulting in a mean gradient ≥ 20 mm Hg with concomitant decrease in EOA ≥0.3 cm^2 or ≥25% **and/or** decrease in DVI ≥0.1 or ≥20% compared with the baseline (1-3 months) postprocedural assessment	• Increase in mean gradient ≥20 mm Hg resulting in a mean gradient ≥ 30 mm Hg with concomitant decrease in EOA ≥0.6 cm^2 or ≥50% **and/or** decrease in DVI ≥0.2 or ≥40% compared with the baseline (1-3 months) postprocedural assessment
• New occurrence or increase of at least one grade of intraprosthetic AR resulting in moderate or greater AR	• New occurrence or increase of at least two grades of intraprosthetic AR resulting in moderate or greater to severe AR

In the setting of concomitant stenosis and regurgitation, the criteria for significant structural valve deterioration may be present at lower thresholds.
*Criteria assume stable LV function and blood pressure.
†Morphologic adverse changes to the prosthesis should be evident.

regard to detect all sites of paravalvular AR. Last, technical limitations and prosthesis-related artifacts with TTE can limit assessment of structural abnormalities related to the mechanism of AR, necessitating the use of other imaging modalities such as TEE or CT (Tables 2 and 3, Figure 15).

ii. **Doppler echocardiography:** Color Doppler evaluation of the AR jet requires visualization of the flow convergence, VC, and proximal jet extension into the LVOT and left ventricle. Limitations of this method include acoustic reverberation and shadowing from the prosthesis that may impair visualization of the flow convergence and VC regions or assessment of the jet width in the LVOT. In this situation, the VC width, area, and circumferential extent could be assessed from a carefully obtained short-axis view.[3] Similar to native valves, measuring the width of an eccentric jet in the outflow tract may overestimate regurgitation severity. Also, entrainment of the regurgitant jet in the LVOT may result in overestimation because of rapid widening of the jet. Conversely, a wall-impinging aortic paravalvular jet may lead to underestimation because of an unimpressive color Doppler jet area.

Semiquantitative and quantitative spectral Doppler methods for grading AR severity are not affected by the prosthetic aortic valve. The presence of a PHT <200 msec or holodiastolic flow reversal in the abdominal aorta suggests the presence of severe regurgitation (Figure 14). Quantitative parameters such as regurgitant volume are calculated using 2D or 3D methods. Note that for stroke volume calculation, care should be taken not to place the sample volume too close to the prosthesis, which would result in overestimation of stroke volume because of proximal acceleration. Methods for quantitation of regurgitant volume and fraction after SAVR and TAVI have been described previously.[1,3]

Classification of intra- and paravalvular prosthetic AR severity is similar to that suggested for native valves in that assessment requires integration of qualitative and semiquantitative parameters (Table 8).[3,58] However, determination of prosthetic valve AR severity may be more complicated because of the presence of combined valvular and paravalvular regurgitant jets, multiple regurgitant jets, or eccentric jets. Figure 16 shows a proposed algorithm for the evaluation of severity of prosthetic valve AR with echocardiography, similar to a recently proposed algorithm.[3] Generally, if the qualitative and semiqualitative parameters are consistent with mild regurgitation, then assessment is complete. If there is a discrepancy or inconsistency among parameters, then explanations from image quality, technical, and physiologic factors should be identified. For patients in whom a consensus grading cannot be determined and there is a need to identify the mechanism and/or quantify the severity of AR, TEE, CMR, or CT is likely required. Each of these modalities has its advantages and limitations (Tables 2 and 3). Note that ASE guidelines describing the assessment of AR after percutaneous aortic valve replacement have been published.[3]

C. Role of CT in the Evaluation of Prosthetic Aortic Valves

CT is a common adjunct imaging modality in patients with PHV dysfunction suspected on echocardiography. CT allows the evaluation of valve morphology, structural abnormalities, stenotic orifices, regurgitant orifices, sewing ring complications, and paravalvular complications. Prospective electrocardiographic triggering is adequate for assessing morphology, but retrospective gating is essential for dynamic 3D evaluation of the valve and functional quantification. A nonenhanced acquisition is useful for detecting calcifications and postsurgical changes, while a delayed phase (60-90 sec) helps in evaluating abscess cavities with rim enhancement and thrombus.

CT has emerged as a useful complementary imaging modality in the follow-up evaluation of transcatheter heart valves.[110] A more recent application of CT (similar to its use in primary TAVI) is for planning of ViV aortic valve implantation. CT is advantageous in preprocedural planning as it is less affected by metal-induced artifacts. Displacement of the native aortic valve leaflets during deployment of the transcatheter valve is associated with a minimal but important risk for subsequent occlusion of the coronary ostia, with a reported incidence of 0.6% to 4.1%.[111] Patients with large and heavily calcified valve leaflets and a short distance between the annular plane and the ostia of the coronary arteries are at greater risk. Hence, it is important to report the distance of coronary ostia from the annular plane.[112]

Table 7 Doppler parameter criteria of aortic valve and mitral valve PPM

	Normal	Moderate	Severe
Aortic EOA*	• >0.85 cm^2/m^2 if BMI < 30 kg/m^2 • >0.70 cm^2/m^2 if BMI ≥ 30 kg/m^2	• 0.85-0.66 cm^2/m^2 if BMI < 30 kg/m^2 • 0.70-0.56 cm^2/m^2 if BMI ≥ 30 kg/m^2	• ≤0.65 cm^2/m^2 if BMI < 30 kg/m^2 • ≤0.55 cm^2/m^2 if BMI ≥ 30 kg/m^2
Mitral EOA*	• >1.2 cm^2/m^2 if BMI < 30 kg/m^2 • >1.0 cm^2/m^2 if BMI ≥ 30 kg/m^2	• 1.2-0.91 cm^2/m^2 if BMI < 30 kg/m^2 • 1.0-0.76 cm^2/m^2 if BMI ≥ 30 kg/m^2	• ≤0.90 cm^2/m^2 if BMI < 30 kg/m^2 • ≤0.75 cm^2/m^2 if BMI ≥ 30 kg/m^2

BMI, Body mass index.
*Valve structure and motion are normal; measured EOA is within 1 SD of the reference EOA.

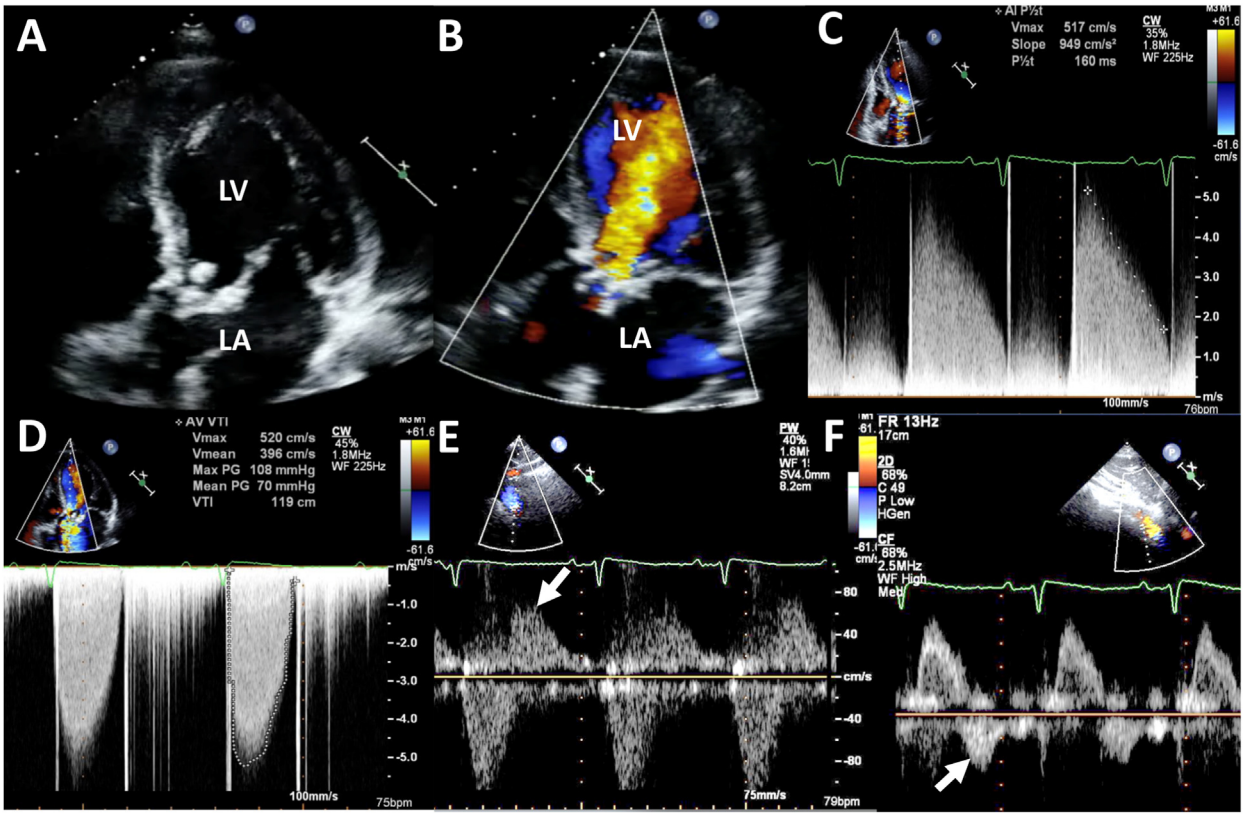

Figure 14 An example of combined AR and stenosis in a patient with a tissue prosthetic aortic valve (AV). **(A)** TTE in the apical five-chamber view during diastole demonstrates a vegetation on the tissue prosthetic AV. **(B)** The corresponding color Doppler image demonstrates severe regurgitation. **(C)** On the CW Doppler image, the PHT is <200 msec, which is consistent with severe regurgitation. **(D)** A high systolic gradient across the valve is evident. **(E)** PW Doppler in the proximal descending thoracic aorta demonstrates flow reversal (*arrow*). **(F)** Flow reversal is also seen in the abdominal aorta (*arrow*). *LA*, Left atrium; *LV*, left ventricle; *Max*, maximal; *PG*, pressure gradient; *Vmax*, maximal velocity; *Vmean*, mean velocity.

The Role of CT in the evaluation of complications is as follows:

i. **Stenosis:** CT can help determine whether pathologic causes of elevated valve pressure gradient exist. These may be difficult to discern on TTE and TEE, particularly in mechanical valves. Possible causes include stenosis from structural failure, calcification, obstruction by pannus or thrombus, or hypoattenuated leaflet thickening with or without restricted motion (Figures 7, 15, and 17).

ii. **Regurgitation:** Structural failure of a bioprosthetic valve is the most common cause of central pathologic regurgitation and often occurs close to the commissure at the site of a tear in the leaflet. CT permits the identification and quantification of a sufficiently large regurgitant orifice, along with evaluation of its secondary consequences. Measurement of regurgitant and stenotic orifice areas with CT shows good accuracy, comparable with that of TTE.[113,114] Computed tomographic angiography can also identify significant valve dehiscence and complications such as pseudoaneurysm formation (Figure 15). Table 9 describes the potential role of CT in evaluating various complications of PHVs, resulting in either stenosis or regurgitation or both. Comparative advantages, limitations, and strengths of CT in relation to TTE and CMR are detailed in Tables 2 and 3.

D. Role of CMR in the Evaluation of Prosthetic Aortic Valves

i. **Prosthetic aortic valve stenosis**

a. Anatomic valve area: Using a stack of thin slices (~4-5 mm) perpendicular to the prosthetic valve in two orthogonal planes (using cross-referenced lines), anatomic valve area can be planimetered via en face tracing of the largest systolic orifice opening (Figure 18).[124] Proper alignment at the leaflet tips is crucial for reproducible and accurate measurement. This can be done on bioprosthetic valves (in the absence of metal struts), but metallic artifact from mechanical valves precludes the assessment of disk motion.[85] Both in vivo and in vitro studies have shown strong agreement between CMR and echocardiography, with superior inter- and intraobserver variability of CMR.[125] One study evaluating 65 bioprosthetic aortic valves showed a strong correlation between CMR-derived anatomic area and echocardiographic effective area measurements (mean differences, 0.02 ± 0.24 cm^2 by TTE and 0.05 ± 0.15 cm^2 by TEE).[85] It is imperative to know that the anatomic valve area is 10% to 20% larger than the effective valve area because of the flow contraction phenomenon.[2]

b. Phase-contrast imaging: In stenosis, flow turbulence creates signal voids because of proton dephasing.[126,127] CMR has the advantage of assessing flow in an in-plane phase (like Doppler echocardiography) and through-plane phase (perpendicular to the maximal velocity across the prosthetic valve). Using two orthogonal in-plane phase-encoding views (derived from cine three-chamber and aorta coronal views to see the site of the jet aliasing), a through-plane image is created perpendicular to the aortic stenosis jet and the highest pixel velocity can be measured (Figure 18). A novel CMR-derived EOA was compared with valve area derived using Doppler echocardiography in native and prosthetic aortic valves.[128,129] Using phase-contrast imaging to assess transvalvular forward flow volume and dividing that by VTI to obtain phase-contrast effective regurgitant orifice area (EROA), this measurement compared favorably and showed excellent agreement with the clinical classification of prosthetic aortic valve stenosis

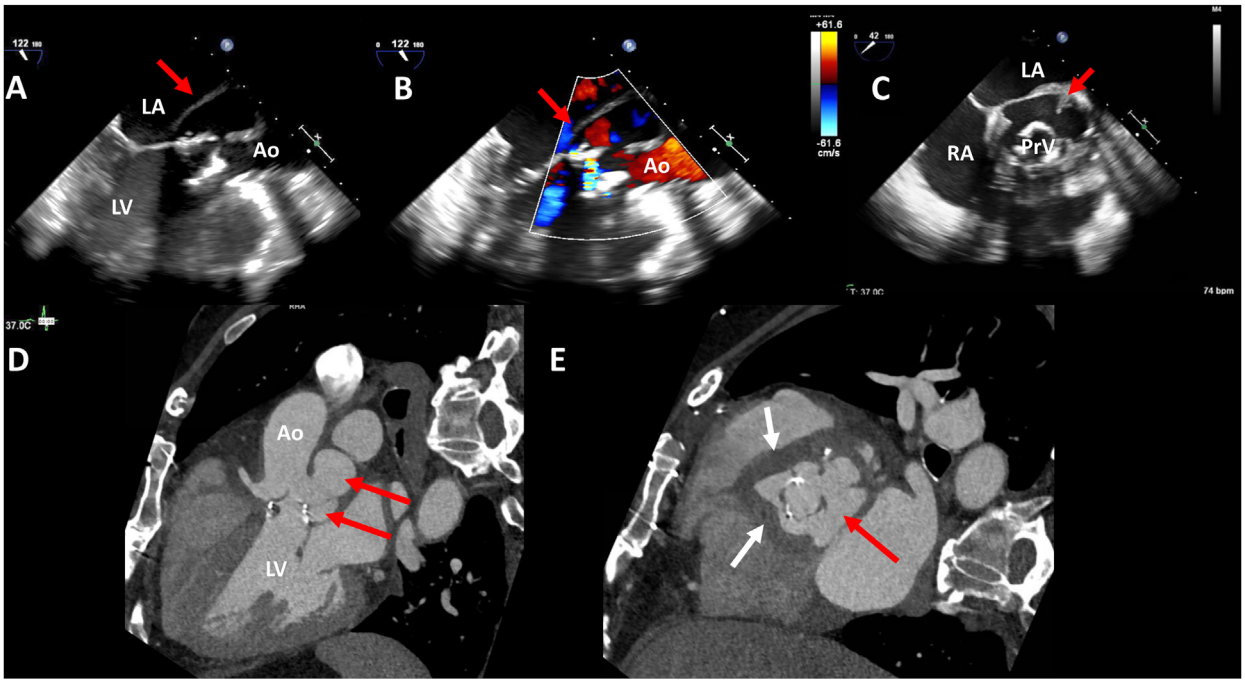

Figure 15 A case of a bioprosthetic aortic valve (AV) complicated by a large aortic root pseudoaneurysm imaged with TEE and computed tomographic angiography. Midesophageal long-axis views **(A, B)** and short-axis view **(C)** show a large pseudoaneurysm (*arrows*). The valve has evidence of calcification but no discrete vegetations. **(B)** Same view with color Doppler showing eccentric paravalvular regurgitation in diastole. **(D)** Cardiac computed tomographic angiographic sagittal view shows dehiscence below the left cusp with a large pseudoaneurysm (*two red arrows*). **(E)** Modified sagittal view shows circumferential hypodensity on the aortic root suggestive of root abscess (*white arrows*). There is mild thickening and calcification of the bioprosthetic AV (visualized in systole). The pseudoaneurysm is seen over the left sinus (*red arrow*). *Ao*, Aorta; *LA*, left atrium; *LV*, left ventricle; *PrV*, prosthetic valve; *RA*, right atrium.

severity.[129] A novel technique using time-resolved 3D flow mapping (four-dimensional [4D] flow) can visualize turbulent flow with vortex formation pattern and measure pressure-drop estimation in a 3D plane. This technique is not widely used and is time consuming.[125,130] In general, as data in CMR are averaged over multiple cardiac cycles, arrhythmias and rapid irregular heart rates can introduce measurement errors. Because of the limited temporal resolution of CMR (from partial volume effect of high jet velocities), there is an underestimation of velocities using phase-contrast CMR sequences compared with Doppler echocardiography.[124]

Adverse cardiac effects of chronic LV pressure overload (LV hypertrophy, replacement fibrosis) can be accurately assessed with CMR. Focal replacement or infarct-like fibrosis (detected by late gadolinium enhancement on CMR) has been seen in 30% to 50% of patients with aortic stenosis and has been shown to predict worse perioperative risk and cardiovascular disease–related survival in patients undergoing TAVI or SAVR.[131,132]

ii. **Prosthetic aortic valve regurgitation:** CMR provides an advantage over echocardiography in providing absolute regurgitant volumes and fractions irrespective of regurgitant jet numbers, eccentricity, or prosthetic valve type.[3,58] In addition, aortic root and aorta anatomy can be simultaneously assessed in patients with aneurysms and/or aortopathy. Cine SSFP sequences along with phase-contrast imaging can help delineate trans- or paravalvular regurgitant jets, the former causing spin dephasing. Depending on the ferromagnetic material in the surgical strut or frame, artifact precluding accurate assessment of the origin of regurgitation can be encountered.

a. Phase-contrast imaging: In-plane phase-contrast imaging can help delineate trans- or paravalvular regurgitation using three-chamber and aorta coronal views. Using through-plane phase-contrast imaging perpendicular to the aortic wall immediately above the prosthetic valve, both antegrade and retrograde flow can be measured directly. The regurgitant volume and hence the fraction (regurgitant volume/forward volume) can then be calculated (Figure 9).[126,133] An alternative method using the difference between forward aortic and net pulmonary flow can be used.[133] In addition, the presence of holodiastolic flow reversal in the descending aorta has shown excellent sensitivity and specificity for severe regurgitation.[134,135]

Studies comparing echocardiography with CMR in assessing paravalvular regurgitation have yielded different results, with underestimation of regurgitant volumes using TTE and TEE.[88] In a recent meta-analysis assessing AR after TAVI, significant discordance was noted between TTE and CMR; however, TTE was able to discriminate moderate or severe AR from mild or none.[136] These studies used different cutoff values for CMR, which could have contributed to the major discrepancies between both imaging modalities. Limitations of the phase-contrast technique include metal-related artifact or nonlaminar flow creating a signal void, arrhythmias reducing the accuracy of measurements, and lower temporal resolution. In addition, the coronary artery diastolic flow is included in the total regurgitant volume. In the future, evolving techniques such as 4D flow may provide direct flow assessment in regurgitant lesions.[127]

Overall, suggested indications for CMR in prosthetic aortic valve assessment are as follows:

1. Discrepancy in clinical history and echocardiographic findings or when imaging quality from TTE or TEE is suboptimal
2. Cases in which valve area–gradient mismatch is seen on TTE; CMR is additive in assessing anatomic bioprosthetic valve area and ensuring highest velocity captured across the valve
3. Assessment of aortic root in complicated endocarditis (paravalvular extension of disease, pseudoaneurysm or root abscess)
4. Quantitation of AR severity
5. Assessing adverse LV remodeling

Table 8 Parameters for evaluation of the severity of prosthetic aortic valve regurgitation

Parameters	Mild	Moderate	Severe
Valve structure and motion			
Mechanical or bioprosthetic	Usually normal	Abnormal*	Abnormal*
Structural parameters			
LV size	Normal†	Normal or mildly dilated†	Dilated†
Doppler parameters (qualitative or semiquantitative)			
Jet width in central jets, % LVOT diameter, (CD)‡	Narrow (≤25%)	Intermediate (26%-64%)	Large (≥65%)
VC width, cm (CD)	<0.3	0.3-0.6	>0.6
VC area, cm^2 (2D/3D CD)§	<0.10	0.10-0.29	≥0.30
Circumferential extent of PVL, % (CD)¶‖	<10	10-29	≥30
Jet density (CW)	Incomplete or faint	Dense	Dense
Jet deceleration rate (PHT), msec (CW)#	Slow (>500)	Variable (200-500)	Steep (<200)
Diastolic flow reversal in the descending aorta (PW)	Absent or brief early diastolic	Intermediate	Prominent, holodiastolic
Doppler parameters (quantitative)			
Regurgitant volume, mL/beat	<30	30-59	≥60
Regurgitant fraction, %	<30	30-50	≥50

CD, Color Doppler.

*Abnormal mechanical valves: for example, immobile occluder (valvular regurgitation), dehiscence or rocking (paravalvular regurgitation); abnormal biological valves: for example, leaflet thickening or prolapse (valvular regurgitation), dehiscence or rocking (paravalvular regurgitation).

†Applies to chronic, late postoperative AR in the absence of other etiologies.

‡Parameter applicable to central jets and less accurate in eccentric jets; Nyquist limit of 50 to 60 cm/sec.

§The VC area is measured by planimetry of the VC of the jet(s) on 2D or 3D CD images in the short-axis view.

¶Measured as the sum of the circumferential lengths of each regurgitant jet VC (not including the nonregurgitant space between the separate jets) divided by the circumference of the outer edge of the valve.

‖Circumferential extent of PVL best not to be used alone but in combination with VC width and/or area.

#Influenced by LV compliance.

Key Points and Recommendations for Prosthetic Aortic Valves

1. Transthoracic echocardiographic assessment of prosthetic valves in the aortic position can be limited by reverberation and shadowing of the posterior annulus/root. TEE is recommended to improve visualization of the posterior annulus/root when poorly imaged with TTE or if there is concern for posterior annulus/root pathology. CMR and CT can offer additional information in these situations.
2. Dedicated imaging of mechanical prosthetic aortic valve leaflets is recommended using radiologic imaging with CT or fluoroscopy when the range of motion cannot be determined with echocardiography and there is clinical concern for prosthetic aortic valve obstruction.
3. In assessing prosthetic aortic valve stenosis, it is recommended that Doppler insonation be acquired from all possible windows and a small nonimaging probe should be used when possible.
4. In patients with elevated prosthetic aortic valve Doppler gradients, it is recommended that causes such as high-flow states, PPM, supra- or subvalvular obstruction, and pressure recovery be excluded.
5. It is recommended to use at least one highly flow-dependent measurement (e.g., peak velocity, mean gradient) and one less flow-dependent measurement (e.g., EOA, DVI) to assess prosthetic aortic valve stenosis.
6. For TAVI valves, in-stent flow acceleration occurs below the valve and at the level of the cusps. It is recommended that the LVOT diameter and velocity measurements be obtained immediately proximal to the stent to prevent overestimation of the EOA by flow acceleration within the stent.
7. Classification of intra- and paravalvular prosthetic aortic valve regurgitation severity is like that in native valves. If there is a discrepancy between echocardiographic qualitative and semiqualitative AR severity parameters that cannot be explained by image quality, technical, or physiologic factors and prevents consensus grading, then TEE, CMR, or CT is required. These additional imaging modalities can also provide information on the etiology of the PHV dysfunction.

III. EVALUATION OF PROSTHETIC MITRAL VALVES

As with prosthetic aortic valves, the initial assessment of prosthetic mitral valve function begins with knowledge of the type and size of the prosthetic valve implanted.

A. Types of Prosthetic Valves in the Mitral Position

The principal mechanical valve used in the mitral position is a bileaflet valve. Bileaflet mechanical valves are prone to pressure recovery from the small orifice between the two tilting disks, which may result in a slight overestimation of the gradient by Doppler and underestimation of EOA with the continuity equation (Figure 3). Three-dimensional planimetry of the orifice has been shown to correlate well with manufacturer-predicted EOA.[137] The EOA of mechanical mitral valves is in the 2- to 3-cm^2 range and the mean gradient ranges from 2 to 3 mm Hg, with some smaller valves having a gradient of up to 5 to 6 mm Hg at physiologic heart rates (Appendix Table A5).

Mitral bioprosthetic valves are stented only. The classic mitral bioprosthetic valve is a stented heterograft consisting of three biological leaflets reconstructed from either porcine aortic valve or bovine pericardium. The hemodynamics of these surgical valves are similar and dependent on implant size but have an expected EOA of 2.2 to

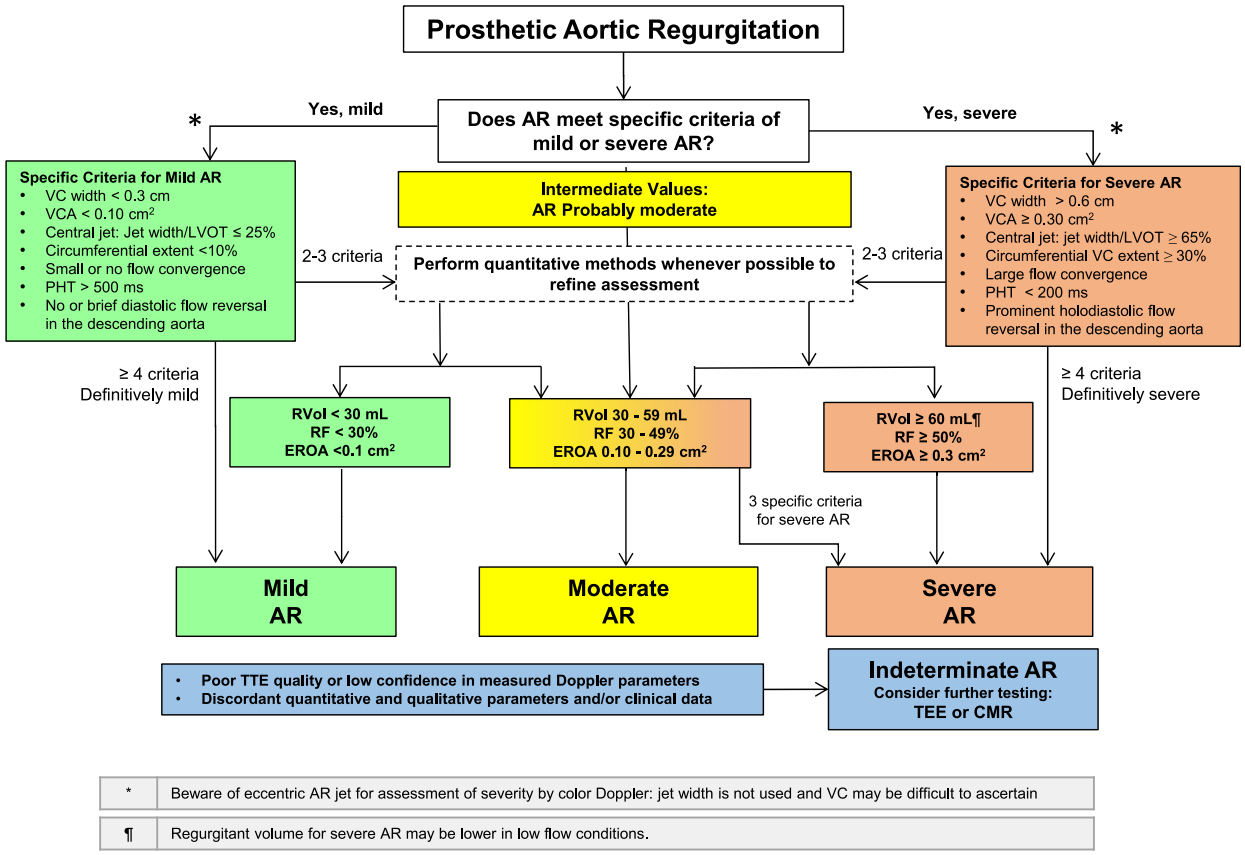

Figure 16 Suggested algorithm to guide integration of multiple parameters of AR severity after aortic valve replacement. Good-quality echocardiographic imaging and complete data acquisition are assumed. If imaging is technically difficult, consider TEE or CMR for evaluation of severity. Regurgitation severity may be indeterminate because of poor image quality, technical issues with data, internal inconsistency among echocardiographic findings, or discordance with clinical findings. *RF*, Regurgitant fraction; *Rvol*, regurgitant volume; *VCA*, VC area.

3.5 cm^2 and a mean gradient of 3 to 5 mm Hg at physiologic heart rates (Table A5).

Only one prosthesis is currently approved for percutaneous placement in the mitral position. The Edwards SAPIEN 3 valve is FDA approved for percutaneous placement in the mitral position for ViV and valve-in-ring (as of July 2021) implantation. At the time of these guidelines, it remains off label for valve–in–mitral annular calcification. The hemodynamics of the SAPIEN 3 valve in the mitral position[138-140] are similar to those of bioprosthetic valves listed above and are summarized in Appendix Table A6. At the time of writing, there are several investigational percutaneous mitral valve replacements as well as systems for mitral valve repair. One of these has recently published excellent 2-year outcomes[141]; however, long-term durability has not been established, and none of these valves are currently approved by the FDA. Therefore, for percutaneous mitral valves, we will focus our discussion on the SAPIEN 3 valve (Appendix Table A6).

B. Echocardiographic Evaluation of Prosthetic Mitral Valves

i. **Evaluation of prosthetic mitral valve function:** Comprehensive evaluation of prosthetic mitral valves with echocardiography is summarized in Table 10 and includes the following: heart rate; peak early velocity; mean pressure gradient; PHT; a statement on the presence or absence of significant regurgitation, LV, right ventricular (RV), and left atrial size; and, if possible, estimation of PA pressure and right atrial (RA) pressure. EOA and DVI are particularly important for evaluation of stenosis but can also provide a clue to the presence of significant MR, which may increase the gradient and DVI because of high flow through the valve and lower systemic output through the LVOT.

Diagnostic criteria of prosthetic mitral stenosis by Doppler echocardiography remain similar to the 2009 guidelines (Table 11). An example of severe prosthetic mitral stenosis is shown in Figure 19. Reporting the heart rate at which Doppler measurements are performed is important. The main criteria for the diagnosis of significant mitral stenosis are a mean gradient >10 mm Hg at a normal heart rate, a PHT >200 msec, a DVI >2.5, and an EOA <1 cm^2.[33,52,142,143] The, DVI derived as VTI_{PrMV}/VTI_{LVOT} has been shown to be the most specific and sensitive Doppler parameter for stenosis in one study.[143] Derivation of EOA is covered earlier in the general section on Doppler. For the mitral valve,

$$EOA = \text{stroke volume}/VTI_{PrMV},$$

where VTI_{PrMV} is the VTI through the prosthetic mitral valve, and stroke volume is measured through the LVOT when there

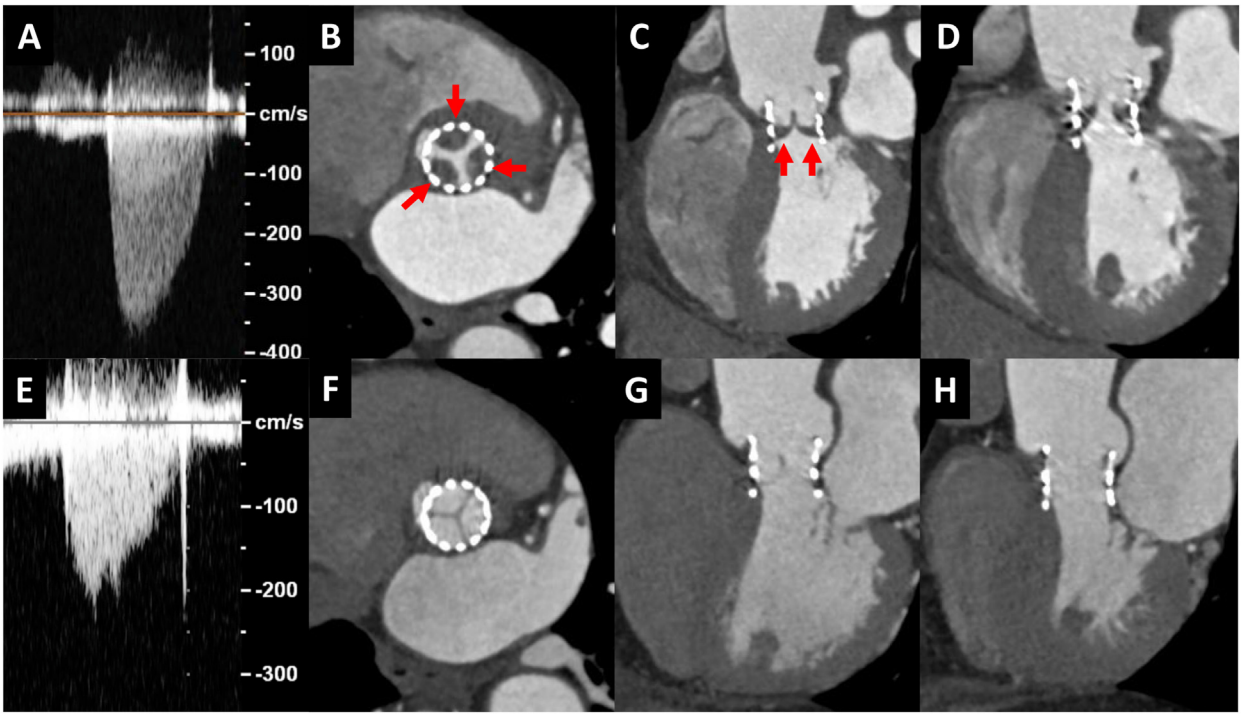

Figure 17 **(Panel A)** Increased mean gradient (28 mm Hg) and peak velocity of 3.6 m/sec across a 23-mm SAPIEN 3 valve were noted approximately 4 months following TAVI. Cardiac CT demonstrated hypoattenuated leaflet thickening (HALT; *red arrows*) with 50% to 75% leaflet involvement **(B, C)** and hypoattenuation affecting motion **(D)**. After initiation of anticoagulation, mean gradient decreased to 14 mm Hg **(E)**. Repeat cardiac CT demonstrated resolution of HALT **(F, G)** with normal leaflet mobility **(H)**.

is no significant AR. Causes of prosthetic mitral stenosis are valve degeneration, valve thrombosis, pannus formation, and large vegetations. Although Doppler echocardiography is the mainstay of the diagnosis of stenosis and obstruction, TEE provides an en face view of the mitral valve, which is essential for confirming the diagnosis and evaluating the mechanism of dysfunction (Figure 19). Other multimodal imaging plays a complementary role (see below).[77,144]

PPM is significantly less common in the mitral compared with the aortic position. However, it may be underdiagnosed. Criteria for PPM are detailed in Table 7. The clinical outcomes may actually be worse when present in the mitral position as opposed to the aortic, particularly in patients <70 years of age.[145]

ii. **Evaluation of prosthetic MR:** TTE is indicated for routine surveillance and may be the initial test of choice when mitral prosthetic valve dysfunction is suspected, but visualization of MR jets by TTE is frequently limited by acoustic reverberation or shadowing from the mitral prosthesis (Figure 6). The parasternal window is often the optimal view for evaluation of prosthetic MR jets, although apical views may be helpful to identify a suspected eccentric regurgitant jet or paravalvular regurgitation.[146] Apical views may also provide better visualization of the prosthetic valve leaflets for identification of vegetation, thrombus, pannus, or leaflet degenerative changes.

Given that transthoracic echocardiographic visualization of prosthetic or paravalvular MR is often limited, it is particularly important to look for indirect spectral Doppler evidence of severe MR. Criteria suggesting significant MR are detailed in Table 12 and include the following:

1. A dense CW MR jet
2. An elevation of the mitral E velocity (>1.9 m/sec in mechanical valves)[1]
3. Low systemic output and VTI_{LVOT} despite a hyperdynamic left ventricle
4. An elevated VTI_{PrMV}/VTI_{LVOT} ratio (>2.5)
5. A large zone of systolic flow convergence seen on the LV side of the mitral prosthesis
6. A significant rise in the PA pressure compared with a previous study

When significant prosthetic or paravalvular MR is suspected on the basis of these parameters, TEE is often helpful to definitively visualize prosthetic leaflet morphology and leaflet or disk mobility and to quantify MR severity (Figure 20). Combined transthoracic and transesophageal echocardiographic parameters and criteria for assessing MR severity are detailed in Table 13. A suggested algorithm for evaluation of MR severity with echocardiography is shown in Figure 21.

iii. **Role of TEE:** TEE has a very important role in the evaluation of prosthetic mitral valves. The prosthetic mitral valve can be visualized en face, allowing thorough assessment of its structure, mobility of the leaflets or the occluder of mechanical valves, and identification of any dehiscence or regurgitation. TEE is crucial in assessing prosthetic valve regurgitation, particularly in mechanical valves where acoustic reverberation and shadowing on TTE is the rule. Three-dimensional TEE has a pivotal role for diagnosing prosthetic mitral valve pathology by providing a full view of the valve, its annulus, and adjacent structures (Figures 19, 20, and 22). The comparative advantages and limitations of TEE and other modalities are detailed in Tables 2 and 3.

C. Role of CT in the Evaluation of Prosthetic Mitral Valves

i. **Valve stenosis:** Cardiac CT is a valuable complementary tool for the evaluation of prosthetic mitral valve stenosis given the high spatial resolution and 3D volume acquisition. Retrospective electrocardiographically gated acquisition is typically performed for prosthetic valve evaluation to allow optimal visualization of the prosthetic valve throughout the cardiac cycle; however, the radiation dose is higher than with prospective electrocardiographically

Table 9 Potential role of CT in various complications of prosthetic aortic valves

Complication	Potential role of MDCT
Mechanical leaflet dysfunction	• Can evaluate motion and opening angle of mechanical leaflet(s) and compare it with manufacturer's specifications • Normal opening angle is 73°-90° for bileaflet valves and 60°-80° for monoleaflet valves
PPM	• Small EOA, normal leaflet motion, lack of masses, and a small geometric orifice area[115]
Structural failure	• Detects valvular calcification despite normal gradients[116]
Prosthesis dehiscence	• Identifies a gap between the annulus and prosthesis sewing ring • For the aortic valve prosthesis, excessive sewing ring motion with rocking >15° implies significant paravalvular regurgitation[1]
PVL	• Contrast material–filled channel in the paravalvular region that connects the lumina proximal and distal to the valve (e.g., for the aortic valve, aorta, and LVOT) • Helps distinguish from pseudoaneurysm and abscess[117] • Helps distinguish from pledget material (the HU of a pledget are significantly higher than those of contrast material [383-494 vs 202-367 HU][118])
Endocarditis	• Large vegetations (>1 cm) seen on the valve leaflet or sewing ring, usually on the ventricular side of the aortic valve[119]; generally inferior to TEE for small vegetations (<4 mm) and perforations (<2 mm) but superior in evaluating paravalvular and extracardiac extension[120] • CT may show other manifestations of infection such as aortic wall thickening, mediastinal gas, fat stranding, collections[119,120]
Pseudoaneurysm	• Contrast material–filled saccular or fusiform outpouchings arising from the annulus, which may contain thrombus • With infection, adjacent soft tissue inflammatory changes may be seen
Thrombus	• Irregular mass commonly mobile, without enhancement, attached to a PHV • Distinguishing from pannus is important • Thrombus is seen more commonly early after surgery, adherent usually to the aortic side of an aortic valve prosthesis, and has lower attenuation (<200 HU) • Pannus is seen late after surgery, is usually located on the ventricular side, and has higher attenuation (>200 HU)[121] • A cutoff of 145 HU is useful in distinguishing thrombus from pannus, with 87.5% sensitivity and 96% specificity[121] • CT allows prediction of response to thrombolysis. Complete lysis is more common in thrombi with attenuation less than 90 HU vs 90-145 HU[121]
HALT and HAM	• Helps identify HALT, with or without restricted motion, which benefits from anticoagulation[122]
Aortic dissection	• Intimal flap with true and false lumina, internal displacement of intimal calcification, delayed enhancement of the false lumen, widening of the aorta and mediastinum, ulcer-like contrast material projections, and compression of the true lumen[123]

HALT, Hypoattenuated leaflet thickening; *HAM*, hypoattenuation affecting motion; *HU*, Hounsfield unit; *MDCT*, multidetector CT.

triggered acquisitions.[147-149] If there are no contraindications, β-blockers can be administered to decrease the heart rate to a goal of 60 beats/min to decrease motion artifacts. Images are reconstructed at 5% to 10% increments of the R-R interval to allow evaluation of the prosthetic valve throughout the cardiac cycle.

Mechanical valve opening and closing angles can be evaluated on non-contrast-enhanced acquisitions such as cine fluoroscopy, but the etiology of limited valve opening cannot be determined.[147] Contrast-enhanced acquisitions can assess bioprosthetic leaflet degeneration (thickening and calcification), leaflet or disk occluder mobility, calcification of the bioprosthetic ring, thrombus, pannus, or vegetation.[150] The geometric orifice area of the prosthetic mitral valve can be measured using multiplanar reconstruction.[151] In mechanical valves, the opening and closing angles in addition to the geometric orifice area can be measured.[152] TEE and CT are more accurate in identifying the etiology of prosthetic mitral stenosis compared with TTE; CT is more sensitive in the identification of pannus as the cause of valve obstruction.[77] There are technical limitations to CT as blooming and beam-hardening artifacts from the valve ring or disk occluders can impair evaluation. These metallic artifacts can be reduced by the use of a higher tube voltage and iterative reconstruction.[153]

ii. **Valve regurgitation:** Excessive rocking of the mitral valve prosthesis during the cardiac cycle is seen in valvular dehiscence. The size of PVL on CT correlated with regurgitant grade on echocardiography in early observations, most of which involved significant regurgitation.[78] Small PVLs can be obscured because of metallic artifacts from the prosthetic ring or disk occluders or confused with a pledget. In these situations, confirmation or exclusion of regurgitation with Doppler echocardiography would be important. Pledgets can be identified also with the addition of a noncontrast acquisition or careful inspection of the attenuation on the contrast-enhanced acquisition, as a felt pledget may have a higher attenuation than contrast-enhanced blood.[153] Regurgitant orifice area can be measured in a systolic phase, with good agreement with TEE and surgical findings reported.[154]

D. Role of CMR in the Evaluation of Prosthetic Mitral Valves

i. **Valve stenosis:** Assessment of mitral valve stenosis by CMR can be performed by three methods: visual assessment of bioprosthetic cusps or occluder excursion, direct planimetry of the valve orifice of a bioprosthetic valve, or

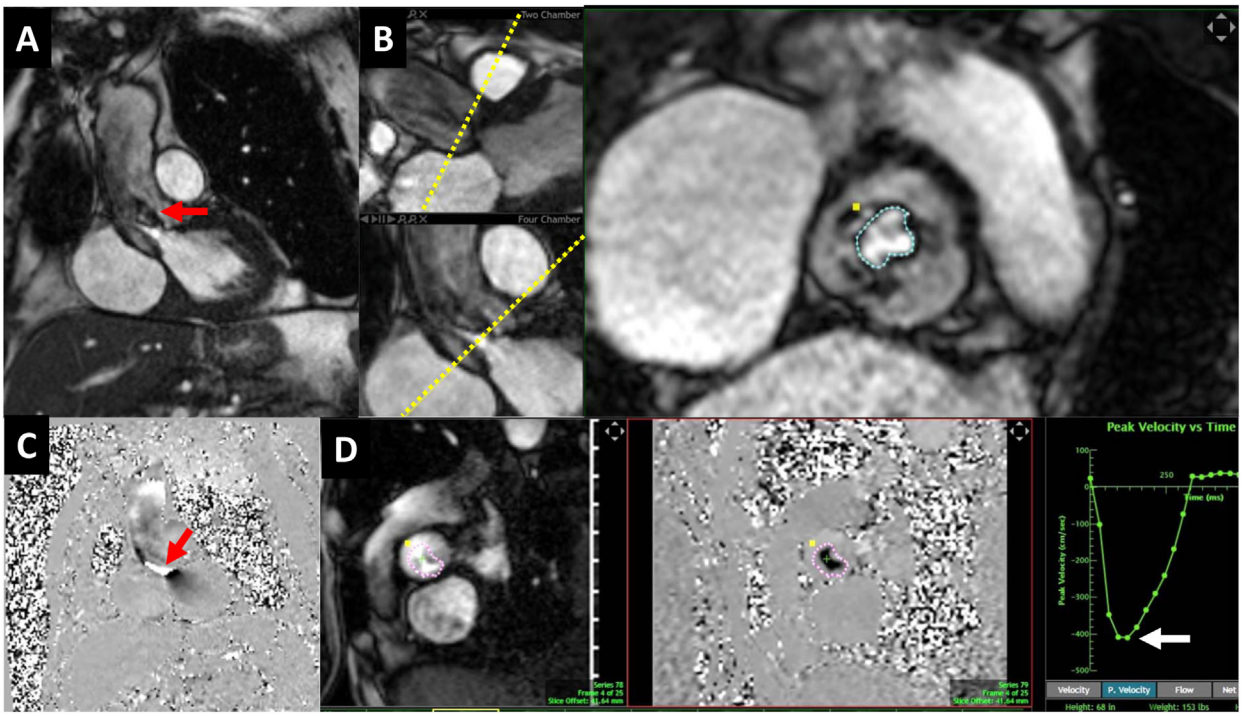

Figure 18 A case of bioprosthetic aortic stenosis evaluated using CMR. **(A)** Aortic long-axis view on steady-state free precession cine CMR shows spin dephasing in systole consistent with high velocities from the stenosis. Note the lack of significant metallic artifact. **(B)** Double orthogonal view at the valve leaflet tips during maximal systolic opening shows a corresponding short-axis view of the prosthetic aortic valve and evidence of stenosis with an anatomic valve area of 0.9 cm^2. **(C, D)** Phase-contrast imaging shows dephasing at the aortic valve level. Magnitude and phase contrast using a double orthogonal plane at the aortic valve level with a velocity-encoded CMR velocity of 450 cm/sec shows no aliasing and a peak transvalvular velocity of 4.1 m/sec (*white arrow* on the flow graph).

measurement of peak velocity through the prosthesis using phase-contrast imaging. A combination of three long-axis and short-axis stack images should be used for visual assessment. This may identify impaired excursion of the mechanical PHV occluders or leaflets of a bioprosthesis and demonstrate a potential cause of stenosis including pannus, thrombosis, or endocarditis. The primary limitation remains susceptibility artifact, especially with mechanical valves. For quantification of stenosis severity, the anatomic orifice area can be measured on bioprosthetic valves.[86,87] If artifact is present that limits assessment of the leaflets, fast-gradient echo sequences could be considered. The

Table 10 Echocardiographic parameters to evaluate prosthetic mitral valve function (stenosis or regurgitation)

Doppler echocardiography of the mitral valve	Peak early velocity
	Mean pressure gradient
	Heart rate at the time of Doppler
	PHT
	DVI (VTI_{PrMV}/VTI_{LVOT})
	EOA*
	Presence, location, and severity of regurgitation
Other pertinent echocardiographic parameters	LV size and function
	Left atrial size
	RV size and function
	Estimation of PA pressure

VTI_{PrMV}, VTI through the prosthetic mitral valve.
*Using the continuity equation.

Table 11 Doppler findings suggestive of prosthetic mitral valve stenosis

	Normal*	Possible stenosis†	Suggests significant stenosis*†
Peak velocity, m/sec‡§	<1.9	1.9-2.5	≥2.5
Mean gradient, mm Hg‡§	≤5	6-10	>10
VTI_{PrMV}/VTI_{LVOT}‡§	<2.2	2.2-2.5	>2.5
EOA, cm^2	≥2.0	1-2	<1
PHT, msec	<130	130-200	>200

VTI_{PrMV}, VTI through the prosthetic mitral valve.
*For either mechanical or bioprosthetic valves; diagnostic accuracy is best if most of the parameters listed are normal or abnormal, respectively.
†Values of the parameters should prompt a closer evaluation of valve function and/or other considerations such as increased flow, increased heart rate, or PPM.
‡These parameters are also abnormal in the presence of significant prosthetic MR.
§Slightly higher cutoff values than shown may be seen in some bioprosthetic valves.

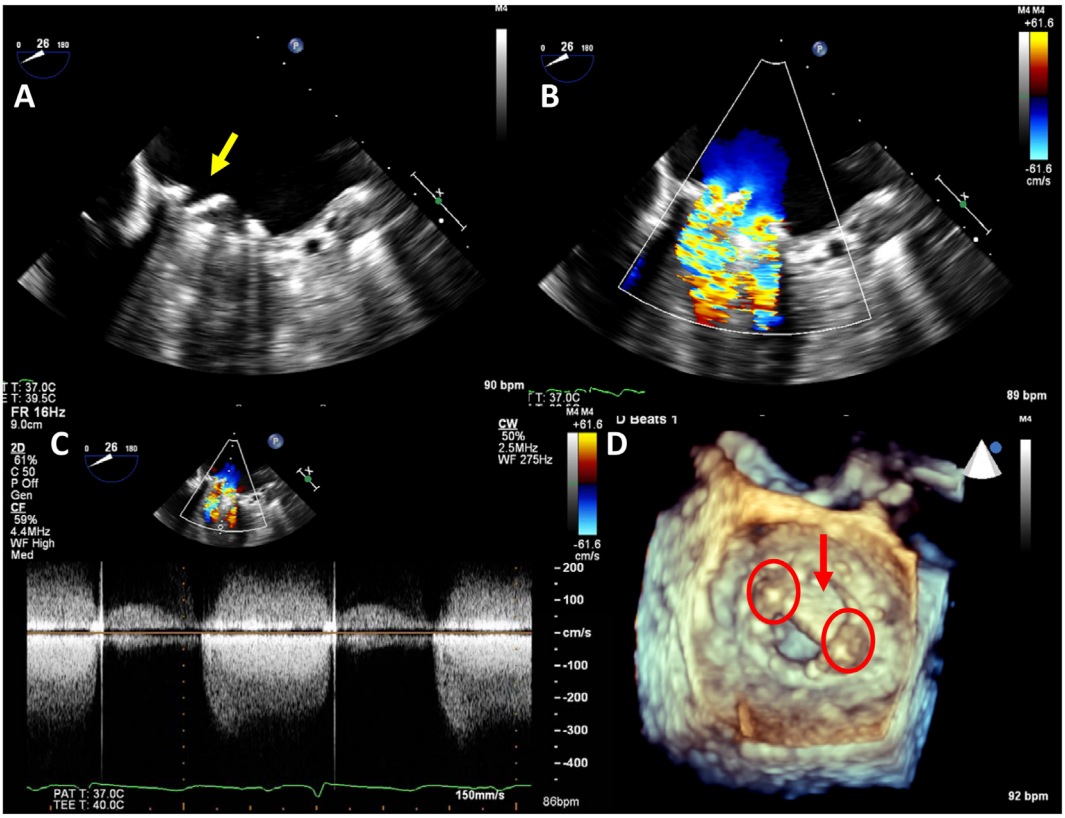

Figure 19 A case of severe mechanical mitral valve stenosis secondary to thrombus formation. **(A)** Two-dimensional TEE, mideso-phageal view in diastole, shows restricted disk motion (*yellow arrow*) with high inflow color aliasing **(B)** and severe prosthetic stenosis (mean gradient, 29 mm Hg at a heart rate of 86 beats/min) on CW Doppler **(C)**. **(D)** Real-time 3D TEE of the mechanical mitral valve (en face view) showing restricted disk motion in diastole (*red arrow*) and two immobile masses (*circles*) along the hinge points of the mechanical valve.

major limitation with this technique is the assumption that the narrowest area is in a single plane, which often is not the case. However, prior small studies have shown high feasibility, good interobserver variability, and agreement with CMR mitral valve planimetry and echocardiography-measured mitral valve area using PHT.[86] Another potential method to assess bioprosthetic valve stenosis is to obtain through-plane phase-contrast images perpendicular to the transprosthetic inflow jet at the level of the valve tips. The Nyquist limit should be carefully chosen to ensure lack of aliasing. Planimetry of the flow area will provide measurement of peak velocity, with recent in vitro data demonstrating the ability to measure VTI and to calculate mitral valve area.[87] The major challenge with this approach is the through-plane motion of the annulus, making it challenging to measure velocity at the same location over the cardiac cycle. Furthermore, this approach is limited with mechanical valves because of susceptibility artifacts. Overall clinical validation of methods to assess prosthetic mitral stenosis remains limited.

ii. **Valve regurgitation:** Prosthetic valve regurgitation can be visually assessed by the presence of CMR-induced intervoxel dephasing in the left atrium on SSFP cines.[155] The jet size can be graded in relation to the area of the left

Table 12 Transthoracic echocardiographic findings suggestive of significant prosthetic MR in mechanical valves with normal PHT

Finding	Sensitivity	Specificity	Comments
Peak mitral velocity ≥1.9 m/sec*	90%	89%	Also consider high flow, PPM
$VTI_{PrMV}/VTI_{LVOT} \geq 2.5$*	89%	91%	Measurement errors increase in atrial fibrillation because of difficulty in matching cardiac cycles; also consider PPM
Mean gradient ≥ 5 mm Hg*	90%	70%	At physiologic heart rates; Also consider high flow, PPM
Maximal TR jet velocity >3 m/sec*	80%	71%	Consider residual postoperative pulmonary hypertension or other causes
LV stroke volume derived by 2D or 3D echocardiography is >30% higher than systemic stroke volume by Doppler	Moderate sensitivity	Specific	Validation lacking; significant MR is suspected when LV function is normal or hyperdynamic and VTI_{LVOT} is small (<16 cm)
Systolic flow convergence seen in the left ventricle toward the prosthesis	Low sensitivity	Specific	Validation lacking; technically challenging to detect readily

VTI_{PrMV}, VTI through the prosthetic mitral valve.
*Data from Olmos *et al*.[33] When both peak velocity and VTI ratio are elevated with a normal PHT, specificity is close to 100%.

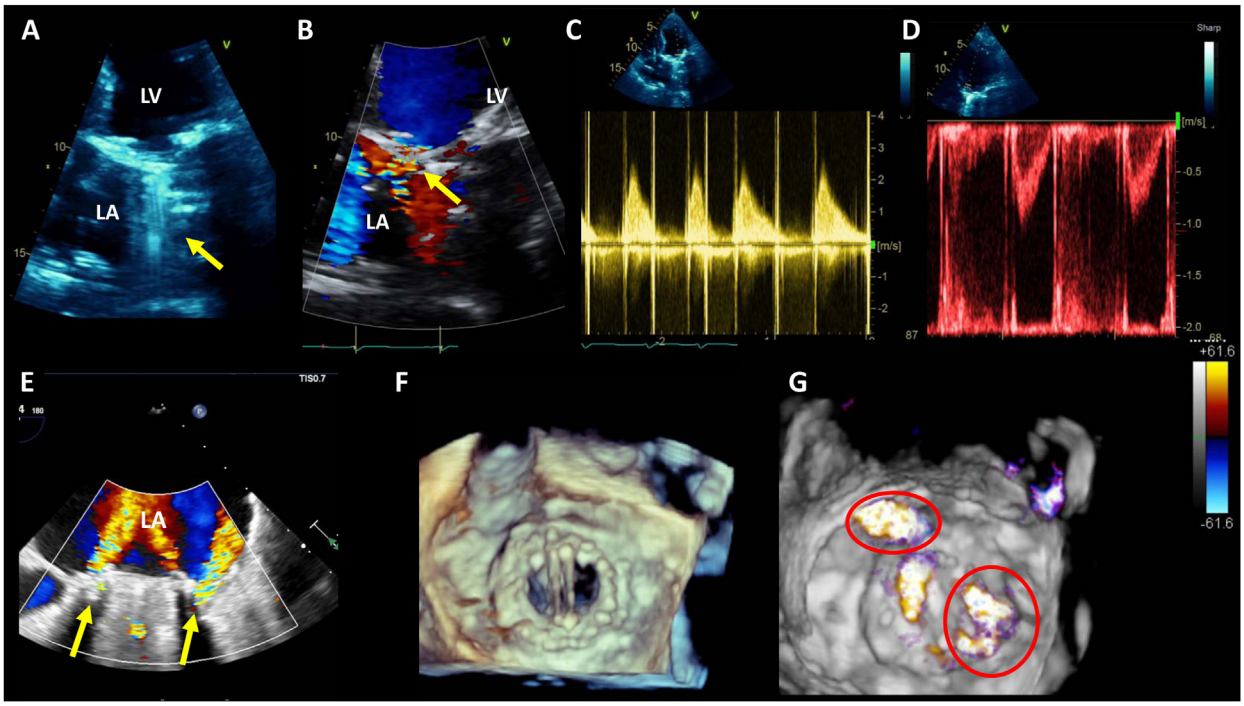

Figure 20 A case of paravalvular MR in a mechanical valve. **(A)** Apical four-chamber view shows acoustic reverberation behind the mechanical mitral valve (MV) in systole (*arrow*). **(B)** Color Doppler shows eccentric MR (*arrow*); artifact makes its origin and extent difficult to ascertain. **(C)** Spectral Doppler shows elevated velocities and gradient across the valve (mean gradient, 9 mm Hg at a heart rate of 87 beats/min) with VTI_{MV} of 52 cm. **(D)** Spectral PW Doppler in the LVOT shows reduced velocity and VTI of 17 cm. A ratio of prosthetic MV VTI to VTI_{LVOT} of 3 alerts to the presence of concomitant regurgitation in the absence of mitral stenosis inferred from a normal PHT. **(E)** Midesophageal TEE shows two paravalvular regurgitant jets (*arrows*). **(F)** Three-dimensional TEE shows a wide-open valve in diastole. **(G)** Three-dimensional TEE with color shows two PVLs, one at 11 o'clock and the other at 5 o'clock (*circles*). The third more central jet is a washing jet, as seen in **(E)**. *LA*, Left atrium; *LV*, left ventricle

atrium (mild, less than one third; moderate, one third to two thirds; severe, more than two thirds) and has good agreement with echocardiography, especially for more than moderate MR.[155] Although intervoxel dephasing may be the first sign of bioprosthetic MR, it may not be reliably identified, because of susceptibility artifacts from the PHV. The cine images may also help identify mechanisms of regurgitation such as dehiscence, vegetation, or abscess. However, the strength of CMR is in quantitative assessment of MR by measurement of regurgitant volume and fraction. This is best achieved using an indirect method. Ideally this should include planimetry of the left ventricle using SSFP cines to measure LV total stroke volume; aortic forward stroke volume is calculated using through-plane phase-contrast images at the level of the proximal ascending aorta. The difference between LV total stroke volume and aortic forward stroke volume is the MR volume.[88] Dividing the regurgitant volume by total LV stroke volume provides the regurgitant fraction. If aortic phase-contrast data are not available, through-plane phase-contrast images at the pulmonary valve can also be used. A potential limitation of this strategy is the risk for susceptibility artifact at the basal short-axis cine images from the PHV, reducing the accuracy of the LV total stroke volume quantification. Finally, in the absence of phase-contrast data and tricuspid, pulmonary, or aortic regurgitation, the difference between LV and RV total stroke volumes can be used to quantify regurgitant volume and fraction.[88]

Key Points for Assessing Prosthetic Mitral Valves

1. Assessment of prosthetic mitral valve function begins with knowledge of the type and size of the prosthetic valve implanted.
2. Structural and hemodynamic evaluation with TTE and TEE provides key understanding of the function of the prosthetic mitral valve.
3. From the Doppler interrogation of prosthetic mitral valves, peak velocity, mean gradient, PHT, EOA or DVI, and heart rate should be measured whenever feasible and reported.
4. Because of shadowing and flow masking in the left atrium, particularly in mechanical mitral valves, significant prosthetic MR may be missed with color Doppler on TTE. Clues for significant MR from spectral Doppler include increased mitral peak early velocity, mean gradient, DVI, and a relatively low systemic stroke volume in relation to total LV stroke volume. TEE is indicated in suspected cases of significant MR.
5. TEE (2D and 3D) provides an en face view of the prosthetic mitral valve which allows the evaluation of valve structure, occluder motion, and the presence, location, and extent of valvular regurgitation; the latter are crucial in guiding interventional procedures.
6. CT and CMR provide complementary evaluation of prosthetic mitral valves, particularly when further information is needed regarding prosthetic structure, function, or associated complications. CT allows the evaluation of valve structure and mechanical valve occluder motion, as well as the localization of significant paravalvular regurgitation and identification of associated complications. CMR allows the evaluation of valvular structure of bioprosthetic valves and is particularly helpful in quantitation of prosthetic MR and LV remodeling.

Table 13 Echocardiographic criteria for severity of prosthetic mitral valve regurgitation using findings from TTE and TEE

	Mild	Moderate	Severe
Structural parameters			
LV size	Normal*	Normal or dilated	Usually dilated†
Prosthetic valve‡	Usually normal	Abnormal§	Abnormal§
Doppler parameters			
Color flow jet area‡¶	Small, central jet (usually <4 cm^2 or <20% of LA area)	Variable	Large central jet (usually >8 cm^2 or >50% of LA area) or variable size wall-impinging jet swirling in left atrium
Flow convergence‖	None or minimal	Intermediate	Large
Jet density (CW)‡	Incomplete or faint	Dense	Dense
Jet contour (CW)‡	Parabolic	Usually parabolic	Early peaking: triangular
Pulmonary venous flow‡	Systolic dominance#	Systolic blunting#	Systolic flow reversal**
Quantitative parameters††			
VC width (cm)‡	<0.3	0.3-0.69	≥0.7
RVol, mL/beat	<30	30-59‡‡	≥60‡‡
RF, %	<30	30-49	≥50
EROA, cm^2	<0.20	0.20-0.39	≥0.40

MV, Mitral valve; *RF*, regurgitant fraction; *RVol*, regurgitant volume.
*LV size applied only to chronic lesions with progressive enlargement.
†In the absence of other etiologies of LV enlargement and acute MR.
‡Parameter may be best evaluated or obtained with TEE, particularly in mechanical valves.
§Abnormal mechanical valves: for example, immobile occluder (valvular regurgitation), dehiscence or rocking (paravalvular regurgitation); abnormal biological valves: for example, leaflet thickening or prolapse (valvular), dehiscence or rocking (paravalvular regurgitation).
¶At a Nyquist limit of 50-60 cm/sec.
‖Minimal and large flow convergence defined as a flow convergence radius <0.4 and ≥0.9 cm for central jets, respectively, with a baseline shift at a Nyquist limit of 40 cm/sec; cutoffs for eccentric jets may be higher.
#Unless other reasons for systolic blunting (e.g., atrial fibrillation, elevated left atrial pressure).
**Pulmonary venous systolic flow reversal is specific but not sensitive for severe MR.
††These quantitative parameters are less well validated than in native MR.
‡‡Regurgitant volume cutoffs may be lower in low-flow conditions.

IV. EVALUATION OF PROSTHETIC PULMONARY VALVES

The native pulmonary valve is located anterior and superior to the aortic valve and is best visualized with TTE using the RVOT view from the parasternal window (modified from the parasternal short-axis view at the aortic valve level) or subcostal window. The prosthetic valve is not always in the same position as the native pulmonary valve, especially when a conduit is involved. It is important to understand that off-axis views may be necessary when using echocardiography. CT and CMR provide improved spatial resolution and should be used to complement the echocardiographic findings. When assessing the pulmonary valve prosthesis, additional information on anatomy of the RVOT and PA as well as RV size, function, and pressures are important to include.

A. Surgical and Transcatheter PVR

The native diseased pulmonary valve may be replaced either by a valved conduit for complete repair of a congenital defect or by a prosthetic valve without a conduit in isolated valve pathology. The most common indication for a valved conduit is tetralogy of Fallot. Other indications include the Rastelli procedure (transposition of the great arteries with ventricular septal defect) or as part of a Ross procedure (congenital aortic valve stenosis) or Yasui repair (interrupted aortic arch with diminutive ascending aorta). The valved conduit is generally a biologic tissue (e.g., homograft, xenograft). Stented biologic prostheses are generally implanted for pulmonary valve regurgitation, which most commonly occurs in patients who have previously undergone RVOT reconstruction.[156]

Transcatheter PVR was first reported in 2000 and has since become a viable alternative to surgical PVR in select patients.[157] Outcomes for both types of interventions are favorable and comparable, with transcatheter PVR associated with shorter hospital stays and periprocedural complications but higher rates of endocarditis.[158] The number of PVR procedures has increased over the years, with a consistently increasing trend in surgical PVR.[159] Additionally, the age at PVR is markedly heterogeneous among centers across the United States, with administrative data indicating an overall increase in younger patients receiving a PVR over time.[160] Trends suggest that more absolute numbers of adult patients are likely to present for evaluation of pathologic complications of replaced prostheses. It is important to understand the types of surgical and transcatheter replacements to better understand the risk for complications.

B. Evaluation of Prosthetic Pulmonary Valve Stenosis

i. **Echocardiographic and Doppler evaluation:** When characterizing the severity of prosthetic stenosis, it is important to remember that high flow velocities may be encountered in locations other than the prosthetic valve. Branch vessel stenosis or conduit edge stenosis may also be present

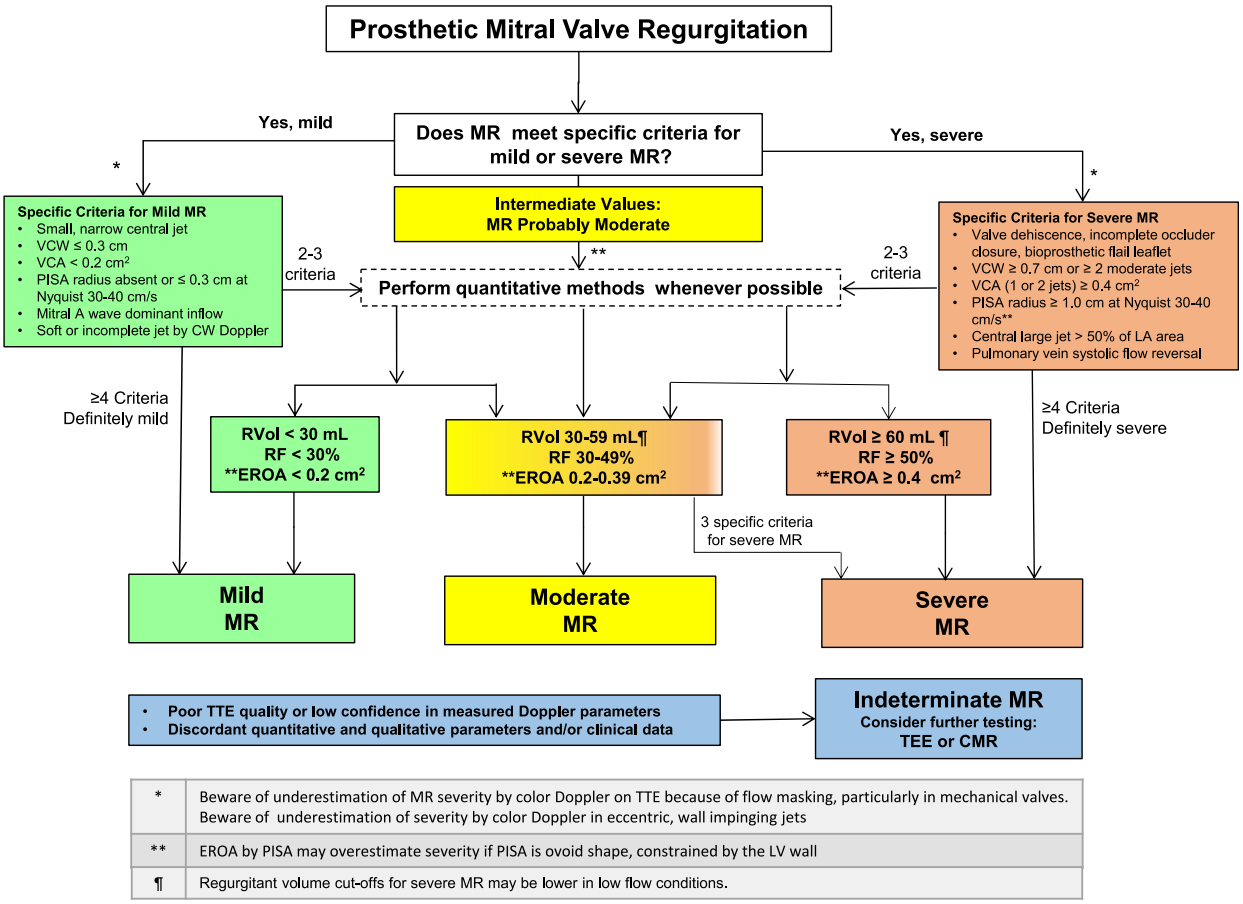

Figure 21 Suggested algorithm to guide integration of multiple parameters of MR severity after mitral valve replacement. Good-quality echocardiographic imaging and complete data acquisition are assumed. If imaging is technically difficult, consider TEE or CMR for evaluation of severity. MR severity may be indeterminate because of poor image quality, technical issues with data, internal inconsistency among echocardiographic findings, or discordance with clinical findings. *LA*, Left atrial; *PISA*, proximal isovelocity surface area; *RF*, regurgitant fraction; *Rvol*, regurgitant volume; *VCA*, VC area; *VCW*, VC width.

and confound CW Doppler interrogation of velocities across the prosthetic valve. Previous ASE guidelines have described the general imaging considerations and challenges of evaluating PVR, including the unconventional shape of the RVOT, the location of the prosthesis, and association with surgically placed conduits.[1] Echocardiographic assessment of valve obstruction should include (1) characterization of the type and size of prosthesis as noted in Table 14, (2) observation of qualitative indicators of obstruction (e.g., thrombus, pannus), (3) quantitation of severity of stenosis, and (4) any changes from previous assessments in serial examinations. In addition, RV systolic pressure should be determined using the jet of TR, if present. Of note, PA systolic pressure in the presence of PVR stenosis is the difference between RV systolic pressure and the gradient across the obstructed valve. Biologic prostheses remain the most common type of PVR. However, these valves are likely to eventually fail and require replacement. Mechanical prostheses are infrequently implanted in this position, thus data on pathology affecting these valves is sparse. Given that a younger age at PVR is prognostic of prosthetic valve failure and that more PVR procedures are being performed in younger individuals, prosthetic pulmonary valve stenosis will become more common.[161] Prosthetic valve failure or dysfunction predominantly manifests as stenosis rather than regurgitation, with an approximately 80% incidence within 10 years of initial implantation.[161] When endocarditis occurs in PVR or conduits, obstruction at the time of diagnosis is more common than severe regurgitation: 53% vs 29%, respectively.[162] Identifying the location of stenosis is important, as the obstruction may occur further along a conduit or in the PA rather than at the valve. PW Doppler is helpful in determining the precise location of obstruction. Narrowing of the conduit and impact on the right ventricle are also indicators of an obstructive lesion. Quantitative parameters are generally limited to peak velocity and mean gradient (Figure 23). Interestingly, there are data to suggest that normally functioning mechanical prostheses are more likely to have lower peak velocity and mean gradient compared with biologic valves in the pulmonary position.[163] Indicators of prosthetic stenosis are provided in Table 15.

ii. **Role of TEE and 3D:** TEE can be challenging when evaluating a PVR, as the pulmonary valve is an anterior structure and if there is a conduit, the location is atypical. Classically, TEE of the pulmonary valve is in the midesophageal view with the transducer angle at 50° to 70° or from the deep transgastric view with transducer angle approximately 50° to 90°.[164] It is helpful to use color Doppler to locate the prosthesis and to pan from 0° to 90° to find the best angle, especially in congenital heart disease (CHD). PW and CW Doppler are important to evaluate for valve or conduit stenosis. Live 3D or 3D zoom using the midesophageal view with the transducer angle at 50° to 70° can be used to display the en face view of the pulmonary valve from the PA side or the RVOT side with rotation to display the anterior leaflet at the 12 o'clock position.[26] Multiplane reconstruction of the 3D data set can quickly be used to evaluate the commissures of the three leaflets for calcification or fusion in addition to tracing the valve orifice.[165] For percutaneous pulmonary valve reimplantation, ICE provides better visualization of the homograft or conduit and may identify infective endocarditis associated with the prosthetic valve.[166,167]

iii. **Role of CMR:** Cine imaging with SSFP or gradient echo allows visualization of the pulmonary prosthesis, the right ventricle, and the PA with its bifurcation. Black blood imaging or gated turbo (fast) spin-echo can be

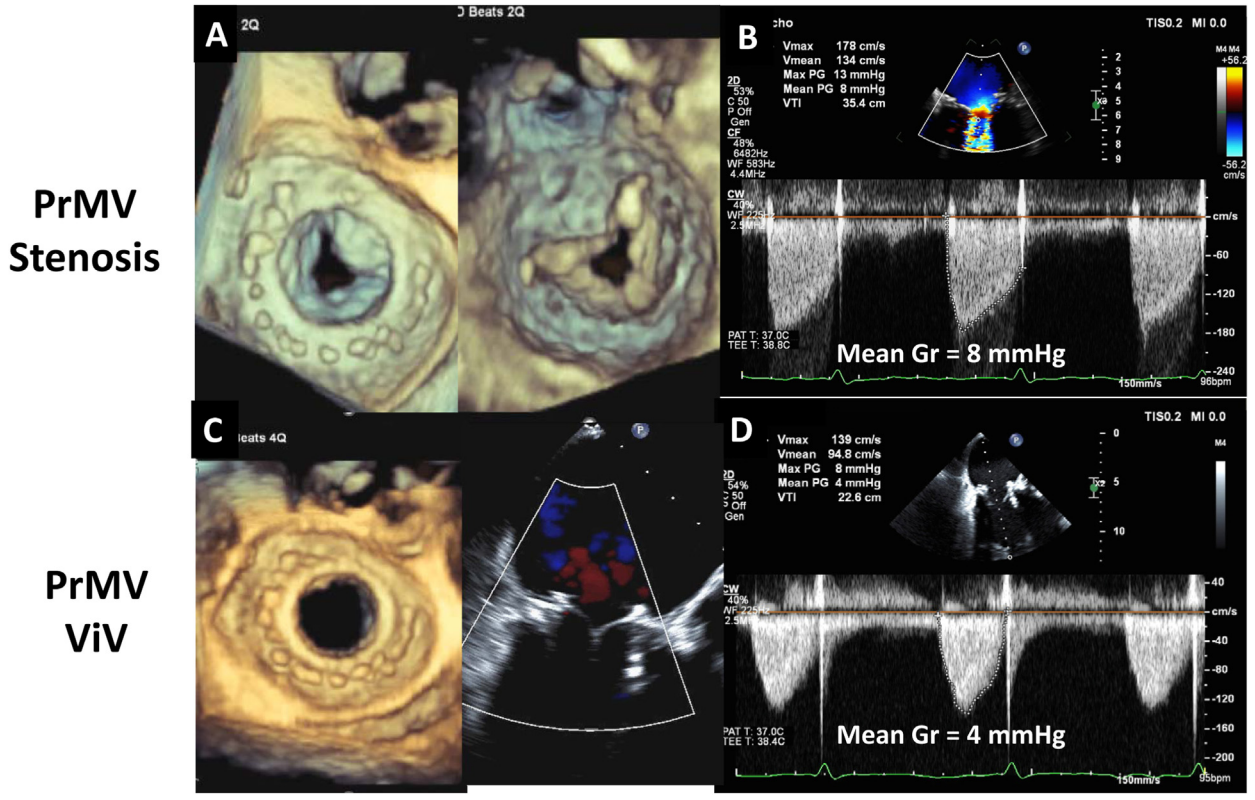

Figure 22 Transesophageal echocardiographic images of a bioprosthetic mitral valve (PrMV) stenosis at baseline and after transcatheter ViV insertion. Baseline 3D transesophageal views **(A)** show thickened leaflets with severely restricted opening in diastole and a mean diastolic gradient (Gr) of 8 mm Hg. **(C)** After transcatheter ViV deployment, the transcatheter valve is well seated with normal leaflet opening in diastole, no significant prosthetic or paravalvular regurgitation, and a mean transvalvular Gr of 4 mm Hg **(D)**. *Max*, Maximal; *PG*, pressure gradient; *Vmax*, maximal velocity; *Vmean*, mean velocity.

used if there is stent artifact and allows assessment of the vessel, as it has decreased sensitivity to metal artifacts, with the limitation of being a static image.[168] Through-plane phase-contrast imaging through the prosthesis allows assessment of the peak velocity through the valve, conduit, and/or the main PA or PAs separately. If there is a stent artifact, phase contrast can be placed just proximal and distal to the stent artifact.[169] The peak velocity generally is slightly lower than that obtained by Doppler echocardiography at an optimal angle. Contrast-enhanced magnetic resonance angiography obtains a 3D data set that can be used to further identify the areas of stenosis. Late gadolinium enhancement with long T1 times can be used to identify thrombus as a cause of stenosis.[127,170] CMR cannot be used to accurately assess calcification of the prosthesis or conduit.

iv. **Role of CT:** When significant stent-related artifact prevents adequate assessment on CMR, CT can be used to evaluate the pulmonary valve or conduit (Figure 24).[171] This can be helpful when the etiology of stenosis is not clear or for evaluation for percutaneous structural intervention.

Table 14 Most common types of PVR

	Type of valve/conduit	Manufacturer; size (valve or conduit diameter)
Surgical	Homograft (cryopreserved aortic or pulmonary)	Variety of sizes
	Xenograft conduits	Medtronic Contegra; 12-22 mm
		Shelhigh; 10-24 mm
		Medtronic Freestyle; 19-29 mm
	Composite synthetic conduits with bioprosthetic/mechanical valves	Carpentier-Edwards Porcine valve; 12-30 mm
		Medtronic Hancock; 12-26 mm
		Manually constructed; various sizes
	Bioprosthetic or mechanical valves	Variety of types and sizes
Transcatheter	Within conduits or bioprosthetic valves	Medtronic Melody; 18 mm
		Edwards SAPIEN; 23-29 mm
	In native outflow tract	Medtronic Harmony; 22 and 25 mm

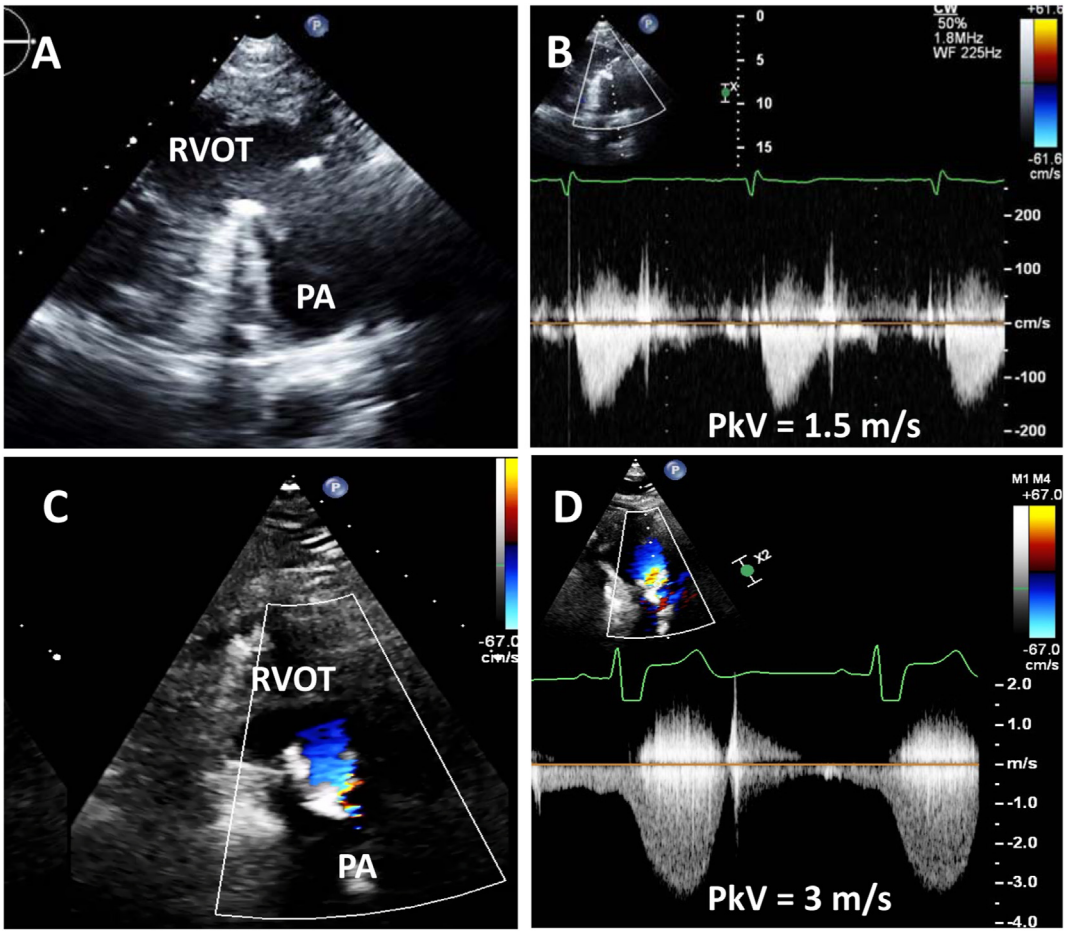

Figure 23 Examples of a normally functioning prosthetic pulmonary valve **(A, B)** and another with significant stenosis **(C, D)**. *PkV*, Peak velocity through the pulmonary valve.

Electrocardiographically gated contrast-enhanced whole–cardiac cycle imaging is recommended, particularly where percutaneous intervention is required. The presence of calcification is indicative of structural valvular degeneration but cannot be used for quantitation of the degree of stenosis. The presence of cusp thickening, pannus, or thrombus can also be assessed for other causes of stenosis.[172] Cardiac CT may be used to determine the size of the valve or conduit using the effective diameter derived from area or perimeter measurement if previous surgical notes are not available. However it should be noted that these measurements are less accurate in conduits, where postoperative calcification can lead to alterations in size and shape.[173]

Table 15 Parameters for prosthetic pulmonary valve stenosis

	Normal	Possible obstruction
Qualitative	• Normal valve structure and motion • Laminar flow	• Abnormal valve structure and motion • Use PW Doppler to determine the location of stenosis • Increased turbulence by color Doppler with a narrow flow jet
Quantitative*	• Peak velocity <3.2 m/sec for bioprosthesis <2.5 m/sec for homograft • Mean gradient <20 mm Hg for bioprosthesis <15 mm Hg for homograft	• Peak velocity ≥3.2 m/sec for bioprosthesis ≥2.5 m/sec for homograft • Mean gradient ≥20 mm Hg for bioprosthesis ≥15 mm Hg for homograft
Serial comparison with baseline	• Stable peak/mean gradient and peak velocity • No change in RV systolic pressures • No change in RV size and systolic function • No change in DVI	• Increased peak/mean gradient and peak velocity • Increased RV systolic pressure • Increased RV size and decreased systolic function • Decrease in DVI

*Measurements assume normal RV stroke volume. Accurate CW Doppler may be challenging because of the position of the homograft or bioprosthetic valve; important to use off-axis parasternal and suprasternal views. Normal values for various prosthetic PVs are shown in Appendix Table A7.

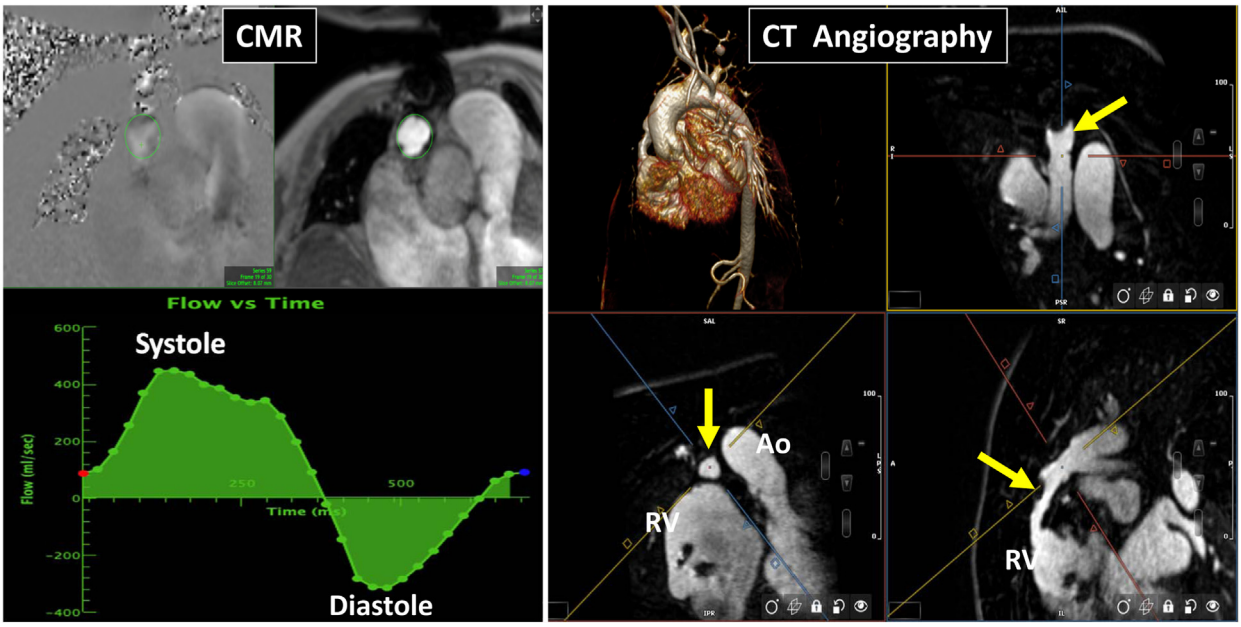

Figure 24 A case of tetralogy of Fallot with a 20-mm homograft placed 25 years earlier. CMR phase contrast systolic and diastolic flow (*left*) shows significant stenosis and regurgitation (4.1 m/sec, with a regurgitation fraction of 41%). Computed tomographic angiography with multiplanar reconstruction (*panels*) shows stenosis of the homograft (14 × 15 mm) secondary to calcification. The *yellow arrows* point to the pulmonary homograft. *Ao*, Aorta; *RV*, right ventricle.

C. Evaluation of Prosthetic Pulmonary Valve Regurgitation

i. **Echocardiographic and Doppler evaluation:** There is a paucity of data specifically evaluating PR in prosthetic valves; therefore, the information available is extrapolated from assessment of PR in native valves. Table 16 details the echocardiographic findings in various degrees of prosthetic PR severity, and Table 17 shows the pros and cons of each imaging modality in assessing PR.

Echocardiographic assessment of PR should include (1) characterization of the type and size of prosthesis; (2) the presence of relevant anatomic abnormalities, such as degeneration or vegetations; (3) quantitation of severity of regurgitation; and (4) any changes from previous assessments in serial examinations. Additionally, assessment of the RV size and interventricular septal position and motion during diastole is needed.

As discussed previously, prosthetic pulmonary stenosis occurs more frequently than regurgitation in both degeneration and endocarditis.

Table 16 Echocardiographic evaluation of severity of prosthetic pulmonary valve regurgitation

Parameters	Mild	Moderate	Severe
Valve structure	Usually normal	Abnormal or valve dehiscence	Abnormal or valve dehiscence
RV size	Normal*	Normal or dilated*	Dilated or progressive dilation†
Jet size by color Doppler (central jets)‡	Thin with a narrow origin; jet width ≤25% of pulmonary annulus	Intermediate; jet width 26%-50% of pulmonary annulus	Usually large, with a wide origin; jet width >50% of pulmonary annulus; may be brief in duration
Jet density by CW Doppler	Incomplete or faint	Dense	Dense
Jet deceleration rate by CW Doppler	Slow deceleration	Variable deceleration	Steep deceleration,§ early termination of diastolic flow
Pulmonary systolic flow compared with systemic flow by PW Doppler¶	Slightly increased	Intermediate	Greatly increased
Diastolic flow reversal in the distal main PA	None	Present	Present

Adapted from Zoghbi *et al*.[1]

*Unless other cause of RV dilatation exists, including residual postsurgical dilatation.

†Unless there are other reasons for baseline RV enlargement. Acute PR is an exception. RV volume overload is usually accompanied with typical paradoxical septal motion.

‡At a Nyquist limit of 50-60 cm/sec; parameter applies to central jets and not eccentric jets.

§Steep deceleration is not specific for severe PR, as it may occur with severe RV diastolic dysfunction.

¶Cutoff values for regurgitant volume and fraction are not well validated.

Table 17 Prosthetic pulmonary valve assessment and multimodality imaging: advantages and limitations

	Echocardiography	CMR	CT
Primary valve failure	Advantages • Qualitative assessment of regurgitation/stenosis • Assessment of peak/mean gradients • Assessment of RV hemodynamics Limitations • Challenging to be coaxial to PVR • Challenging to evaluate PA stenosis	Advantages • Spatial resolution • Quantification of stenosis/regurgitation • Quantification of RV volume/function • Anatomic visualization of PA/bifurcation Limitations • Some valves can create artifacts	Advantages • Spatial resolution • Visualization of leaflets for stenosis • Assessment of calcification of valve/conduit • Anatomic visualization of PA/bifurcation Limitations • Assessment of regurgitation • No hemodynamic assessment • Radiation/contrast use
Thrombosis /Pannus	Advantages • Qualitative assessment regurgitation/stenosis • Assessment of peak/mean gradients • Assessment of RV hemodynamics Limitations • Difficult to visualize valve structure	Not ideal for assessment	Advantages • Good visualization and spatial resolution • Differentiates between thrombus and pannus Limitations • Radiation/contrast
Endocarditis	Advantages • Temporal resolution • Qualitative assessment of regurgitation/stenosis Limitations • Dependent on acoustic windows	Not ideal for assessment of small vegetations	Not ideal for assessment of small vegetations

However, when a valved conduit is present, both stenosis of the conduit and regurgitation of the valve can occur (Figure 23). Color, PW, and CW Doppler are used to assist with the evaluation (Table 16). Color Doppler demonstrates diastolic flow into the RVOT, and jet duration and jet width assist in determining the severity. Severe PR has a short jet duration, as the PA and RV diastolic pressures equalize quickly, making it challenging to visually appreciate the PR. A color jet width >50% of the prosthesis annulus suggests severe PR. These parameters are less reliable in eccentric and paravalvular regurgitation. Reversal of flow in the distal main PA by PW Doppler is suggestive of at least moderate PR. A brief diastolic deceleration time is also suggestive of severe PR, but this is also dependent on the compliance of the right ventricle. In a study comparing CMR with echocardiography, a PHT <95 msec and a slope >4.9 m/sec^2 indicated a need for pulmonary valve intervention.[174] There are limited methods for quantification of PR that can be extrapolated to prosthetic valves. A comparison of stroke volume obtained just below the PVR and stroke volume obtained at the aortic or mitral valve can provide a measurement of regurgitant volume and fraction (in the absence of AR or MR, respectively). A regurgitant fraction <30% is considered mild, and >50% is considered severe.[1]

ii. **Role of TEE and 3D:** The use of TEE described previously in the section on pulmonary stenosis can help evaluate the severity of PR (Table 17).[3] Prosthetic valves can have calcification and thrombus, which are better visualized using TEE. The evaluation of PR using 3D TEE can also be achieved with live 3D, 3D zoom, or multiplanar reconstruction. The added value of 3D TEE is to see the valve en face with the regurgitant orifice.[26] ICE may be a consideration in evaluating a PVR when TEE is inconclusive.[166,167]

iii. **Role of CT:** Although CT can be used to detect leaflet mobility and the presence of prolapse, its temporal resolution is limited. Furthermore, although the anatomic regurgitant orifice area has been demonstrated as a useful tool for the quantification of AR, no studies are available for PR. However, CT may be useful for the precise localization and sizing of PVLs.[78]

iv. **Role of CMR:** The benefit of CMR for assessment of regurgitation is quantification using phase-contrast imaging (Figure 24).[169] CMR is

Table 18 Echocardiographic parameters required for comprehensive prosthetic TV assessment

Standard parameters	Size and type of prosthesis, and implantation date
2D or 3D imaging	Heart rate and blood pressure
	Leaflet thickening/mobility
	Mechanical occluder mobility
	Presence of thrombus, vegetation, or pannus
	Prosthesis stability/dehiscence
Color Doppler	Regurgitant jet location (central, eccentric, or paravalvular)
	Proximal flow convergence location, radius
	Regurgitant jet VC
	Regurgitant jet area
CW Doppler	Peak and mean diastolic gradient
	PHT
	DVI (VTI_{PrTV}/SV_{LVOT})
	EOA
	Peak TR velocity
	TR contour and density
Related cardiac chambers	RA, RV size and function
	Size and respiratory variation of IVC
	Hepatic vein flow profile

IVC, Inferior vena cava; *SV*, stroke volume; *VTI_{PrTV}*, VTI through the prosthetic TV.

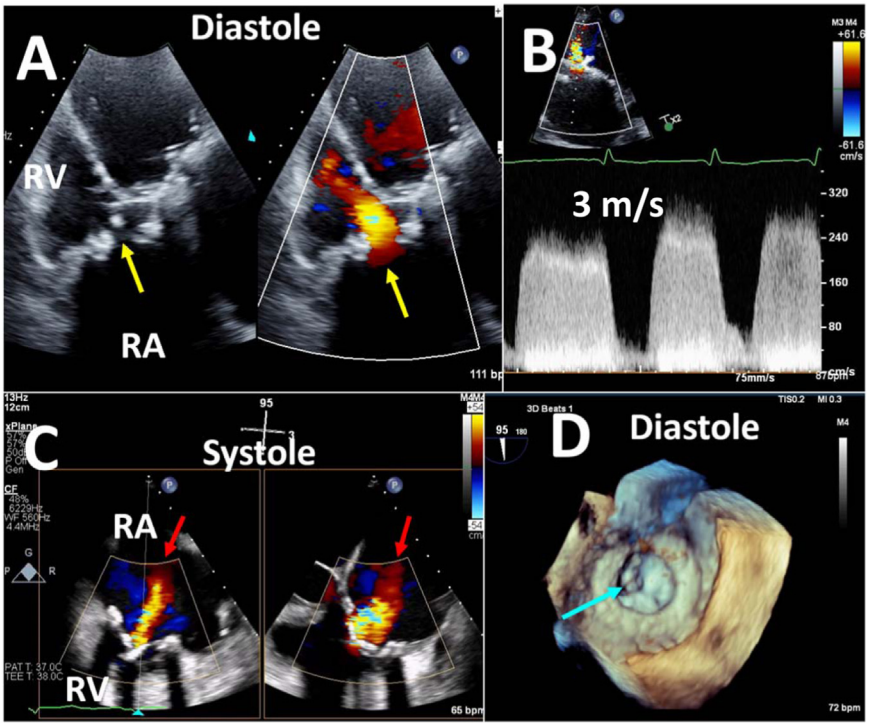

Figure 25 Transthoracic **(A, B)** and transesophageal **(C, D)** imaging of a patient with severe bioprosthetic TV stenosis. **(A)** Color-compare diastolic image shows the calcified and restricted leaflets (*yellow arrow*) with turbulent diastolic flow. CW Doppler **(B)** shows a peak velocity of 3.0 m/sec, with a mean gradient of 20 mm Hg. The transesophageal systolic image shows concomitant TR (*red arrows*) in the setting of markedly restricted bioprosthetic leaflet mobility. Three-dimensional imaging confirms severe restriction of all three leaflets with a small diastolic orifice (*blue arrow*). *RA*, Right atrium; *RV*, right ventricle.

Table 19 Doppler parameters suggestive of prosthetic TV stenosis

	Bioprosthetic	Mechanical
Peak E velocity, m/sec)	≥2.1	≥1.9
Mean gradient, mm Hg	≥9	≥6
PHT, msec	≥200	≥130
EOA, cm^2	<1.5	<2.0
DVI (VTI_{PrTV}/VTI_{LVOT})*	≥3.3	≥2.1

VTI_{PrTV}, VTI through the prosthetic TV.
*Assessed in the absence of AR or TR. Upper limits of normal DVI vary by valve size and type.

superior to echocardiography for quantification of PR.[168] On the basis of measured regurgitant fraction, the severity of PR is mild when <26%, moderate when 26% to 35%, and severe when >35%.[175] Other investigators consider a regurgitant fraction >40% as severe.[176] Phase-contrast CMR is not affected by multiple or eccentric jets. The through plane can be placed outside of the valvular artifact if need. Newer sequences such as 4D flow can be used to better understand the direction of the flow and quantitate the regurgitation, however its reliability has not been proven at this time. Additionally, quantification of RV volumes is important in the assessment of PR and is best evaluated using CMR.

Key Points for Assessing Prosthetic Pulmonary Valves and Conduits

1. Assessment of a prosthetic pulmonary valve requires an understanding of the different types of valves and valved conduits that are placed.
2. Evaluation with echocardiography may require off-axis, unconventional views.
3. Doppler-derived peak velocity and mean gradient (and possibly DVI) where feasible should be measured and reported.
4. For valve regurgitation, color Doppler interrogation, spectral Doppler recording of the jet with attention to its intensity and slope are necessary.
5. CT and CMR offer better delineation of prosthetic pulmonary valves regarding thrombus and calcification. CMR is particularly helpful in quantitation of PR.
6. There is a paucity of data evaluating PR in prosthetic valves; the information available is mostly extrapolated from assessment of native valves.

V. EVALUATION OF PROSTHETIC TRICUSPID VALVES

Evaluation of the TV is in evolution, as the once "forgotten" valve has received greater attention following natural history studies showing poor outcomes associated with progressively worse disease.[177,178] Given the current guideline recommendations,[5] the majority of TV repairs or TV replacements (TVRs) are performed at the time of left heart surgery, most commonly mitral valve surgery alone.[179] Almost 90% of TV procedures in the United States are repairs, with a decline in the number of replacements over the past decades. For

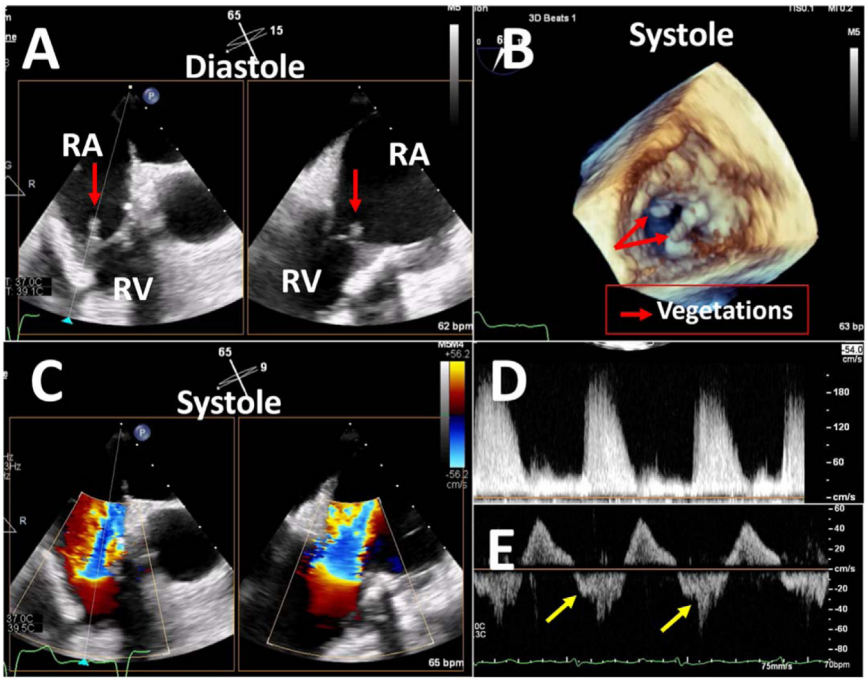

Figure 26 Example of bioprosthetic TV with severe regurgitation. TEE shows multiple vegetations (*red arrows*, **A** and **B**) on the bioprosthetic TV, resulting in severe regurgitation **(C)**. CW Doppler **(D)** shows a low-velocity dense and early systolic peaking profile. PW Doppler of the hepatic vein **(E)** shows systolic flow reversal (*arrows*) consistent with severe regurgitation. *RA*, Right atrium; *RV*, right ventricle.

isolated TV procedures, however, replacements continue to predominate, likely related to the late presentation of isolated disease.[180]

Although the majority of TVRs are bioprosthetic, meta-analyses suggest that there is an equal risk for 30-day and late mortality, reoperation, and 5-year valve failure in patients with mechanical vs biological TVR.[181] Some investigators have shown that bioprosthetic degeneration rate is steeper after 7 years.[182]

Prosthetic valves and prosthetic rings have different presentations and modes of failure. Surgical bioprostheses can fail because of prosthetic stenosis or regurgitation. The mean time period between tricuspid bioprosthesis implantation and dysfunction requiring ViV implantation was 12 years (range, 3-32 years).[183] Longitudinal studies of TV repairs have shown that significant recurrent regurgitation occurs within 5 to 7 years of repair.[184,185]

In the setting of inpatient mortality of 10% to 13% associated with both isolated and redo TV surgery,[180,186] transcatheter options have become more common to address both native TV and prosthetic device failure.[183,185,187,188] The assessment of prosthetic TV function thus involves the evaluation of surgical and transcatheter TV repair and replacement, as well as ViV and valve-in-ring procedures.

A. Echocardiographic Assessment of Prosthetic TV Function

The comprehensive evaluation of TVR requires multiple imaging planes where both 2D and 3D echocardiography are used (Table 18). TTE of the TVR is particularly useful because of the anterior position of the valve. All standard imaging planes for native TV assessment should be performed.[189] Native and prosthetic TV velocity varies with cycle length and respiration and therefore multiple cardiac cycles should be obtained by Doppler.[190,191] For PW and CW Doppler, a minimum of five cardiac cycles should be averaged in atrial fibrillation and sinus rhythm, or measurements can be performed in midexpiratory apnea.[1] PHT is influenced by heart rate, chamber compliance, and loading conditions and thus should be interpreted with caution when used as a stand-alone indicator of TV function. In addition, the PHT-derived EOA calculation overestimates TV area for bioprosthetic valves compared with continuity equation–derived methods and is not recommended.[192]

The new ASE guidelines for performance of a comprehensive TEE before structural valve intervention suggest strategies for complete visualization of the native TV.[193] In general, these same strategies should be used to assess prosthetic TVs. Guidelines have suggested standardized imaging display for the en face view of the native TV and the same standards should be used for en face display of TV prosthetic valves.[26,194] Imaging the TV with TEE may be more difficult than with TTE because of the position of the valve relative to the esophagus (anterior and medial). Acoustic noise from the fibrous body of the heart, as well as left heart prosthetic material, makes TEE from the midesophageal views particularly problematic. Imaging from deep esophageal or transgastric transducer positions places the probe closer to the TV and can therefore eliminate both shadowing caused by left heart structures and far-field attenuation.[92,194] Understanding these limitations can help determine the optimal image plane for detection of specific abnormalities.[68,195,196]

B. Evaluation of Prosthetic TV Stenosis

i. **Echocardiographic evaluation:** TVR may fail early or late after implantation. Echocardiographic evaluation of prosthetic TV function includes assessment of the parameters listed in Table 18. Two-dimensional or 3D images demonstrating thickened and/or restricted motion of bioprosthetic

Table 20 Echocardiographic parameters for determining prosthetic TV regurgitation: advantages and limitations

Parameter	Advantages	Limitations
TV morphology (e.g., flail leaflet, perforation, dehiscence)	• Abnormalities should be seen if severe TR is present	• Influenced by machine settings and physics of ultrasound (e.g., depth, acoustic artifact by prosthetic material)
RA and RV size and function	• Dilatation of both right atrium and right ventricle is typically seen in significant TR • Absence of RA and RV dilatation argues against severe chronic TR	• Underlying pathology of left and right heart as well as pulmonary hypertension may also cause right heart chamber dilatation
IVC and hepatic vein flow	• In the setting of significant TR, dilatation of the IVC and holosystolic flow reversal in the hepatic vein are seen	• Changes in RA compliance are frequently seen following TVR, resulting in blunting of hepatic vein flow and/or late systolic reversal. • Dilatation of IVC may be seen in other conditions with high RA/RV diastolic pressure
CW Doppler	• Dense systolic spectral recording with triangular, early peaking velocity are suggestive of severe TR	• Jet alignment is required • Diastolic peak and mean gradients are influenced not only by TR but also by RV/LV function and prosthetic stenosis.
Color Doppler jet (size, number of jets, location, eccentricity)	• Real time and rapid • Large central jet (area > 10 cm^2) suggestive of severe TR	• Influenced by machine settings and physics of ultrasound (e.g., depth, acoustic artifact by prosthetic material), and hemodynamics • Multiple and eccentric jets are more difficult to interpret
VCW	• Real time and rapid • VCW ≥ 0.7 cm suggestive of severe TR	• Difficult to assess in jets with temporal variability • Limited validation for multiple jets • Limited validation for noncircular orifice shape
PISA radius and EROA*	• Large flow convergence (>0.9 cm) suggests severe • EROA < 0.2 cm^2 usually mild TR; ≥0.4 cm^2 usually severe TR	• May underestimate TR severity in presence of multiple jets, temporal variability or markedly asymmetric orifice shape • Device interference with flow convergence zone limits accuracy
VC area by 3D planimetry	• May be the most accurate assessment of TR; however, poorly validated	• Limitations of resolution (axial, lateral, and temporal) as well as blooming artifacts • Accuracy in nonplanar orifices may be limited • 3D reconstruction of each orifice is time consuming • Temporal averaging may be necessary

IVC, Inferior vena cava; *PISA*, proximal isovelocity surface area; *VCW*, VC width.
*Not well validated for quantitation in TVR; for PISA, baseline Nyquist limit shift to 25-35 cm/sec.

leaflets or reduced excursion of one or more mechanical disks are obvious signs of prosthetic stenosis. Stenosis should also be suspected when there is a narrowed, aliased high-velocity color Doppler TV inflow pattern (Figure 25). Degeneration of TV bioprostheses is not uncommon and occurs in 0.4% to 2.2% patients/year.[197,198] The rate of freedom from TV bioprosthetic dysfunction has been estimated at 66% at 5 years.[199] Mechanical prostheses typically become obstructed by thrombosis, pannus, or vegetation with reported thrombosis rates of 0.5% to 3.3% patients/year.[197,200,201]

Normal Doppler values for various prosthetic TVs are detailed in Appendix Tables A8 and A9. Mean gradient values <6 to 9 mm Hg have been associated with normal bioprosthetic function across a wide variety of bioprosthesis.[192] Similarly, a mean gradient <6 mm Hg was found to be a marker of normal mechanical TV function.[202] It should be emphasized, however, that there are several factors that can significantly affect mean gradient in the absence of prosthetic valve dysfunction, including a smaller valve and high output states. In patients undergoing ViV or valve-in-ring procedures, a postimplantation mean gradient of >10 mm Hg is considered evidence of stenosis.[203]

In the absence of tachycardia, bioprosthetic TV obstruction is suspected when CW Doppler E-wave velocity is ≥2.1 m/sec, whereas mechanical prosthetic obstruction is suggested when E-wave velocity is ≥1.9 m/sec (Table 19).[191,192,204] Previous guidelines recommended that a PHT<230 msec is consistent with absence of prosthetic stenosis.[1] In a series

Table 21 Echocardiographic grading of TR after TVR or TV repair

Parameters	Mild	Moderate	Severe
Qualitative			
Color jet area*	Small, narrow, central	Moderate central	Large central jet or eccentric wall-impinging jet(s) of variable size swirling in right atrium
Flow convergence zone†	Not visible or small	Intermediate in size	Large
TR CW Doppler velocity waveform (density and shape)	Faint/partial/parabolic	Dense, parabolic or triangular	Dense, often triangular
Tricuspid inflow	A-wave dominant	Variable	E-wave dominant‡
Semiquantitative			
VC width, cm*	<0.3	0.3-0.69	≥0.7 or ≥2 moderate jets
PISA radius, cm†	≤0.5	0.6-0.9	>0.9
Hepatic vein flow§	Systolic dominance	Systolic blunting	Systolic flow reversal
Quantitative			
EROA, cm^2§	<0.20	0.20-0.39	≥0.40
RVol, mL§	<30	30-44	≥45

PISA, Proximal isovelocity surface area; *RVol*, regurgitant volume.
*With Nyquist limit > 50-60 cm/sec.
†Not well validated for quantitation in TVR; baseline Nyquist limit shift to 25-35 cm/sec.
‡Nonspecific, influenced by other factors (RV diastolic function, atrial fibrillation, RA pressure).
§EROA and RVol from 2D PISA need further validation of cutoffs by either PISA or volumetric methods.

of 285 bioprostheses, Blauwet *et al.*[202] found that a PHT <200 msec was representative of normal bioprosthetic function early after implantation. Mechanical bileaflet TV prostheses, in contrast, have a lower normal cut point for PHT (<130 msec). PHT is not recommended in the presence of rounded spectral Doppler contours, as measurement of PHT cannot be performed reliably in these circumstances.[205] It should also be noted that PHT is influenced by both heart rate and right-sided chamber compliance.

Although prior guidelines have suggested the use of prosthetic gradients and PHT to evaluate prosthetic function, the DVI (DVI = VTI_{PrTV}/VTI_{LVOT}) and EOA have more recently been included as part of a comprehensive Doppler assessment of TVR. The DVI associated with normal bioprosthetic TV function varies significantly by valve type and size, with upper values ranging from 2.4 to 3.6.[192] Likewise, the DVI associated with normal mechanical TV function varies significantly by valve type and size, with upper limits ranging from 2.3 to 2.8.[202] EOA can be calculated by dividing the stroke volume in the LVOT by the diastolic tricuspid prosthetic VTI.[192,202] This method is most accurate if there is mild or less TR and AR, though there is a dearth of normative data. If there is significant AR, the forward stroke volume can be measured from the RVOT.[206]

Table 22 List of CHD anatomies likely to require a prosthetic heart valve after primary surgery

	CHD anatomy	Surgical interventions	Percutaneous valve interventions
Aortic valve	• Severe aortic stenosis • Shone complex • Interrupted aortic arch with small aortic annulus • Bicuspid aortic valve • Unicuspid aortic valve	• Ross procedure • Ross-Konno procedure • Yasui procedure • Aortic valve replacement	• Balloon valvuloplasty • ViV TAVI
Mitral valve	• Congenital mitral valve stenosis • Parachute mitral valve • Arcade mitral valve • Shone complex • AVSD	• Mitral valve repair • AVSD repair • Mechanical mitral valve replacement	• Balloon valvuloplasty • ViV (Melody or Edwards SAPIEN valve)
TV	• AVSD • Ebstein anomaly • TV dysplasia • Tricuspid atresia	• TV repair • Cone reconstruction • Mechanical TVR • Bjork procedure	• ViV (Melody valve)
Pulmonary valve	• Truncus arteriosus • Transposition with LVOT obstruction • TOF/pulmonary atresia • Congenital pulmonary valve stenosis	• RV-to-PA conduit • Rastelli operation • Homograft	• Balloon valvuloplasty • Melody valve • Edwards SAPIEN valve • Harmony transcatheter pulmonary valve

AVSD, Atrioventricular septal defect; *TOF*, tetralogy of Fallot.

Table 23 Challenges to prosthetic valve evaluation in patients with CHD

- Poor echocardiographic windows due to
  - Previous surgery
  - Chest deformities
  - Artifacts from prosthetic materials
  - Body size
- Underestimation of prosthetic valve/conduit gradients due to
  - The presence of associated shunts
  - Serial stenoses
  - Eccentric jets
- EOA calculation may be limited by
  - Serial stenoses, which affect use of the continuity equation
  - Noncircular LVOT or RVOT shape affecting calculation of pre-prosthesis flow
  - Inaccurate VTI in patients with subaortic or subpulmonary stenosis when the preobstruction flow velocity pattern is not laminar
- Long tubular narrowing in conduits will affect the pressure gradient calculated by the modified Bernoulli equation using peak flow velocity

The Doppler parameters suggestive of prosthetic TV stenosis are listed in Table 19.

Although high pressure gradients can be indicative of prosthetic stenosis, high transprosthetic gradients can also reflect PPM. Proposed values of EOA for TV PPM have ranged from <0.9 to 1.19 cm^2/m^2.[192,207] At present, data are lacking regarding the impact of these indexed EOA thresholds on outcomes in longitudinal cohorts.

ii. **Role of CT:** CT can aid in the evaluation of TVR stenosis by measurement of the geometric orifice area and determination of the etiology of stenosis. It shows etiologies such as leaflet degeneration, abnormal leaflet or disk occluder mobility, calcification of the bioprosthetic ring, thrombus, pannus, or vegetation.[150] Adequate RA and RV opacification with limited mixing artifact is required for CT evaluation of the prosthetic TV. This can be achieved with a triphasic contrast injection protocol and timing of acquisition for right heart opacification rather than the left heart.[208] The maximal geometric orifice area of the prosthetic TV can be measured in diastole using multiplanar reconstruction in short axis at the bioprosthetic leaflet tip.[151] In mechanical valves, the opening and closing angles in addition to the geometric orifice area can be measured.[152] Careful consideration of these measurements is required as the geometric orifice area by CT is larger than the EOA by TTE, as expected.[151]

iii. **Role of CMR:** Prosthetic tricuspid stenosis can be quantified on CMR with planimetry of the geometric orifice area on cine imaging or peak velocity and gradient on through-plane contrast-velocity mapping. Susceptibility artifact from a metal ring and disk occluder can limit visualization of the valve opening but can be minimized with a gradient-echo sequence rather than SSFP sequence.[209] The use of through-plane velocity mapping may be limited because of the susceptibility artifact from the valve ring or disk occluder and the annular motion in the TV position.

C. Evaluation of Prosthetic TV Regurgitation

i. **Echocardiographic evaluation:** TR may be either transvalvular or paravalvular in origin, and careful assessment of the prosthetic TV from all available windows is necessary. Regurgitation after use of a transcatheter device in native TV disease has been addressed in recent guidelines[3] and is not covered here. As for all valvular regurgitation assessments by echocardiography, an integrative approach using color, PW, and CW Doppler is needed in the overall evaluation of TR (Figure 26, Tables 20 and 21). Color Doppler should be performed from multiple transthoracic echocardiographic views for the assessment of TR severity with attention to the three components of the jet—flow convergence, VC, and jet direction—as well as jet effects on the right atrium. To compensate for acoustic shadowing from the prosthetic valve stent or disk occluders, it is important to acquire modified RV inflow and subcostal views. Numerous studies have suggested significant pitfalls of color Doppler jet area alone for the assessment of TR severity.[1,210] Quantitative measurements should be performed whenever possible. However, proximal isovelocity surface area quantitation of both native and prosthetic valve TR has several pitfalls (e.g., low flow, irregular orifice shape, temporal variability), and few studies have validated the methodology in native or prosthetic valve disease.[211,212] Progressive dilatation of cardiac chambers or alterations in hepatic vein size and flow at follow-up may also be indications of a change in prosthetic valve function.

Echocardiographic criteria for assessing TR severity are shown in Table 21. On color Doppler imaging, a large flow convergence, increased VC width (>0.7 cm), EROA > 0.4 cm^2, and regurgitant volume > 45 mL all suggest severe TR. A dense CW Doppler tracing with a triangular, early peaking velocity as well as increased transvalvular diastolic peak velocity and mean gradient also suggests severe TR. A DVI of >3.3 in the context of increased transvalvular gradient and normal PHT help confirm the presence of significant TR. Few studies have shown the feasibility of 3D color Doppler planimetry of the VC area by both TTE[211] and TEE in native valve disease.[213] Compared with the multiparametric assessment of severe TR, the 3D VC area cutoff[211,213] and Doppler EROA cutoff are nearly double the proximal isovelocity surface area EROA.[211] Whether these methods can be used to assess prosthetic valves requires further study.

ii. **Role of CMR:** CMR is able to evaluate the status of the right ventricle in the setting of TR because of its ability to quantify RV volumes and ejection fraction without geometric assumptions.[5] Although there are currently no published data on prosthetic TR, the approaches used are analogous to those for native TR. Typically, quantitation of regurgitant volumes by CMR relies on velocity-encoded phase-contrast images to measure forward flow across the pulmonary valve, then subtract this from the total RV stroke volume measured using short-axis planimetry of multiple disks. This quantitative approach demonstrated modest agreement with a multiparametric echocardiographic approach in native TR.[214] A recent study that used CMR to assess outcomes in native functional TR showed that both regurgitant volume and regurgitant fraction are associated with increased mortality after adjustment for clinical and imaging covariates, including RV ejection fraction.[215] Although the risk was progressive with increasing TR volume and regurgitant fraction, a TR volume of ≥45 mL or regurgitant fraction of ≥50% identified patients in the highest risk stratum for mortality. Specific CMR thresholds for intervention in prosthetic TR are not established.

iii. **Role of CT:** The role of CT in prosthetic TV regurgitation is similar to that in prosthetic MR. Excessive rocking of the prosthesis during the cardiac cycle is seen in valvular dehiscence and significant PVLs can be identified and localized. Small PVLs can be obscured because of metallic artifacts from the prosthetic ring or disk occluders. The role of CT is currently primarily to help in planning transcatheter TV interventions.[216]

Key Points for Assessing Prosthetic TVs

1. A comprehensive evaluation of TVR requires multiple imaging planes in which 2D and 3D and Doppler echocardiography are used to assess valvular structure and function, as well as right heart chamber size and function. Because of shadowing and flow masking in the right atrium, particularly in mechanical TVs, screening for TR should include modified RV inflow and subcostal views as well as PW Doppler interrogation of hepatic vein flow, where feasible.
2. From the Doppler recordings of prosthetic TVs, peak velocity, mean gradient, PHT, and heart rate should be measured and reported whenever feasible. There is less experience with EOA and DVI of TVR.
3. Several factors can affect mean TV gradient in the absence of prosthetic valve dysfunction, including heart rate, flow, prosthesis size and type; considering these confounders, we suggest use of prosthesis type-specific cutoffs for determination of prosthetic TV stenosis.
4. A multiparametric echocardiographic approach for assessing prosthetic TV regurgitation is required, as validation of quantitative methods is lacking.
5. CMR may be useful for quantifying regurgitant volume and fraction; however, validation of its use in prosthetic valve function is lacking.
6. CT is helpful in identifying mechanisms of valve dysfunction, localization of significant PVLs and is essential in planning percutaneous interventions on the TV.

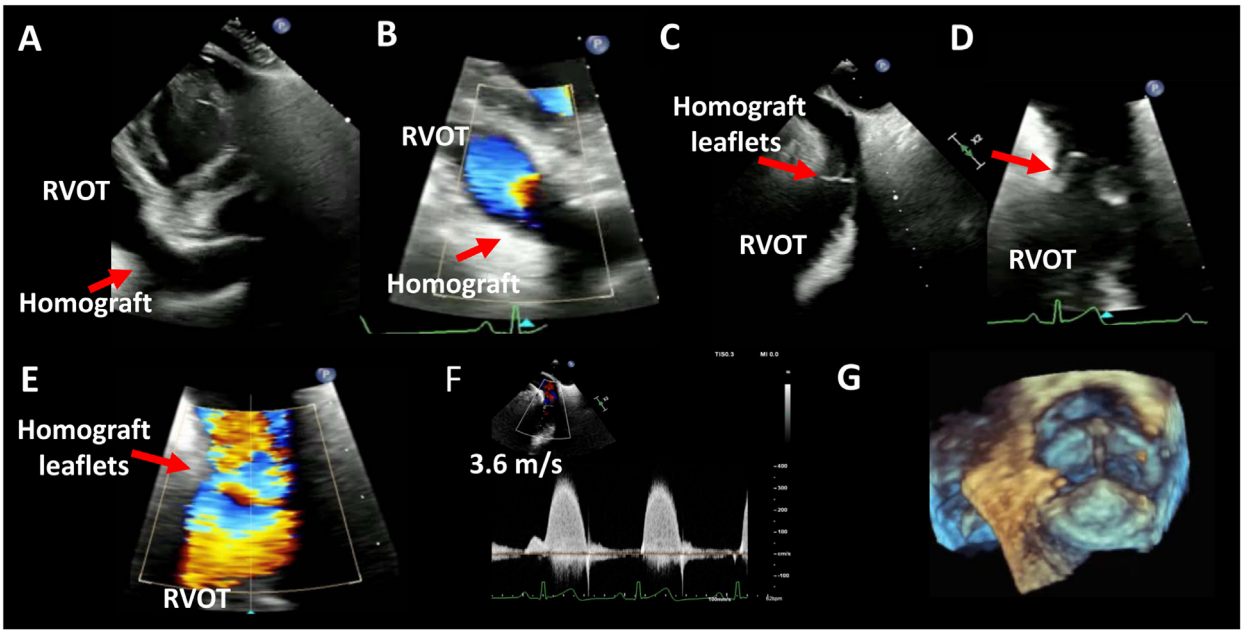

Figure 27 Transesophageal echocardiographic image from a deep transgastric window at about 60°, in a patient who underwent a Ross procedure for infective endocarditis, demonstrating the cardiac structures surrounding the pulmonary homograft **(A)**. The zoomed deep transgastric images with color Doppler demonstrate flow acceleration in the homograft **(B)**. A high esophageal view at about 130° provides a clear view of the homograft leaflets (*red arrows*, **C**), with restricted motion **(D)** and flow acceleration across the leaflets by color Doppler **(E)**. CW Doppler **(F)** measures peak and mean systolic gradients of 52 and 30 mm Hg, respectively. The patient underwent surgical replacement of the pulmonary valve with a Sorin prosthesis; a 3D image of the valve is shown **(G)**.

VI. EVALUATION OF PROSTHETIC VALVES IN CHD

A. Prosthetic Valves in CHD

The advent of interventional transcatheter approaches to deploying PHV has benefited many patients with CHD. In children with valve disease, repair is preferred over replacement, as PPM is inevitable as children grow. Balloon valvuloplasty is the first line of treatment for congenital valvular stenosis and some patients receive ViV implantation in the respective atrioventricular or semilunar valve position using a percutaneous approach before valve replacement.[217] This allows patients to grow before they receive mechanical valves after failed repair.[218,219] The evaluation of PHV in CHD using the described approach in adults in this document generally works, though there are some limitations and differences as described below. Table 22 lists all the CHD lesions that may require surgical and/or percutaneous interventions for PHV. Use of 2D and 3D

Table 24 Use of 3D echocardiography in patients with CHD*

Region of interest	3D modality	Information	Feasibility
Aortic valve	• GS/color Doppler • TTE: PLAX, PSAX, apical • TEE: ME 60°, 120°	• Prosthetic valve leaflet appearance/ motion • Regurgitation origin • Improved LVOT area measurement	Moderate
Mitral valve	• GS/color Doppler • TTE: PLAX, PSAX, apical • TEE: ME 0°, 90°, 120°	• Prosthetic valve leaflet appearance/ motion • Regurgitation origin	High
TV	• GS/color Doppler • TTE: apical, RV inflow, subcostal • TEE: ME 0°, 40°-60°, transgastric	• Prosthetic valve leaflet appearance/ motion • Regurgitation origin	Moderate
Pulmonary valve/pulmonary homografts	• GS/color Doppler • TTE: PSAX • TEE: high esophageal 0°-40°, transgastric	• Prosthetic valve leaflet appearance/ motion • Regurgitation origin • Improves RVOT area measurement	Low

GS, Grayscale; *ME*, midesophageal; *PLAX*, parasternal long-axis view; *PSAX*, parasternal short-axis view.
*Edited from Simpson *et al*.[224]

echocardiography, CMR, and CT is delineated in the evaluation of PHV in adolescents and adults with CHD.

B. Echocardiography in the Evaluation of PHVs Associated With CHD

Echocardiography is the primary noninvasive imaging modality used to assess prosthetic valves in patients with CHD. It allows both appraisal of valve function and hemodynamic impact of valve dysfunction on the left and/or right ventricles. Comprehensive echocardiographic assessment includes 2D and 3D transthoracic or transesophageal imaging with the use of color, CW, and PW Doppler.[164] It can also include agitated saline, ultrasound-enhancing agents, and stress echocardiography. One of the most important steps before imaging the patient with moderate or great complexity CHD is to understand the flow of blood through the heart to determine which images are needed. This requires an appreciation of the original cardiac anatomy and the changes introduced with surgical repairs or percutaneous interventions. Information regarding CHD classification is available in the American College of Cardiology and American Heart Association adult CHD guidelines.[217]

i. **TTE:** Several guidelines and recommendations have been published regarding TTE in patients with CHD. These include a general transthoracic echocardiographic protocol from the International Society for Adult Congenital Heart Disease.[220] Also, the ASE has published guidelines for multimodality imaging for patients with tetralogy of Fallot and transposition of the great arteries.[170,221] Challenges in imaging and assessing prosthetic valves in patients with CHD are summarized in Table 23.
Transthoracic echocardiographic images from patients with CHD may be suboptimal because of body size, chest wall deformities, and multiple surgical procedures. The artifacts from prosthetic materials and valves are additional obstacles to obtaining interpretable echocardiographic images. Off-axis and nonconventional imaging windows are frequently required. In particular, right heart structures can be challenging to image because of their location. For example, right-sided conduits (e.g., RV-PA or RA-RV) are anteriorly located and can be situated behind the sternum. Significant gradients in these conduits can be missed if the image is not optimized. Color flow mapping can be used to identify their location.[220] Views that are not often acquired, such as an anteriorly tilted image in the apical window, could be attempted to improve visualization of RA-RV conduits or pulmonary valves. The higher heart rate of pediatric patients may cause low-frame-rate images that can be addressed by using M-mode echocardiography. If images are inadequate, TEE should be considered (see the following section). Furthermore, use of ultrasound-enhancing agent is recommended to improve assessment of cardiac chamber size and function. Changes could indicate possible prosthetic valve/conduit dysfunction and necessitate further imaging with CMR or CT. Beyond echocardiographic image quality, evaluation of prosthetic valves in patients with CHD may be complicated by the coexistence of multiple levels of obstruction and the presence of additional shunts. Serial stenoses will affect the application of the continuity equation to determine EOA. For instance, pressure gradient measurements across the valve in a RV-PA conduit will be affected by the presence of a stenosis extending to the right or left PA. The presence of additional shunts, either untreated or residual after treatment, will affect flow and pressure gradients and therefore the EOA calculation.

ii. **Stress echocardiography:** The use of stress echocardiography in native and prosthetic valves is well established.[60] Current European Association of Cardiovascular Imaging and ASE recommendations on the clinical use of stress echocardiography in nonischemic heart disease include a description of its application in patients with CHD.[60] Patients with CHD with prosthetic valves or valved conduits can undergo stress echocardiography to assess symptoms, exercise capacity, ventricular dysfunction and contractile reserve, and pulmonary vascular response.[217,222,223] Importantly, exercise testing can be used to increase early diagnosis and intervention.

iii. **TEE:** TEE is predominantly used when transthoracic imaging is inadequate to assess prosthetic valve function. However, it is also indicated when there are concerns regarding prosthetic valve infective endocarditis, a need to reevaluate the valve after treatment for thrombosis or infection, or to guide surgical or percutaneous valve interventions. The ASE has published guidelines for the performance of TEE in patients with CHD.[164] Similar to TTE, some transesophageal echocardiographic views need to be modified to thoroughly assess the prosthetic valve/conduit in patients with CHD (Figure 27).

iv. **Three-dimensional echocardiography:** In patients with good acoustic windows, 3D echocardiography can provide valuable anatomic information. It can also improve assessment of valve dysfunction severity and quantification of LV, RV, and stroke volumes.[224] An expert consensus statement on the use of 3D echocardiography in patients with CHD was published in 2017.[224] Table 24 summarizes its feasibility in patients with CHD. Of note, patients with complex anatomy will likely need multibeat acquisition to obtain a data set that encompasses the prosthetic valve and conduit and adjacent structures needed for orientation with adequate spatial and temporal resolution. It may also be necessary for high quality 3D color images.

C. Role of Cardiac CT

CT with 4D imaging is a useful complementary method for the evaluation of PHVs in patients with CHD. CT may be particularly useful in patients with CHD for the following reasons: (1) the position of the PHV may not always lend itself to assessment with traditional echocardiographic windows given multiple prior surgical procedures, atypical anatomy, or unusual locations (e.g., RA-to-RV conduit in Bjork procedure); (2) valves can be placed within conduits in patients with CHD (e.g., RV-to-PA conduit), making assessment challenging because of the location and artifacts related to the conduit; and (3) the potential presence of multiple sequential obstructions, making Doppler assessment difficult.

Potential causes of PHV dysfunction in patients with CHD are similar to those without CHD. Once an increased gradient or valvular regurgitation is identified by echocardiography or is clinically suspected, CT can be considered. To assess the cause of increased gradients across a mechanical prosthetic valve, noncontrast CT (especially in the context of renal dysfunction) with retrospective gating may be sufficient to assess the motion of the occluders. Noncontrast CT can also identify the presence of valve stent fracture (e.g., from transcutaneous pulmonary valves) and perivalvular calcification, as well as help differentiate pledgets from potential PVL that may be contributing to increased transvalvular gradients. If there is suspicion of valve thrombosis, pannus formation, vegetations, or dysfunction of a bioprosthetic valve, retrospectively gated CT with contrast should be performed. The site of contrast injection (right arm, left arm, leg) should be carefully determined on the basis of knowledge of the known venous anatomy.

Specific scenarios in which cardiac CT is useful in patients with CHD to assess PHV beyond their usual location include assessment of valved conduits (e.g., tetralogy of Fallot) or percutaneous valve within an RV-to-PA conduit (e.g., Melody valve[172]), a valve within an RA-to-RV conduit (Bjork procedure), to differentiate conduit edge stenosis from valvular dysfunction, and to identify the presence of concomitant sub- or supravalvular stenosis (e.g., branch PA stenosis; Figure 24). For these specific indications, given the right-sided location of these abnormalities, the timing of image acquisition in relation to contrast administration should maximize the presence of contrast in the right-sided structures. Triphasic injections may be useful for this purpose.[172] A retrospectively gated study should be performed to assess the dynamic nature of the prosthetic valve and mobility of

the valved stent if applicable. Assessing valve regurgitation is not directly possible because of the lack of flow data, however, retrospective gated acquisition can identify the presence of valve rocking. If dehiscence is clearly present, CT can characterize its location, length, and width to allow planning for potential percutaneous procedures. In addition, in the context of single valve disease, RV and LV stroke volumes could be measured to quantify regurgitant volume and fraction.

An important limitation of CT is the potential for beam hardening or blooming artifacts that affect diagnostic accuracy, especially in the context of multiple valves, stents, coils, and pacemaker leads. These must be carefully avoided whenever possible using techniques described above.

D. Role of CMR

CMR is widely used in both the preoperative and postoperative assessment of simple to complex CHD. CMR's strength in CHD is its ability to (1) image the valve in planes that may be challenging for echocardiography, such as behind the sternum; (2) provide chamber quantification; (3) assess great vessel and conduit anatomy by 3D contrast-enhanced magnetic resonance angiography; and (4) characterize tissue for a comprehensive evaluation of valvular function.[225]

In a prospective evaluation of cases, the most common PHV for CHD was PVR, followed by aortic valve replacement and homograft or autograft.[226] Currently, there is a paucity of published literature focused specifically on PHVs in CHD. The use of CMR in this population is extrapolated from literature primarily involving native valves that are similar to homografts or autografts and with data from surgical prostheses as discussed above.[124]

The use of both 1.5- and 3-T CMR magnets is safe in patients with all types of PHVs. When evaluating which magnet strength to use in CHD, it is important to consider other interventions the patient may have had, such as vascular plugs, coils, or pacemakers or defibrillators, which may require a 1.5-T magnet or be contraindicated for CMR. Various sequences can be used, as described earlier (Figure 8) to evaluate leaflet morphology and motion and delineate prosthetic vs periprosthetic regurgitation complementary to echocardiography. Phase-contrast velocity mapping can measure velocity and flow through a specific plane slice (Figure 24).[124] When performing phase contrast, depending on the signal void that occurs with PHV, the assessment may be placed 0.25 to 0.4 mm downstream from the PHV. Additionally, contrast-enhanced tissue characterization of pulmonary conduits is noted with stenosis and correlated with inflammation and fibrosis of the conduit.

Four-dimensional flow CMR is a newer modality that allows comprehensive study of flow in the heart and thoracic vessels in all three spatial directions. This technique allows flow visualization, flow quantification, and advanced hemodynamic parameters including wall shear stress and kinetic energy evaluation. In CHD, 4D flows have been studied in patients with d-transposition of the great arteries with arterial switch, who can develop neo-AR and supravalvular pulmonary or aortic stenosis at the anastomotic site. Studies show increased asymmetric flow in the anterior main PA, better visualization of the supravalvular pulmonary stenosis, and asymmetrical wall stress in the distal ascending aorta.[227] Calkoen *et al.*[228] studied atrioventricular septal defect patients after correction, which can involve mitral valve surgery, and showed the ability of 4D flow to accurately quantitate and visualize eccentric left atrioventricular valve regurgitation. These findings can help understand complications that these patients may encounter in the long term.[228]

Key Points for the Evaluation of Prosthetic Valves in CHD

1. Evaluation of prosthetic valves in CHD may require modifications to standard transthoracic and transesophageal echocardiographic views.
2. An understanding of different CHD anatomy, conduits, and hemodynamics is required in the evaluation of PHV in CHD.
3. Three-dimensional echocardiography can provide valuable anatomic information and en face views of the PHV in CHD.
4. CT and CMR provide additional means of imaging PHVs in CHD.

VII. CONCLUSIONS AND FUTURE DIRECTIONS

Echocardiography is the imaging modality of choice for the initial evaluation and management of PHVs. A comprehensive approach is needed to assess valve structure and function in addition to the extent of reverse remodeling of cardiac chambers after percutaneous or surgical valve replacement. Color and spectral Doppler play a central role in evaluating prosthetic valve function and related complications. In general, assessment of prosthetic valve function is more challenging than native valves because of suboptimal visualization of prosthetic valve structure and occluder devices with TTE and the inherent variability of valve hemodynamics and orifice areas observed with the wide range of prosthetic valve types and sizes. Thus, documentation of the type and size of the inserted valve or conduit is paramount in assessment of prosthetic valves. Furthermore, serial comparison with a baseline postoperative study is essential in facilitating accurate evaluation of valve function.

In patients with suspected prosthetic valvular dysfunction, advanced imaging is frequently needed to identify the mechanism of dysfunction or severity of regurgitation, particularly in mechanical valves. In addition to the traditional role of 2D and 3D TEE in assessing valve dysfunction, CT and CMR have emerged as powerful imaging modalities that complement echocardiography. CT offers high-resolution imaging with particular advantage in mechanical valves, while CMR's main strength is quantitation of regurgitation severity. Thus, the role of imaging has significantly expanded since the initial ASE document on prosthetic valves in 2009. The choice of advanced imaging modality, if needed after an initial TTE, should be carefully decided, as each modality has advantages and limitations. This choice is best tailored to the patient's clinical condition, the type and position of prosthetic valve, and the suspected underlying condition of obstruction and/or regurgitation. Goals of future research will include enhancing automated quantitation of regurgitation severity with color and spectral Doppler, increasing temporal resolution with CT and CMR, and decreasing artifacts emanating from metallic structures, thus improving valve visualization.

NOTICE AND DISCLAIMER

any decision made or action taken by you or such other parties in reliance on this information. Nor does your use of this information constitute the offering of medical advice by ASE or create any physician-patient relationship between ASE and your patients or anyone else.

ACKNOWLEDGMENT

This document was reviewed by members of the 2023-2024 ASE Guidelines and Standards Committee, the ASE Board of Directors, the ASE Executive Committee, and designated reviewers (Jacqueline Danik, MD, DrPH, Noreen Kelly, MD, MBA, Smadar Kort, MD, Anuj Mediratta, MD, Matthew Parker, MD, Alan Pearlman, MD, Andrew Pellet, RDCS, PhD, Patricia Pellikka, MD, David A. Orsinelli, MD, Anita Sadeghpour, MD, Brian Soriano, MD, Leif Selamet Tierney, MD, David H. Wiener, MD, and Bo Xu, MD).

SUPPLEMENTARY DATA

Supplementary data to this article can be found online at https://doi.org/10.1016/j.echo.2023.10.004.

REFERENCES

1. Zoghbi WA, Chambers JB, Dumesnil JG, et al. Recommendations for evaluation of prosthetic valves with echocardiography and Doppler ultrasound: a report from the American Society of Echocardiography's guidelines and standards Committee and the Task force on prosthetic valves, developed in conjunction with the American College of Cardiology Cardiovascular Imaging Committee, Cardiac Imaging Committee of the American Heart Association, the European Association of Echocardiography, a registered branch of the European Society of Cardiology, the Japanese Society of Echocardiography and the Canadian Society of Echocardiography, endorsed by the American College of Cardiology Foundation, American Heart Association, European Association of Echocardiography, a registered branch of the European Society of Cardiology, the Japanese Society of Echocardiography, and Canadian Society of Echocardiography. J Am Soc Echocardiogr 2009;22:975-1014; quiz 1082-4.
2. Lancellotti P, Pibarot P, Chambers J, et al. Recommendations for the imaging assessment of prosthetic heart valves: a report from the European association of cardiovascular imaging endorsed by the Chinese Society of Echocardiography, the inter-American Society of Echocardiography, and the Brazilian Department of Cardiovascular Imaging. Eur Heart J Cardiovasc Imaging 2016;17:589-90.
3. Zoghbi WA, Asch FM, Bruce C, et al. Guidelines for the evaluation of valvular regurgitation after percutaneous valve repair or replacement: a report from the American society of echocardiography developed in collaboration with the society for cardiovascular angiography and interventions, Japanese Society of Echocardiography, and Society for Cardiovascular Magnetic Resonance. J Am Soc Echocardiogr 2019;32:431-75.
4. Goldstone AB, Chiu P, Baiocchi M, et al. Mechanical or biologic prostheses for aortic-valve and mitral-valve replacement. N Engl J Med 2017;377:1847-57.
5. Otto CM, Nishimura RA, Bonow RO, et al. 2020 ACC/AHA guideline for the management of patients with valvular heart disease: a report of the American College of Cardiology/American Heart Association Joint Committee on clinical practice guidelines. J Am Coll Cardiol 2021;77:e25-197.
6. Alkhouli M, Alqahtani F, Simard T, et al. Predictors of use and outcomes of mechanical valve replacement in the United States (2008-2017). J Am Heart Assoc 2021;10:e019929.
7. Eugène M, Duchnowski P, Prendergast B, et al. Contemporary management of severe symptomatic aortic stenosis. J Am Coll Cardiol 2021;78:2131-43.
8. Halkos ME, Puskas JD. Are all bileaflet mechanical valves equal? Curr Opin Cardiol 2009;24:136-41.
9. Yang B, Malik A, Farhat L, et al. Influence of age on longevity of a stentless aortic valve. Ann Thorac Surg 2020;110:500-7.
10. Windecker S, Okuno T, Unbehaun A, et al. Which patients with aortic stenosis should be referred to surgery rather than transcatheter aortic valve implantation? Eur Heart J 2022;43:2729-50.
11. Hahn RT, Leipsic J, Douglas PS, et al. Comprehensive echocardiographic assessment of normal transcatheter valve function. JACC Cardiovasc Imaging 2019;12:25-34.
12. Kunadian B, Vijayalakshmi K, Thornley AR, et al. Meta-analysis of valve hemodynamics and left ventricular mass regression for stentless versus stented aortic valves. Ann Thorac Surg 2007;84:73-8.
13. Varc-3 Writing C, Genereux P, Piazza N, et al. Valve academic research Consortium 3: updated Endpoint definitions for aortic valve clinical research. J Am Coll Cardiol 2021;77:2717-46.
14. Butany J, Collins MJ, Nair V, et al. Morphological findings in explanted Toronto stentless porcine valves. Cardiovasc Pathol 2006;15:41-8.
15. Vongpatanasin W, Hillis LD, Lange RA. Prosthetic heart valves. N Engl J Med 1996;335:407-16.
16. Barbetseas J, Nagueh SF, Pitsavos C, et al. Differentiating thrombus from pannus formation in obstructed mechanical prosthetic valves: an evaluation of clinical, transthoracic and transesophageal echocardiographic parameters. J Am Coll Cardiol 1998;32:1410-7.
17. Ueda T, Teshima H, Fukunaga S, et al. Evaluation of prosthetic valve obstruction on electrocardiographically gated multidetector-row computed tomography–identification of subprosthetic pannus in the aortic position. Circ J 2013;77:418-23.
18. Habib G, Hoen B, Tornos P, et al. Guidelines on the prevention, diagnosis, and treatment of infective endocarditis (new version 2009): the Task force on the prevention, diagnosis, and treatment of infective endocarditis of the European Society of Cardiology (ESC). Endorsed by the European Society of Clinical Microbiology and Infectious Diseases (ESCMID) and the International Society of Chemotherapy (ISC) for infection and Cancer. Eur Heart J 2009;30:2369-413.
19. Afridi I, Apostolidou MA, Saad RM, et al. Pseudoaneurysms of the mitral-aortic intervalvular fibrosa: dynamic characterization using transesophageal echocardiographic and Doppler techniques. J Am Coll Cardiol 1995;25:137-45.
20. Kouchoukos NT, Wareing TH, Murphy SF, et al. Sixteen-year experience with aortic root replacement. Results of 172 operations. Ann Surg 1991;214:308-18. discussion 318-20.
21. Summers MR, Leon MB, Smith CR, et al. Prosthetic valve endocarditis after TAVR and SAVR: insights from the PARTNER trials. Circulation 2019;140:1984-94.
22. Roudaut R, Serri K, Lafitte S. Thrombosis of prosthetic heart valves: diagnosis and therapeutic considerations. Heart 2007;93:137-42.
23. Egbe AC, Pislaru SV, Pellikka PA, et al. Bioprosthetic valve thrombosis versus structural failure: clinical and echocardiographic predictors. J Am Coll Cardiol 2015;66:2285-94.
24. Salah HM, Almaddah N, Xu J, et al. Gender differences and outcomes of hypoattenuated leaflet thickening (HALT) following transcatheter aortic valve replacement: a meta-analysis of randomized and cohort studies. Curr Probl Cardiol 2022;48:101155.
25. Carlson S, Habib G, Chen T, et al. Multimodality imaging for prosthetic valves evaluation: current understanding and future directions. Prog Cardiovasc Dis 2022;72:66-77.
26. Lang RM, Badano LP, Tsang W, et al. EAE/ASE recommendations for image acquisition and display using three-dimensional echocardiography. J Am Soc Echocardiogr 2012;25:3-46.
27. Baumgartner H, Schima H, Tulzer G, et al. Effect of stenosis geometry on the Doppler-catheter gradient relation in vitro: a manifestation of pressure recovery. J Am Coll Cardiol 1993;21:1018-25.
28. Baumgartner H, Stefenelli T, Niederberger J, et al. "Overestimation" of catheter gradients by Doppler ultrasound in patients with aortic stenosis:

a predictable manifestation of pressure recovery. J Am Coll Cardiol 1999;33:1655-61.
29. Chafizadeh ER, Zoghbi WA. Doppler echocardiographic assessment of the St. Jude Medical prosthetic valve in the aortic position using the continuity equation. Circulation 1991;83:213-23.
30. Muraru D, Cecchetto A, Cucchini U, et al. Intervendor consistency and accuracy of left ventricular volume measurements using three-dimensional echocardiography. J Am Soc Echocardiogr 2018;31:158-68.e1.
31. Kitano T, Nabeshima Y, Otsuji Y, et al. Accuracy of left ventricular volumes and ejection fraction measurements by contemporary three-dimensional echocardiography with Semi- and fully automated software: systematic review and meta-analysis of 1,881 Subjects. J Am Soc Echocardiogr 2019;32:1105-15.e5.
32. Hahn RT, Douglas PS, Jaber WA, et al. Doppler velocity index outcomes following surgical or transcatheter aortic valve replacement in the PARTNER trials. JACC Cardiovasc Interv 2021;14:1594-606.
33. Olmos L, Salazar G, Barbetseas J, et al. Usefulness of transthoracic echocardiography in detecting significant prosthetic mitral valve regurgitation. Am J Cardiol 1999;83:199-205.
34. Baumgartner H, Khan S, DeRobertis M, et al. Discrepancies between Doppler and catheter gradients in aortic prosthetic valves in vitro. A manifestation of localized gradients and pressure recovery. Circulation 1990;82:1467-75.
35. Heinrich RS, Fontaine AA, Grimes RY, et al. Experimental analysis of fluid mechanical energy losses in aortic valve stenosis: importance of pressure recovery. Ann Biomed Eng 1996;24:685-94.
36. Levine RA, Schwammenthal E. Stenosis is in the eye of the observer: impact of pressure recovery on assessing aortic valve area. J Am Coll Cardiol 2003;41:443-5.
37. Herrmann HC, Pibarot P, Wu C, et al. Bioprosthetic aortic valve hemodynamics: definitions, outcomes, and evidence gaps: JACC state-of-the-art review. J Am Coll Cardiol 2022;80:527-44.
38. Baumgartner H, Khan S, DeRobertis M, et al. Effect of prosthetic aortic valve design on the Doppler-catheter gradient correlation: an in vitro study of normal St. Jude, Medtronic-Hall, Starr-Edwards and Hancock valves. J Am Coll Cardiol 1992;19:324-32.
39. Pibarot P, Dumesnil JG. Hemodynamic and clinical impact of prosthesis-patient mismatch in the aortic valve position and its prevention. J Am Coll Cardiol 2000;36:1131-41.
40. Pibarot P, Magne J, Leipsic J, et al. Imaging for predicting and assessing prosthesis-patient mismatch after aortic valve replacement. JACC Cardiovasc Imaging 2019;12:149-62.
41. Abbas AE, Ternacle J, Pibarot P, et al. Impact of flow on prosthesis-patient mismatch following transcatheter and surgical aortic valve replacement. Circ Cardiovasc Imaging 2021;14:e012364.
42. Dumesnil JG, Honos GN, Lemieux M, et al. Validation and applications of indexed aortic prosthetic valve areas calculated by Doppler echocardiography. J Am Coll Cardiol 1990;16:637-43.
43. Schwammenthal E, Chen C, Benning F, et al. Dynamics of mitral regurgitant flow and orifice area. Physiologic application of the proximal flow convergence method: clinical data and experimental testing. Circulation 1994;90:307-22.
44. Schwammenthal E, Vered Z, Agranat O, et al. Impact of atrioventricular compliance on pulmonary artery pressure in mitral stenosis: an exercise echocardiographic study. Circulation 2000;102:2378-84.
45. Zorn GL 3rd, Little SH, Tadros P, et al. Prosthesis-patient mismatch in high-risk patients with severe aortic stenosis: a randomized trial of a self-expanding prosthesis. J Thorac Cardiovasc Surg 2016;151:1014-22.1023.e1-3.
46. Pibarot P, Weissman NJ, Stewart WJ, et al. Incidence and sequelae of prosthesis-patient mismatch in transcatheter versus surgical valve replacement in high-risk patients with severe aortic stenosis: a PARTNER trial cohort–a analysis. J Am Coll Cardiol 2014;64:1323-34.
47. Blais C, Dumesnil JG, Baillot R, et al. Impact of valve prosthesis-patient mismatch on short-term mortality after aortic valve replacement. Circulation 2003;108:983-8.
48. Ruel M, Al-Faleh H, Kulik A, et al. Prosthesis-patient mismatch after aortic valve replacement predominantly affects patients with preexisting left ventricular dysfunction: effect on survival, freedom from heart failure, and left ventricular mass regression. J Thorac Cardiovasc Surg 2006;131:1036-44.
49. Castro LJ, Arcidi JM Jr., Fisher AL, et al. Routine enlargement of the small aortic root: a preventive strategy to minimize mismatch. Ann Thorac Surg 2002;74:31-6. discussion 36.
50. Pibarot P, Dumesnil JG. Prosthesis-patient mismatch: definition, clinical impact, and prevention. Heart 2006;92:1022-9.
51. Pibarot P, Dumesnil JG. Prosthesis-patient mismatch in the mitral position: old concept, new evidences. J Thorac Cardiovasc Surg 2007;133:1405-8.
52. Bitar JN, Lechin ME, Salazar G, et al. Doppler echocardiographic assessment with the continuity equation of St. Jude Medical mechanical prostheses in the mitral valve position. Am J Cardiol 1995;76:287-93.
53. Dumesnil JG, Honos GN, Lemieux M, et al. Validation and applications of mitral prosthetic valvular areas calculated by Doppler echocardiography. Am J Cardiol 1990;65:1443-8.
54. Pibarot P, Herrmann HC, Wu C, et al. Standardized definitions for bioprosthetic valve dysfunction following aortic or mitral valve replacement: JACC state-of-the-art review. J Am Coll Cardiol 2022;80:545-61.
55. Hwang HY, Kim YH, Kim KH, et al. Patient-prosthesis mismatch after mitral valve replacement: a propensity score analysis. Ann Thorac Surg 2016;101:1796-802.
56. Tomšič A, Arabkhani B, Schoones JW, et al. Prosthesis-patient mismatch after mitral valve replacement: a pooled meta-analysis of Kaplan-Meier-derived individual patient data. J Card Surg 2020;35:3477-85.
57. Ionescu A, Fraser AG, Butchart EG. Prevalence and clinical significance of incidental paraprosthetic valvar regurgitation: a prospective study using transoesophageal echocardiography. Heart 2003;89:1316-21.
58. Zoghbi WA, Adams D, Bonow RO, et al. Recommendations for noninvasive evaluation of native valvular regurgitation: a report from the American society of echocardiography developed in collaboration with the society for cardiovascular magnetic resonance. J Am Soc Echocardiogr 2017;30:303-71.
59. Kinno M, Raissi SR, Olson KA, et al. Three-dimensional echocardiography in the evaluation and management of paravalvular regurgitation. Echocardiography 2018;35:2056-70.
60. Lancellotti P, Pellikka PA, Budts W, et al. The clinical use of stress echocardiography in non-ischaemic heart disease: recommendations from the European Association of Cardiovascular Imaging and the American Society of Echocardiography. J Am Soc Echocardiogr 2017;30:101-38.
61. Gentry Iii JL, Phelan D, Desai MY, et al. The role of stress echocardiography in valvular heart disease: a current appraisal. Cardiology 2017;137:137-50.
62. Nicoara A, Skubas N, Ad N, et al. Guidelines for the use of transesophageal echocardiography to assist with surgical decision-making in the operating room: a surgery-based approach: from the American society of echocardiography in collaboration with the Society of Cardiovascular Anesthesiologists and the Society of Thoracic Surgeons. J Am Soc Echocardiogr 2020;33:692-734.
63. Little SH, Bapat V, Blanke P, et al. Imaging guidance for transcatheter mitral valve intervention on prosthetic valves, rings, and annular calcification. JACC Cardiovasc Imaging 2021;14:22-40.
64. Hahn RT, Nicoara A, Kapadia S, et al. Echocardiographic imaging for transcatheter aortic valve replacement. J Am Soc Echocardiogr 2018;31:405-33.
65. Hahn RT, Kodali S, Tuzcu EM, et al. Echocardiographic imaging of procedural complications during balloon-expandable transcatheter aortic valve replacement. JACC Cardiovasc Imaging 2015;8:288-318.

66. Sündermann SH, Biaggi P, Grünenfelder J, et al. Safety and feasibility of novel technology fusing echocardiography and fluoroscopy images during MitraClip interventions. EuroIntervention 2014;9:1210-6.
67. Hahn RT, Kodali SK. State-of-the-art intra-procedural imaging for the mitral and tricuspid PASCAL Repair System. Eur Heart J Cardiovasc Imaging 2022;23:e94-110.
68. Muraru D, Hahn RT, Soliman OI, et al. 3-Dimensional echocardiography in imaging the tricuspid valve. JACC Cardiovasc Imaging 2019;12:500-15.
69. Hahn RT, Kodali S, Fam N, et al. Early multinational experience of transcatheter tricuspid valve replacement for treating severe tricuspid regurgitation. JACC Cardiovasc Interv 2020;13:2482-93.
70. Hahn RT, George I, Kodali SK, et al. Early single-site experience with transcatheter tricuspid valve replacement. JACC Cardiovasc Imaging 2019;12:416-29.
71. Cianciulli TE, Lax JA, Beck MA, et al. Cinefluoroscopic assessment of mechanical disc prostheses: its value as a complementary method to echocardiography. J Heart Valve Dis 2005;14:664-73.
72. Gorlin R, Gorlin SG. Hydraulic formula for calculation of the area of the stenotic mitral valve, other cardiac valves, and central circulatory shunts. I. Am Heart J 1951;41:1-29.
73. Kober G, Hilgermann R. Catheter entrapment in a Bjöurk-Shiley prosthesis in aortic position. Cathet Cardiovasc Diagn 1987;13:262-5.
74. Burstow DJ, Nishimura RA, Bailey KR, et al. Continuous wave Doppler echocardiographic measurement of prosthetic valve gradients: a simultaneous Doppler-catheter correlative study. Circulation 1989;80:504-14.
75. Schoenfeld MH, Palacios IF, Hutter AM, et al. Underestimation of prosthetic mitral valve areas: role of transseptal catheterization in avoiding unnecessary repeat mitral valve surgery. JAm Coll Cardiol 1985;5:1387-92.
76. Suh YJ, Im DJ, Hong YJ, et al. Absolute-delay multiphase reconstruction reduces prosthetic valve-related and atrial fibrillation-related artifacts at cardiac CT. AJR Am J Roentgenol 2017;208:W160-7.
77. Kim JY, Suh YJ, Han K, et al. Diagnostic value of advanced imaging modalities for the detection and differentiation of prosthetic valve obstruction: a systematic review and meta-analysis. JACC Cardiovasc Imaging 2019;12:2182-92.
78. Koo HJ, Lee JY, Kim GH, et al. Paravalvular leakage in patients with prosthetic heart valves: cardiac computed tomography findings and clinical features. Eur Heart J Cardiovasc Imaging 2018;19:1419-27.
79. Makkar RR, Blanke P, Leipsic J, et al. Subclinical leaflet thrombosis in transcatheter and surgical bioprosthetic valves: PARTNER 3 cardiac computed tomography substudy. J Am Coll Cardiol 2020;75:3003-15.
80. Cartlidge TRG, Doris MK, Sellers SL, et al. Detection and prediction of bioprosthetic aortic valve degeneration. J Am Coll Cardiol 2019;73:1107-19.
81. Jain V, Wang TKM, Bansal A, et al. Diagnostic performance of cardiac computed tomography versus transesophageal echocardiography in infective endocarditis: a contemporary comparative meta-analysis. J Cardiovasc Comput Tomogr 2021;15:313-21.
82. Edwards MB, Ordidge RJ, Hand JW, et al. Assessment of magnetic field (4.7 T) induced forces on prosthetic heart valves and annuloplasty rings. J Magn Reson Imaging 2005;22:311-7.
83. Shellock FG. Prosthetic heart valves and annuloplasty rings: assessment of magnetic field interactions, heating, and artifacts at 1.5 Tesla. J Cardiovasc Magn Reson 2001;3:317-24.
84. Shellock FG. Biomedical implants and devices: assessment of magnetic field interactions with a 3.0-Tesla MR system. J Magn Reson Imaging 2002;16:721-32.
85. von Knobelsdorff-Brenkenhoff F, Rudolph A, Wassmuth R, et al. Feasibility of cardiovascular magnetic resonance to assess the orifice area of aortic bioprostheses. Circ Cardiovasc Imaging 2009;2:397-404. 2 p following 404.
86. von Knobelsdorff-Brenkenhoff F, Rudolph A, Wassmuth R, et al. Assessment of mitral bioprostheses using cardiovascular magnetic resonance. J Cardiovasc Magn Reson 2010;12:36.
87. Maragiannis D, Jackson MS, Autry K, et al. Functional assessment of bioprosthetic mitral valves by cardiovascular magnetic resonance: an in vitro validation and comparison to Doppler echocardiography. J Cardiovasc Magn Reson 2020;22:55.
88. Haberka M, Malczewska M, Pysz P, et al. Cardiovascular magnetic resonance and transesophageal echocardiography in patients with prosthetic valve paravalvular leaks: towards an accurate quantification and stratification. J Cardiovasc Magn Reson 2021;23:31.
89. Habib G, Lancellotti P, Antunes MJ, et al. 2015 ESC guidelines for the management of infective endocarditis: the Task force for the management of infective endocarditis of the European Society of Cardiology (ESC). Endorsed by: European Association for Cardio-thoracic Surgery (EACTS), the European Association of Nuclear Medicine (EANM). Eur Heart J 2015;36:3075-128.
90. Roque A, Pizzi MN, Fernández-Hidalgo N, et al. Morpho-metabolic post-surgical patterns of non-infected prosthetic heart valves by [18F]FDG PET/CTA: "normality" is a possible diagnosis. Eur Heart J Cardiovasc Imaging 2020;21:24-33.
91. Wahadat AR, Tanis W, Scholtens AM, et al. Normal imaging findings after aortic valve implantation on 18F-Fluorodeoxyglucose positron emission tomography with computed tomography. J Nucl Cardiol 2021;28:2258-68.
92. Hahn RT, Abraham T, Adams MS, et al. Guidelines for performing a comprehensive transesophageal echocardiographic examination: recommendations from the American Society of Echocardiography and the Society of Cardiovascular Anesthesiologists. J Am Soc Echocardiogr 2013;26:921-64.
93. Winter MP, Zbiral M, Kietaibl A, et al. Normal values for Doppler echocardiographic assessment of prosthetic valve function after transcatheter aortic valve replacement: a systematic review and meta-analysis. Eur Heart J Cardiovasc Imaging 2018;19:361-8.
94. Capodanno D, Petronio AS, Prendergast B, et al. Standardized definitions of structural deterioration and valve failure in assessing long-term durability of transcatheter and surgical aortic bioprosthetic valves: a consensus statement from the European Association of Percutaneous Cardiovascular Interventions (EAPCI) endorsed by the European Society of Cardiology (ESC) and the European Association for Cardio-Thoracic Surgery (EACTS). Eur Heart J 2017;38:3382-90.
95. Dvir D, Bourguignon T, Otto CM, et al. Standardized definition of structural valve degeneration for surgical and transcatheter bioprosthetic aortic valves. Circulation 2018;137:388-99.
96. Roslan AB, Naser JA, Nkomo VT, et al. Performance of echocardiographic algorithms for assessment of high aortic bioprosthetic valve gradients. J Am Soc Echocardiogr 2022;35:682-91.e2.
97. Shames S, Koczo A, Hahn R, et al. Flow characteristics of the SAPIEN aortic valve: the importance of recognizing in-stent flow acceleration for the echocardiographic assessment of valve function. J Am Soc Echocardiogr 2012;25:603-9.
98. Hahn RT, Pibarot P, Stewart WJ, et al. Comparison of transcatheter and surgical aortic valve replacement in severe aortic stenosis: a longitudinal study of echocardiography parameters in cohort A of the PARTNER trial (placement of aortic transcatheter valves). J Am Coll Cardiol 2013;61:2514-21.
99. Pibarot P, Salaun E, Dahou A, et al. Echocardiographic results of transcatheter versus surgical aortic valve replacement in low-risk patients: the PARTNER 3 trial. Circulation 2020;141:1527-37.
100. Duncan A, Moat N, Simonato M, et al. Outcomes following transcatheter aortic valve replacement for degenerative stentless versus stented bioprostheses. JACC Cardiovasc Interv 2019;12:1256-63.
101. Alnasser S, Cheema AN, Simonato M, et al. Matched comparison of self-expanding transcatheter heart valves for the treatment of failed aortic surgical bioprosthesis: insights from the valve-in-valve International data registry (VIVID). Circ Cardiovasc Interv 2017;10:e004392.
102. Bleiziffer S, Erlebach M, Simonato M, et al. Incidence, predictors and clinical outcomes of residual stenosis after aortic valve-in-valve. Heart 2018;104:828-34.
103. Abbas AE, Mando R, Hanzel G, et al. Invasive versus echocardiographic evaluation of transvalvular gradients immediately post-transcatheter aortic valve replacement. Circ Cardiovasc Interv 2019;12:e007973.

104. Rodes-Cabau J, Abbas AE, Serra V, et al. Balloon- vs self-expanding valve systems for failed small surgical aortic valve bioprostheses. J Am Coll Cardiol 2022;80:681-93.
105. Hatoum H, Hahn RT, Lilly S, et al. Differences in pressure recovery between balloon expandable and self-expandable transcatheter aortic valves. Ann Biomed Eng 2020;48:860-7.
106. Hatoum H, Samaee M, Sathananthan J, et al. Comparison of performance of self-expanding and balloon-expandable transcatheter aortic valves. JTCVS Open 2022;10:128-39.
107. Alperi A, Robichaud M, Panagides V, et al. Impact of residual transvalvular gradient on clinical outcomes following valve-in-valve transcatheter aortic valve replacement. Int J Cardiol 2022;366:90-6.
108. de Freitas Campos Guimaraes L, Urena M, Wijeysundera HC, et al. Long-term outcomes after transcatheter aortic valve-in-valve replacement. Circ Cardiovasc Interv 2018;11:e007038.
109. Hahn RT, Webb J, Pibarot P, et al. 5-Year follow-up from the PARTNER 2 aortic valve-in-valve registry for degenerated aortic surgical bioprostheses. JACC Cardiovasc Interv 2022;15:698-708.
110. Otto CM, Kumbhani DJ, Alexander KP, et al. 2017 ACC expert consensus decision pathway for transcatheter aortic valve replacement in the management of adults with aortic stenosis: a report of the American College of Cardiology Task force on clinical expert consensus documents. J Am Coll Cardiol 2017;69:1313-46.
111. Ribeiro HB, Rodes-Cabau J, Blanke P, et al. Incidence, predictors, and clinical outcomes of coronary obstruction following transcatheter aortic valve replacement for degenerative bioprosthetic surgical valves: insights from the VIVID registry. Eur Heart J 2018;39:687-95.
112. Blanke P, Weir-McCall JR, Achenbach S, et al. Computed tomography imaging in the context of transcatheter aortic valve implantation (TAVI)/Transcatheter aortic valve replacement (TAVR): an expert consensus document of the society of cardiovascular computed tomography. JACC Cardiovasc Imaging 2019;12:1-24.
113. Feuchtner GM, Spoeck A, Lessick J, et al. Quantification of aortic regurgitant fraction and volume with multi-detector computed tomography comparison with echocardiography. Acad Radiol 2011;18:334-42.
114. Feuchtner GM, Dichtl W, Friedrich GJ, et al. Multislice computed tomography for detection of patients with aortic valve stenosis and quantification of severity. J Am Coll Cardiol 2006;47:1410-7.
115. Freeman M, Webb JG, Willson AB, et al. Multidetector CT predictors of prosthesis-patient mismatch in transcatheter aortic valve replacement. J Cardiovasc Comput Tomogr 2013;7:248-55.
116. Saleeb SF, Newburger JW, Geva T, et al. Accelerated degeneration of a bovine pericardial bioprosthetic aortic valve in children and young adults. Circulation 2014;130:51-60.
117. Pham N, Zaitoun H, Mohammed TL, et al. Complications of aortic valve surgery: manifestations at CT and MR imaging. Radiographics 2012;32:1873-92.
118. Habets J, Meijer TS, Meijer RC, et al. CT attenuation measurements are valuable to discriminate pledgets used in prosthetic heart valve implantation from paravalvular leakage. Br J Radiol 2012;85:e616-21.
119. Feuchtner GM, Stolzmann P, Dichtl W, et al. Multislice computed tomography in infective endocarditis: comparison with transesophageal echocardiography and intraoperative findings. J Am Coll Cardiol 2009;53:436-44.
120. Fagman E, Perrotta S, Bech-Hanssen O, et al. ECG-gated computed tomography: a new role for patients with suspected aortic prosthetic valve endocarditis. Eur Radiol 2012;22:2407-14.
121. Gunduz S, Ozkan M, Kalcik M, et al. Sixty-four-section cardiac computed tomography in mechanical prosthetic heart valve dysfunction: thrombus or pannus. Circ Cardiovasc Imaging 2015;8:e003246.
122. Pache G, Schoechlin S, Blanke P, et al. Early hypo-attenuated leaflet thickening in balloon-expandable transcatheter aortic heart valves. Eur Heart J 2016;37:2263-71.
123. McMahon MA, Squirrell CA. Multidetector CT of aortic dissection: a pictorial review. Radiographics 2010;30:445-60.
124. Gulsin GS, Singh A, McCann GP. Cardiovascular magnetic resonance in the evaluation of heart valve disease. BMC Med Imaging 2017;17:67.
125. von Knobelsdorff-Brenkenhoff F, Dieringer MA, Greiser A, et al. In vitro assessment of heart valve bioprostheses by cardiovascular magnetic resonance: four-dimensional mapping of flow patterns and orifice area planimetry. Eur J Cardiothorac Surg 2011;40:736-42.
126. Myerson SG. CMR in evaluating valvular heart disease: diagnosis, severity, and outcomes. JACC Cardiovasc Imaging 2021;14:2020-32.
127. Leiner T, Bogaert J, Friedrich MG, et al. SCMR Position Paper (2020) on clinical indications for cardiovascular magnetic resonance. J Cardiovasc Magn Reson 2020;22:76.
128. Garcia J, Kadem L, Larose E, et al. Comparison between cardiovascular magnetic resonance and transthoracic Doppler echocardiography for the estimation of effective orifice area in aortic stenosis. J Cardiovasc Magn Reson 2011;13:25.
129. Maragiannis D, Jackson MS, Flores-Arredondo JH, et al. Functional assessment of bioprosthetic aortic valves by CMR. JACC Cardiovasc Imaging 2016;9:785-93.
130. Ha H, Kvitting JP, Dyverfeldt P, et al. 4D Flow MRI quantification of blood flow patterns, turbulence and pressure drop in normal and stenotic prosthetic heart valves. Magn Reson Imaging 2019;55:118-27.
131. Barone-Rochette G, Pierard S, De Meester de Ravenstein C, et al. Prognostic significance of LGE by CMR in aortic stenosis patients undergoing valve replacement. J Am Coll Cardiol 2014;64:144-54.
132. Musa TA, Treibel TA, Vassiliou VS, et al. Myocardial scar and mortality in severe aortic stenosis. Circulation 2018;138:1935-47.
133. Lee JC, Branch KR, Hamilton-Craig C, et al. Evaluation of aortic regurgitation with cardiac magnetic resonance imaging: a systematic review. Heart 2018;104:103-10.
134. Bolen MA, Popovic ZB, Rajiah P, et al. Cardiac MR assessment of aortic regurgitation: holodiastolic flow reversal in the descending aorta helps stratify severity. Radiology 2011;260:98-104.
135. Kammerlander AA, Wiesinger M, Duca F, et al. Diagnostic and prognostic utility of cardiac magnetic resonance imaging in aortic regurgitation. JACC Cardiovasc Imaging 2019;12:1474-83.
136. Papanastasiou CA, Kokkinidis DG, Jonnalagadda AK, et al. Meta-analysis of transthoracic echocardiography versus cardiac magnetic resonance for the assessment of aortic regurgitation after transcatheter aortic valve implantation. Am J Cardiol 2019;124:1246-51.
137. Krim SR, Vivo RP, Patel A, et al. Direct assessment of normal mechanical mitral valve orifice area by real-time 3D echocardiography. JACC Cardiovasc Imaging 2012;5:478-83.
138. Whisenant B, Kapadia SR, Eleid MF, et al. One-year outcomes of mitral valve-in-valve using the SAPIEN 3 transcatheter heart valve. JAMA Cardiol 2020;5:1245-52.
139. Guerrero M, Vemulapalli S, Xiang Q, et al. Thirty-day outcomes of transcatheter mitral valve replacement for degenerated mitral bioprostheses (Valve-in-Valve), failed surgical rings (Valve-in-Ring), and native valve with severe mitral annular calcification (Valve-in-Mitral annular calcification) in the United States: data from the Society of Thoracic Surgeons/American College of Cardiology/Transcatheter Valve Therapy Registry. Circ Cardiovasc Interv 2020;13:e008425.
140. Eleid MF, Cabalka AK, Williams MR, et al. Percutaneous Transvenous transseptal transcatheter valve implantation in failed bioprosthetic mitral valves, ring annuloplasty, and severe mitral annular calcification. JACC Cardiovasc Interv 2016;9:1161-74.
141. Muller DWM, Sorajja P, Duncan A, et al. 2-Year outcomes of transcatheter mitral valve replacement in patients with severe symptomatic mitral regurgitation. J Am Coll Cardiol 2021;78:1847-59.
142. Fernandes V, Olmos L, Nagueh SF, et al. Peak early diastolic velocity rather than pressure half-time is the best index of mechanical prosthetic mitral valve function. Am J Cardiol 2002;89:704-10.
143. Spencer RJ, Gin KG, Tsang MY, et al. Doppler parameters derived from transthoracic echocardiography accurately detect bioprosthetic mitral valve dysfunction. J Am Soc Echocardiogr 2017;30:966-73.e1.
144. Chang S, Suh YJ, Han K, et al. The clinical significance of perivalvular pannus in prosthetic mitral valves: can cardiac CT be helpful? Int J Cardiol 2017;249:344-8.

145. Tsubota H, Sakaguchi G, Arakaki R, et al. Impact of prosthesis-patient mismatch after mitral valve replacement: a propensity score analysis. Semin Thorac Cardiovasc Surg 2021;33:347-53.
146. Cohen GI, Davison MB, Klein AL, et al. A comparison of flow convergence with other transthoracic echocardiographic indexes of prosthetic mitral regurgitation. J Am Soc Echocardiogr 1992;5:620-7.
147. Konen E, Goitein O, Feinberg MS, et al. The role of ECG-gated MDCT in the evaluation of aortic and mitral mechanical valves: initial experience. AJR Am J Roentgenol 2008;191:26-31.
148. Symersky P, Budde RP, de Mol BA, et al. Comparison of multidetector-row computed tomography to echocardiography and fluoroscopy for evaluation of patients with mechanical prosthetic valve obstruction. Am J Cardiol 2009;104:1128-34.
149. LaBounty TM, Agarwal PP, Chughtai A, et al. Evaluation of mechanical heart valve size and function with ECG-gated 64-MDCT. AJR Am J Roentgenol 2009;193:W389-96.
150. Grunenfelder J, Plass A, Alkadhi H, et al. Evaluation of biological aortic valve prostheses by dual source computer tomography and anatomic measurements for potential transapical valve-in-valve procedure. Interact Cardiovasc Thorac Surg 2008;7:195-9. discussion 199-200.
151. Chenot F, Montant P, Goffinet C, et al. Evaluation of anatomic valve opening and leaflet morphology in aortic valve bioprosthesis by using multidetector CT: comparison with transthoracic echocardiography. Radiology 2010;255:377-85.
152. LaBounty TM, Agarwal PP, Chughtai A, et al. Hemodynamic and functional assessment of mechanical aortic valves using combined echocardiography and multidetector computed tomography. J Cardiovasc Comput Tomogr 2009;3:161-7.
153. Habets J, Symersky P, Leiner T, et al. Artifact reduction strategies for prosthetic heart valve CT imaging. Int J Cardiovasc Imaging 2012;28:2099-108.
154. Suh YJ, Hong GR, Han K, et al. Assessment of mitral paravalvular leakage after mitral valve replacement using cardiac computed tomography: comparison with surgical findings. Circ Cardiovasc Imaging 2016;9:e004153.
155. Simprini LA, Afroz A, Cooper MA, et al. Routine cine-CMR for prosthesis-associated mitral regurgitation: a multicenter comparison to echocardiography. J Heart Valve Dis 2014;23:575-82.
156. Emani SM. Options for prosthetic pulmonary valve replacement. Semin Thorac Cardiovasc Surg Pediatr Card Surg Annu 2012;15:34-7.
157. Bonhoeffer P, Boudjemline Y, Saliba Z, et al. Percutaneous replacement of pulmonary valve in a right-ventricle to pulmonary-artery prosthetic conduit with valve dysfunction. Lancet 2000;356:1403-5.
158. Ribeiro JM, Teixeira R, Lopes J, et al. Transcatheter versus surgical pulmonary valve replacement: a systemic review and meta-analysis. Ann Thorac Surg 2020;110:1751-61.
159. Egbe AC, Vallabhajosyula S, Connolly HM. Trends and outcomes of pulmonary valve replacement in tetralogy of Fallot. Int J Cardiol 2020;299:136-9.
160. O'Byrne ML, Glatz AC, Mercer-Rosa L, et al. Trends in pulmonary valve replacement in children and adults with tetralogy of fallot. Am J Cardiol 2015;115:118-24.
161. Caldarone CA, McCrindle BW, Van Arsdell GS, et al. Independent factors associated with longevity of prosthetic pulmonary valves and valved conduits. J Thorac Cardiovasc Surg 2000;120:1022-30. discussion 1031.
162. Miranda WR, Connolly HM, Bonnichsen CR, et al. Prosthetic pulmonary valve and pulmonary conduit endocarditis: clinical, microbiological and echocardiographic features in adults. Eur Heart J Cardiovasc Imaging 2016;17:936-43.
163. Sadeghpour A, Saadatifar H, Kiavar M, et al. Doppler echocardiographic assessment of pulmonary prostheses: a comprehensive assessment including velocity time integral ratio and prosthesis effective orifice area. Congenit Heart Dis 2008;3:415-21.
164. Puchalski MD, Lui GK, Miller-Hance WC, et al. Guidelines for performing a comprehensive transesophageal echocardiographic: examination in children and all patients with congenital heart disease: recommendations from the American Society of Echocardiography. J Am Soc Echocardiogr 2019;32:173-215.
165. Ahmed MI, Escanuela MG, Crosland WA, et al. Utility of live/real time three-dimensional transesophageal echocardiography in the assessment and percutaneous intervention of bioprosthetic pulmonary valve stenosis. Echocardiography 2014;31:531-3.
166. Ostergaard L, Vejlstrup N, Kober L, et al. Diagnostic potential of intracardiac echocardiography in patients with suspected prosthetic valve endocarditis. J Am Soc Echocardiogr 2019;32:1558-64.e3.
167. Bouajila S, Chalard A, Dauphin C. Usefulness of intracardiac echocardiography for the diagnosis of infective endocarditis following percutaneous pulmonary valve replacement. Cardiol Young 2017;27:1406-9.
168. Sucha D, Symersky P, Tanis W, et al. Multimodality imaging assessment of prosthetic heart valves. Circ Cardiovasc Imaging 2015;8:e003703.
169. Nayak KS, Nielsen JF, Bernstein MA, et al. Cardiovascular magnetic resonance phase contrast imaging. J Cardiovasc Magn Reson 2015;17:71.
170. Valente AM, Cook S, Festa P, et al. Multimodality imaging guidelines for patients with repaired tetralogy of fallot: a report from the American Society of Echocardiography: developed in collaboration with the Society for Cardiovascular Magnetic Resonance and the Society for Pediatric Radiology. J Am Soc Echocardiogr 2014;27:111-41.
171. Chung R, Taylor AM. Imaging for preintervention planning: transcatheter pulmonary valve therapy. Circ Cardiovasc Imaging 2014;7:182-9.
172. Han BK, Moga FX, Overman D, et al. Diagnostic value of contrast-enhanced multiphase computed tomography for assessment of percutaneous pulmonary valve obstruction. Ann Thorac Surg 2016;101:e115-6.
173. Curran L, Agrawal H, Kallianos K, et al. Computed tomography guided sizing for transcatheter pulmonary valve replacement. Int J Cardiol Heart Vasc 2020;29:100523.
174. Dellas C, Kammerer L, Gravenhorst V, et al. Quantification of pulmonary regurgitation and prediction of pulmonary valve replacement by echocardiography in patients with congenital heart defects in comparison to cardiac magnetic resonance imaging. Int J Cardiovasc Imaging 2018;34:607-13.
175. Lotz J, Sohns JM. [Imaging technique and current status of valvular heart disease using cardiac MRI]. Radiologe 2013;53:872-9.
176. Mercer-Rosa L, Yang W, Kutty S, et al. Quantifying pulmonary regurgitation and right ventricular function in surgically repaired tetralogy of Fallot: a comparative analysis of echocardiography and magnetic resonance imaging. Circ Cardiovasc Imaging 2012;5:637-43.
177. Wang N, Fulcher J, Abeysuriya N, et al. Tricuspid regurgitation is associated with increased mortality independent of pulmonary pressures and right heart failure: a systematic review and meta-analysis. Eur Heart J 2019;40:476-84.
178. Benfari G, Antoine C, Miller WL, et al. Excess mortality associated with functional tricuspid regurgitation complicating heart failure with reduced ejection fraction. Circulation 2019;140:196-206.
179. Kilic A, Saha-Chaudhuri P, Rankin JS, et al. Trends and outcomes of tricuspid valve surgery in North America: an analysis of more than 50,000 patients from the Society of Thoracic Surgeons database. Ann Thorac Surg 2013;96:1546-52. discussion 1552.
180. Zack CJ, Fender EA, Chandrashekar P, et al. National trends and outcomes in isolated tricuspid valve surgery. J Am Coll Cardiol 2017;70:2953-60.
181. Negm S, Arafat AA, Elatafy EE, et al. Mechanical versus bioprosthetic valve replacement in the tricuspid valve position: a systematic review and meta-analysis. Heart Lung Circ 2021;30:362-71.
182. Rizzoli G, Vendramin I, Nesseris G, et al. Biological or mechanical prostheses in tricuspid position? A meta-analysis of intra-institutional results. Ann Thorac Surg 2004;77:1607-14.
183. Godart F, Baruteau AE, Petit J, et al. Transcatheter tricuspid valve implantation: a multicentre French study. Arch Cardiovasc Dis 2014;107:583-91.
184. Taramasso M, Gavazzoni M, Pozzoli A, et al. Tricuspid regurgitation: predicting the need for intervention, procedural success, and recurrence of disease. JACC Cardiovasc Imaging 2019;12:605-21.

185. Aboulhosn J, Cabalka AK, Levi DS, et al. Transcatheter valve-in-ring implantation for the treatment of residual or recurrent tricuspid valve dysfunction after prior surgical repair. JACC Cardiovasc Interv 2017;10:53-63.
186. Dreyfus J, Flagiello M, Bazire B, et al. Isolated tricuspid valve surgery: impact of aetiology and clinical presentation on outcomes. Eur Heart J 2020;41:4304-17.
187. Rahgozar K, Ho E, Goldberg Y, et al. Transcatheter tricuspid valve repair and replacement: a landscape review of current techniques and devices for the treatment of tricuspid valve regurgitation. Expert Rev Cardiovasc Ther 2021;19:399-411.
188. Sanon S, Cabalka AK, Babaliaros V, et al. Transcatheter tricuspid valve-in-valve and valve-in-ring implantation for degenerated surgical prosthesis. JACC Cardiovasc Interv 2019;12:1403-12.
189. Mitchell C, Rahko PS, Blauwet LA, et al. Guidelines for performing a comprehensive transthoracic echocardiographic examination in adults: recommendations from the American society of echocardiography. J Am Soc Echocardiogr 2019;32:1-64.
190. Yuan L, Cao T, Duan Y, et al. Noninvasive assessment of influence of resistant respiration on blood flow velocities across the cardiac valves in humans–a quantification study by echocardiography. Echocardiography 2004;21:391-8.
191. Connolly HM, Miller FA Jr., Taylor CL, et al. Doppler hemodynamic profiles of 82 clinically and echocardiographically normal tricuspid valve prostheses. Circulation 1993;88:2722-7.
192. Blauwet LA, Danielson GK, Burkhart HM, et al. Comprehensive echocardiographic assessment of the hemodynamic parameters of 285 tricuspid valve bioprostheses early after implantation. J Am Soc Echocardiogr 2010;23:1045-59. 1059.e1-2.
193. Hahn R, Saric M, Faletra FF, et al. Recommended standards for the performance of transesophageal echocardiographic screening for structural heart intervention: from the American society of echocardiography. J Am Soc Echocardiogr 2022;35:1-76. Erratum in: J Am Soc Echocardiogr. 2022 Apr;35(4):447.
194. Hahn RT. State-of-the-Art review of echocardiographic imaging in the evaluation and treatment of functional tricuspid regurgitation. Circ Cardiovasc Imaging 2016;9:e005332.
195. Badano LP, Agricola E, Perez de Isla L, et al. Evaluation of the tricuspid valve morphology and function by transthoracic real-time three-dimensional echocardiography. Eur J Echocardiogr 2009;10:477-84.
196. Hahn RT. Transcathether valve replacement and valve repair: review of procedures and intraprocedural echocardiographic imaging. Circ Res 2016;119:341-56.
197. Garatti A, Nano G, Bruschi G, et al. Twenty-five year outcomes of tricuspid valve replacement comparing mechanical and biologic prostheses. Ann Thorac Surg 2012;93:1146-53.
198. Ratnatunga CP, Edwards MB, Dore CJ, et al. Tricuspid valve replacement: UK Heart Valve Registry mid-term results comparing mechanical and biological prostheses. Ann Thorac Surg 1998;66:1940-7.
199. Burri M, Vogt MO, Horer J, et al. Durability of bioprostheses for the tricuspid valve in patients with congenital heart disease. Eur J Cardiothorac Surg 2016;50:988-93.
200. Nakano K, Koyanagi H, Hashimoto A, et al. Tricuspid valve replacement with the bileaflet St. Jude Medical valve prosthesis. J Thorac Cardiovasc Surg 1994;108:888-92.
201. Peterffy A, Szentkiralyi I. Mechanical valves in tricuspid position: cause of thrombosis and prevention. Eur J Cardiothorac Surg 2001;19:735-6.
202. Blauwet LA, Burkhart HM, Dearani JA, et al. Comprehensive echocardiographic assessment of mechanical tricuspid valve prostheses based on early post-implantation echocardiographic studies. J Am Soc Echocardiogr 2011;24:414-24.
203. McElhinney DB, Aboulhosn JA, Dvir D, et al. Mid-term valve-related outcomes after transcatheter tricuspid valve-in-valve or valve-in-ring replacement. J Am Coll Cardiol 2019;73:148-57.
204. Kobayashi Y, Nagata S, Ohmori F, et al. Serial Doppler echocardiographic evaluation of bioprosthetic valves in the tricuspid position. J Am Coll Cardiol 1996;27:1693-7.
205. Maragiannis D, Aggeli C, Nagueh SF. Echocardiographic evaluation of tricuspid prosthetic valves: an update. Hellenic J Cardiol 2016;57:145-51.
206. Rudski LG, Lai WW, Afilalo J, et al. Guidelines for the echocardiographic assessment of the right heart in adults: a report from the American Society of Echocardiography endorsed by the European Association of Echocardiography, a registered branch of the European Society of Cardiology, and the Canadian Society of Echocardiography. J Am Soc Echocardiogr 2010;23:685-713. quiz 786-8.
207. van Slooten YJ, Freling HG, van Melle JP, et al. Long-term tricuspid valve prosthesis-related complications in patients with congenital heart disease. Eur J Cardiothorac Surg 2014;45:83-9.
208. Han BK, Rigsby CK, Leipsic J, et al. Computed tomography imaging in patients with congenital heart disease, Part 2: technical recommendations. An expert consensus document of the Society of Cardiovascular Computed Tomography (SCCT): endorsed by the Society of Pediatric Radiology (SPR) and the North American Society of Cardiac Imaging (NASCI). J Cardiovasc Comput Tomogr 2015;9:493-513.
209. Saremi F, Grizzard JD, Kim RJ. Optimizing cardiac MR imaging: practical remedies for artifacts. Radiographics 2008;28:1161-87.
210. Hahn RT, Thomas JD, Khalique OK, et al. Imaging assessment of tricuspid regurgitation severity. JACC Cardiovasc Imaging 2019;12:469-90.
211. Dahou A, Ong G, Hamid N, et al. Quantifying tricuspid regurgitation severity: a comparison of proximal isovelocity surface area and novel quantitative Doppler methods. JACC Cardiovasc Imaging 2019;12:560-2.
212. Hahn RT, Meduri CU, Davidson CJ, et al. Early feasibility study of a transcatheter tricuspid valve annuloplasty: SCOUT trial 30-day results. J Am Coll Cardiol 2017;69:1795-806.
213. Utsunomiya H, Harada Y, Susawa H, et al. Comprehensive evaluation of tricuspid regurgitation location and severity using vena contracta analysis: a color Doppler three-dimensional transesophageal echocardiographic study. J Am Soc Echocardiogr 2019;32:1526-37.e2.
214. Zhan Y, Senapati A, Vejpongsa P, et al. Comparison of echocardiographic assessment of tricuspid regurgitation against cardiovascular magnetic resonance. JACC Cardiovasc Imaging 2020;13:1461-71.
215. Zhan Y, Debs D, Khan MA, et al. Natural history of functional tricuspid regurgitation quantified by cardiovascular magnetic resonance. J Am Coll Cardiol 2020;76:1291-301.
216. Pulerwitz TC, Khalique OK, Leb J, et al. Optimizing cardiac CT protocols for comprehensive acquisition prior to percutaneous MV and TV repair/replacement. JACC Cardiovasc Imaging 2020;13:836-50.
217. Stout KK, Daniels CJ, Aboulhosn JA, et al. 2018 AHA/ACC guideline for the management of adults with congenital heart disease: a report of the American College of Cardiology/American Heart Association Task force on clinical practice guidelines. Circulation 2019;139:e698-800.
218. Choi PS, Sleeper LA, Lu M, et al. Revisiting prosthesis choice in mitral valve replacement in children: Durable alternatives to traditional bioprostheses. J Thorac Cardiovasc Surg 2021;61:213-25.
219. Ibezim C, Sarvestani AL, Knight JH, et al. Outcomes of mechanical mitral valve replacement in children. Ann Thorac Surg 2019;107:143-50.
220. Li W, West C, McGhie J, et al. Consensus recommendations for echocardiography in adults with congenital heart defects from the International Society of Adult Congenital Heart Disease (ISACHD). Int J Cardiol 2018;272:77-83.
221. Cohen MS, Eidem BW, Cetta F, et al. Multimodality imaging guidelines of patients with transposition of the great arteries: a report from the American Society of Echocardiography developed in collaboration with the Society for Cardiovascular Magnetic Resonance and the Society of Cardiovascular Computed Tomography. J Am Soc Echocardiogr 2016;29:571-621.

222. Hasan BS, Lunze FI, Chen MH, et al. Effects of transcatheter pulmonary valve replacement on the hemodynamic and ventricular response to exercise in patients with obstructed right ventricle-to-pulmonary artery conduits. JACC Cardiovasc Interv 2014;7:530-42.
223. Hasan BS, Lunze FI, McElhinney DB, et al. Exercise stress echocardiographic assessment of outflow tract and ventricular function in patients with an obstructed right ventricular-to-pulmonary artery conduit after repair of conotruncal heart defects. Am J Cardiol 2012;110:1527-33.
224. Simpson J, Lopez L, Acar P, et al. Three-dimensional echocardiography in congenital heart disease: an expert consensus document from the European association of cardiovascular imaging and the American society of echocardiography. J Am Soc Echocardiogr 2017;30:1-27.
225. Fratz S, Chung T, Greil GF, et al. Guidelines and protocols for cardiovascular magnetic resonance in children and adults with congenital heart disease: SCMR expert consensus group on congenital heart disease. J Cardiovasc Magn Reson 2013;15:51.
226. Freling HG, van Slooten YJ, van Melle JP, et al. Prosthetic valves in adult patients with congenital heart disease: rationale and design of the Dutch PROSTAVA study. Neth Heart J 2012;20:419-24.
227. Rizk J. 4D flow MRI applications in congenital heart disease. Eur Radiol 2021;31:1160-74.
228. Calkoen EE, Westenberg JJ, Kroft LJ, et al. Characterization and quantification of dynamic eccentric regurgitation of the left atrioventricular valve after atrioventricular septal defect correction with 4D Flow cardiovascular magnetic resonance and retrospective valve tracking. J Cardiovasc Magn Reson 2015;17:18.
229. Duncan A, Davies S, Di Mario C, et al. Valve-in-valve transcatheter aortic valve implantation for failing surgical aortic stentless bioprosthetic valves: a single-center experience. J Thorac Cardiovasc Surg 2015;150:91-8.
230. Webb JG, Murdoch DJ, Alu MC, et al. 3-Year outcomes after valve-in-valve transcatheter aortic valve replacement for degenerated bioprostheses: the PARTNER 2 registry. J Am Coll Cardiol 2019;73:2647-55.
231. Rajani R, Mukherjee D, Chambers JB. Doppler echocardiography in normally functioning replacement aortic valves: a review of 129 studies. J Heart Valve Dis 2007;16:519-35.
232. Rosenhek R, Binder T, Maurer G, et al. Normal values for Doppler echocardiographic assessment of heart valve prostheses. J Am Soc Echocardiogr 2003;16:1116-27.
233. Egbe AC, Connolly HM, Miranda WR, et al. Outcomes of bioprosthetic valves in the pulmonary position in adults with congenital heart disease. Ann Thorac Surg 2019;108:1410-5.
234. Jalal Z, Valdeolmillos E, Malekzadeh-Milani S, et al. Mid-term outcomes following percutaneous pulmonary valve implantation using the "Folded Melody valve" technique. Circ Cardiovasc Interv 2021;14:e009707.
235. Shojaeifard M, Daryanavard A, Karimi Behnagh A, et al. Assessment of normal hemodynamic profile of mechanical pulmonary prosthesis by Doppler echocardiography: a prospective cross-sectional study. Cardiovasc Ultrasound 2020;18:14.

Table A1 Normal Doppler echocardiographic values for percutaneous SAPIEN valves in native aortic stenosis by valve size

Valve iteration	Normal values				
SAPIEN	**20 mm**	**23 mm**	**26 mm**	**29 mm**	**All sizes**
EOA, cm^2	NA	1.56 ± 0.43	1.84 ± 0.52	NA	1.70 ± 0.49
Mean gradient, mm Hg	NA	9.92 ± 4.27	8.76 ± 3.89	NA	9.36 ± 4.13
DVI	NA	0.53 ± 0.13	0.53 ± 0.13	NA	0.53 ± 0.13
SAPIEN XT	**20 mm**	**23 mm**	**26 mm**	**29 mm**	**All sizes**
EOA, cm^2	NA	1.41 ± 0.30	1.74 ± 0.42	2.06 ± 0.52	1.67 ± 0.46
Mean gradient, mm Hg	NA	10.41 ± 3.74	9.24 ± 3.57	8.36 ± 3.14	9.52 ± 3.64
DVI	NA	0.52 ± 0.10	0.54 ± 0.11	0.53 ± 0.11	0.53 ± 0.11
SAPIEN 3	**20 mm**	**23 mm**	**26 mm**	**29 mm**	**All sizes**
EOA, cm^2	1.22 ± 0.22	1.45 ± 0.26	1.74 ± 0.35	1.89 ± 0.37	1.66 ± 0.38
Mean gradient, mm Hg	16.23 ± 5.01	12.79 ± 4.65	10.59 ± 3.88	9.28 ± 3.16	11.18 ± 4.35
DVI	0.42 ± 0.07	0.43 ± 0.08	0.43 ± 0.09	0.40 ± 0.09	0.43 ± 0.09

NA, Not applicable.
Data are expressed as mean ± SD. Data are modified from Hahn *et al*.[11] with permission.

Table A2 Normal Doppler echocardiographic values for percutaneous CoreValve and Evolut R valves by valve size in native aortic stenosis

Valve iteration	Normal values				
CoreValve	**23 mm**	**26 mm**	**29 mm**	**31 mm**	**All sizes**
EOA, cm^2	1.12 ± 0.36	1.74 ± 0.49	1.97 ± 0.53	2.15 ± 0.72	1.88 ± 0.56
Mean gradient, mm Hg	14.43 ± 5.72	8.27 ± 3.82	8.85 ± 4.17	9.55 ± 3.44	8.85 ± 4.14
DVI	0.44 ± 0.09	0.59 ± 0.15	0.54 ± 0.12	0.49 ± 0.12	0.55 ± 0.13
Evolut R (30 d)	**23 mm**	**26 mm**	**29 mm**	**34 mm**	**All sizes**
EOA, cm^2	1.09 ± 0.26	1.69 ± 0.40	1.97 ± 0.54	2.60 ± 0.75	2.01 ± 0.65
Mean gradient, mm Hg	14.97 ± 7.15	7.53 ± 2.65	7.85 ± 3.08	6.30 ± 3.23	7.52 ± 3.19
DVI	0.42 ± 0.04	0.61 ± 0.13	0.59 ± 0.14	0.58 ± 0.15	0.59 ± 0.14

Data are expressed as mean ± SD. Data are modified from Hahn *et al*.[11] with permission.

Table A3 Doppler echocardiographic parameters for percutaneous aortic ViV at 1 year after the procedure

TAVI ViV	THV size	Peak gradient, mm Hg	Mean gradient, mm Hg	EOA, cm^2
CoreValve[100]	All	23.48 ± 12.10	12.89 ± 0.20	1.62 ± 0.14
Evolut[141,229]	All	22.43 ± 5.72	14.70 ± 9.11	1.36 ± 0.07
SAPIEN 3[100]	All	33.93 ±10.11	27.00 ±10.20	1.07 ± 0.32
SAPIEN XT[100,230]	All	31.31± 3.75	18.02 ± 4.22	1.31 ± 0.25

THV, Transcatheter heart valve.
Data are expressed as mean ± SD. Data are derived from the respective publications.

Table A4 Normal Doppler echocardiographic values for surgical prosthetic aortic valves

Valve	Size, mm	Peak gradient, mm Hg	Mean gradient, mm Hg	EOA, cm^2
Abbott *Epic*	21		19.1 ± 8.2	1.0 ± 0.3
	23		13.9 ± 6.0	1.4 ± 0.5
	25		12.1 ± 5.1	1.5 ± 0.5
	27		11.4 ± 4.1	1.6 ± 0.4
	29		7.5 ± 3.3	2.4 ± 1.1
Abbott *Trifecta*	19		10.7 ± 4.6	1.41 ± 0.24
	21		8.1 ± 3.5	1.63 ± 0.29
	23		7.2 ± 2.8	1.81 ± 0.30
	25		6.2 ± 2.7	2.02 ± 0.32
	27		4.8 ± 2.0	2.20 ± 0.20
	29		4.7 ± 1.6	2.35 ± 0.22
Arbor Surgical *Trilogy*	21	21 ± 8	11 ± 6	1.9 ± 0.2
	23	15 ± 7	8 ± 4	2.0 ± 0.3
ATS *Bileaflet*	19	47.0 ± 12.6	25.3 ± 8.0	1.1 ± 0.3
	21	23.7 ± 6.8	15.9 ± 5.0	1.4 ± 0.5
	23		14.4 ± 4.9	1.7 ± 0.5
	25		11.3 ± 3.7	2.1 ± 0.7
	27		8.4 ± 3.7	2.5 ± 0.1
	29		8.0 ± 3.0	3.1 ± 0.8
ATS AP *Bileaflet*	18		21.0 ± 1.8	1.2 ± 0.3
	20	21.4± 4.2	11.1 ± 3.5	1.3 ± 0.3
	22	18.7± 8.3	10.5 ± 4.5	1.7 ± 0.4
	24	15.1± 5.6	7.5 ± 3.1	2.0 ± 0.6
	26		6.0 ± 2.0	2.1 ± 0.4
ATS *3F Enable*	21	27.0 ± 8.4	15.0 ± 4.6	1.1 ± 0.4
	22	25.7 ± 10.8	14.5 ± 6.0	1.4 ± 0.4
	25	20.3 ± 7.4	11.4 ± 4.0	1.6 ± 0.5
	27	16.8 ± 6.3	9.4 ± 3.3	1.9 ± 0.5
	29	14.3 ± 6.7	7.8 ± 3.8	2.4 ± 0.8
Baxter Perimount *Stented bovine pericardial*	19	32.5 ± 8.5	19.5 ± 5.5	1.3 ± 0.2
	21	24.9 ± 7.7	13.8 ± 4.0	1.3 ± 0.3
	23	19.9 ± 7.4	11.5 ± 3.9	1.6 ± 0.3
	25	16.5 ± 7.8	10.7 ± 3.8	1.6 ± 0.4
	27	12.8 ± 5.4	4.8 ± 2.2	2.0 ± 0.4
Biocor *Stented porcine*	23	30.0 ± 10.7	20 ± 6.6	1.3 ± 0.3
	25	23.0 ± 7.9	16 ± 5.1	1.7 ± 0.4
	27	22.0 ± 6.5	15.0 ± 3.7	2.2 ± 0.4
Extended Biocor *Stentless*	19-21	17.5 ± 6.5	9.6 ± 3.6	1.4 ± 0.4
	23	14.7 ± 7.3	7.7 ± 3.8	1.7 ± 0.4
	25	14.0 ± 4.3	7.4 ± 2.5	1.8 ± 0.4

(*Continued*)

Table A4 (*Continued*)

Valve	Size, mm	Peak gradient, mm Hg	Mean gradient, mm Hg	EOA, cm^2
Bioflo *Stented bovine pericardial*	19	37.2 ± 8.8	26.4 ± 5.5	0.7 ± 0.1
	21	28.7 ± 6.2	18.7 ± 5.5	1.1 ± 0.1
Bjork-Shiley *Single tilting disk*	21	38.9 ± 11.9	21.8 ± 3.4	1.1 ± 0.3
	23	28.8 ± 11.2	15.7 ± 5.3	1.3 ± 0.3
	25	23.7 ± 8.2	13.0 ± 5.0	1.5 ± 0.4
	27		10.0 ± 2.0	1.6 ± 0.3
Carbomedics reduced *Bileaflet*	19	43.4 ± 1.2	24.4 ± 1.2	1.2 ± 0.1
Carbomedics Standard *Bileaflet*	19	38.0 ± 12.8	18.9 ± 8.3	1.0 ± 0.3
	21	26.8 ± 10.1	12.9 ± 5.4	1.5 ± 0.4
	23	22.5 ± 7.4	11.0 ± 4.6	1.4 ± 0.3
	25	19.6 ± 7.8	9.1 ± 3.5	1.8 ± 0.4
	27	17.5 ± 7.1	7.9 ± 3.2	2.2 ± 0.2
	29	9.1 ± 4.7	5.6 ± 3.0	3.2 ± 1.6
Carbomedics Tophat *Bileaflet*	21	30.2 ± 10.9	14.9 ± 5.4	1.2 ± 0.3
	23	24.2 ± 7.6	12.5 ± 4.4	1.4 ± 0.4
	25		9.5 ± 2.9	1.6 ± 0.32
Carpentier Edwards Pericardial *Stented bovine pericardial*	19	32.1 ± 3.4	24.2 ± 8.6	1.2 ± 0.3
	21	25.7 ± 9.9	20.3 ± 9.1	1.5 ± 0.4
	23	21.7 ± 8.6	13.0 ± 5.3	1.8 ± 0.3
	25	16.5 ± 5.4	9.0 ± 2.3	
Carpentier Edwards Standard *Stented porcine*	19	43.5 ± 12.7	25.6 ± 8.0	0.9 ± 0.2
	21	27.7 ± 7.6	17.3 ± 6.2	1.5 ± 0.3
	23	28.9 ± 7.5	16.1 ± 6.2	1.7 ± 0.5
	25	24.0 ± 7.1	12.9 ± 4.6	1.9 ± 0.5
	27	22.1 ± 8.2	12.1 ± 5.5	2.3 ± 0.6
	29		9.9 ± 2.9	2.8 ± 0.5
Carpentier Supra-Annular *Stented porcine*	19	34.1 ± 2.7		1.1 ± 0.1
	21	28.0 ± 10.5	17.5 ± 3.8	1.4 ± 0.9
	23	25.3 ± 10.5	13.4 ± 4.5	1.6 ± 0.6
	25	24.4 ± 7.6	13.2 ± 4.8	1.8 ± 0.4
	27	16.7 ± 4.7	8.8 ± 2.8	1.9 ± 0.7
Cryolife *Stentless*	19		9.0 ± 2.0	1.5 ± 0.3
	21		6.6 ± 2.9	1.7 ± 0.4
	23		6.0 ± 2.3	2.3 ± 0.2
	25		6.1 ± 2.6	2.6 ± 0.2
	27		4.0 ± 2.4	2.8 ± 0.3
Edwards Duromedics *Bileaflet*	21	39.0 ± 13		
	23	32.0 ± 8.0		
	25	26.0 ± 10.0		
	27	24.0 ± 10.0		

(*Continued*)

Table A4 (*Continued*)

Valve	Size, mm	Peak gradient, mm Hg	Mean gradient, mm Hg	EOA, cm^2
Edwards *Inspiris Resilia*	19		17.6 ± 7.8	1.1 ± 0.2
	21		12.6 ± 4.7	1.3 ± 0.3
	23		10.1 ± 3.8	1.6 ± 0.4
	25		9.6 ± 5.2	1.8 ± 0.5
	27		8.2 ± 3.5	2.2 ± 0.6
Edwards *Intuity*	19		13.9 ± 3.9	1.1 ± 0.1
	21		11.6 ± 3.6	1.3 ± 0.1
	23		10.4 ± 3.5	1.7 ± 0.2
	25		9.1 ± 3.2	1.9 ± 0.2
	27		8.3 ± 3.7	2.2 ± 0.2
Edwards Mira *Bileaflet*	19		18.2 ± 5.3	1.2 ± 0.4
	21		13.3 ± 4.3	1.6 ± 0.4
	23		14.7 ± 2.8	1.6 ± 0.6
	25		13.1 ± 3.8	1.9
Edwards *Mosaic*	21		13.3 ± 5.3	1.4 ± 0.4
	23		11.8 ± 4.9	1.6 ± 0.5
	25		10.6 ± 4.4	1.8 ± 0.5
	27		9.1 ± 4.0	2.0 ± 0.5
	29		8.6 ± 2.9	2.3 ± 0.6
Hancock *Stented porcine*	21	18.0 ± 6.0	12.0 ± 2.0	
	23	16.0 ± 2.0	11.0 ± 2.0	
	25	15.0 ± 3.0	10.0 ± 3.0	
Hancock II *Stented porcine*	21		14.8 ± 4.1	1.3 ± 0.4
	23	34.0 ± 13.0	16.6 ± 8.5	1.3 ± 0.4
	25	22.0 ± 5.3	10.8 ± 2.8	1.6 ± 0.4
	29	16.2 ± 1.5	8.2 ± 1.7	1.6 ± 0.2
Homograft *Homograft valves*	17-19		9.7 ± 4.2	4.2 ± 1.8
	19-21			5.4 ± 0.9
	20-21		7.9 ± 4.0	3.6 ± 2.0
	20-22		7.2 ± 3.0	3.5 ± 1.5
	22	1.7 ± 0.3		5.8 ± 3.2
	22-23		5.6 ± 3.1	2.6 ± 1.4
	22-24			5.6 ± 1.7
	24-27		6.2 ± 2.6	2.8 ± 1.1
	26	1.4 ± 0.6		6.8 ± 2.9
	25-28			6.2 ± 2.5
Intact *Stented porcine*	19	40.4 ± 15.4	24.5 ± 9.3	
	21	40.9 ± 15.6	19.6 ± 8.1	1.6 ± 0.4
	23	32.7 ± 9.6	19.0 ± 6.1	1.6 ± 0.4
	25	29.7 ± 15.0	17.7 ± 7.9	1.7 ± 0.3
	27	25.0 ± 7.6	15.0 ± 4.5	

(*Continued*)

Table A4 (*Continued*)

Valve	Size, mm	Peak gradient, mm Hg	Mean gradient, mm Hg	EOA, cm^2
Ionescu-Shiley *Stented bovine pericardial*	17	23.8 ± 3.4		0.9 ± 0.1
	19	19.7 ± 5.9	13.3 ± 3.9	1.1 ± 0.1
	21	26.6 ± 9.0		
	23		15.6 ± 4.4	
Labcor Santiago *Stented bovine pericardial*	19	18.6 ± 5.0	11.8 ± 3.3	1.2 ± 0.1
	21	17.5 ± 6.6	8.2 ± 4.5	1.3 ± 0.1
	23	14.8 ± 5.2	7.8 ± 2.9	1.8 ± 0.2
	25	12.3 ± 3.4	6.8 ± 2.0	2.1 ± 0.3
Labcor Synergy *Stented porcine*	21	24.3 ± 8.1	13.3 ± 4.2	1.1 ± 0.3
	23	27.3 ± 13.7	15.3 ± 6.9	1.4 ± 0.4
	25	22.5 ± 11.9	13.2 ± 6.4	1.5 ± 0.4
	27	17.8 ± 7.0	10.6 ± 4.6	1.8 ± 0.5
MCRI On-X *Bileaflet*	19	21.3 ± 10.8	11.8 ± 3.4	1.5 ± 0.2
	21	16.4 ± 5.9	9.9 ± 3.6	1.7 ± 0.4
	23	15.9 ± 6.4	8.6 ± 3.4	1.9 ± 0.6
	25	16.5 ± 10.2	6.9 ± 4.3	2.4 ± 0.6
Medtronic Advantage *Bileaflet*	23		10.4 ± 3.1	2.2 ± 0.3
	25		9.0 ± 3.7	2.8 ± 0.6
Medtronic Advantage *Bileaflet*	27		7.6 ± 3.6	3.3 ± 0.7
	29		6.1 ± 3.8	3.9 ± 0.7
Medtronic *Avalus*	19		17.1 ± 5.0	1.11 ± 0.25
	21		14.5 ± 4.3	1.25 ± 0.25
	23		12.1 ± 3.8	1.47 ± 0.32
	25		11.7 ± 4.0	1.57 ± 0.31
	27		10.3 ± 4.2	1.77 ± 0.41
Medtronic Freestyle *Stentless*	19		13.0 ± 3.9	
	21		9.1 ± 5.1	1.4 ± 0.3
	23	11.0 ± 4.0	8.1 ± 4.6	1.7 ± 0.5
	25		5.3 ± 3.1	2.1 ± 0.5
	27		4.6 ± 3.1	2.5 ± 0.1
Medtronic-Hall *Single tilting disk*	21	26.9 ± 10.5	14.1 ± 5.9	1.1 ± 0.2
	23	26.9 ± 8.9	13.5 ± 4.8	1.4 ± 0.4
	25	17.1 ± 7.0	9.5 ± 4.3	1.5 ± 0.5
	27	18.9 ± 9.7	8.7 ± 5.6	1.9 ± 0.2
Medtronic-Hall *Single tilting disk*	20	34.4 ± 13.1	17.1 ± 5.3	1.2 ± 0.5
Medtronic Mosaic *Stented porcine*	21		14.2 ± 5.0	1.4 ± 0.4
	23	23.8 ± 11.0	13.7 ± 4.8	1.5 ± 0.4
	25	22.5 ± 10.0	11.7 ± 5.1	1.8 ± 0.5
	27		10.4 ± 4.3	1.9 ± 0.1
	29		11.1 ± 4.3	2.1 ± 0.2

(*Continued*)

Table A4 (*Continued*)

Valve	Size, mm	Peak gradient, mm Hg	Mean gradient, mm Hg	EOA, cm^2
Mitroflow *Stented bovine pericardial*	19	18.6 ± 5.3	13.1 ± 3.3	1.1 ± 0.2
Monostrut Bjork-Shiley *Single tilting disk*	19		27.4 ± 8.8	
	21	27.5 ± 3.1	20.5 ± 6.2	
	23	20.3 ± 0.7	17.4 ± 6.4	
	25		16.1 ± 4.9	
	27		11.4 ± 3.8	
Prima *Stentless*	21	28.8 ± 6.0	13.7 ± 1.9	1.4 ± 0.7
	23	21.5 ± 7.5	11.5 ± 4.9	1.5 ± 0.3
	25	22.1 ± 12.5	11.6 ± 7.2	1.8 ± 0.5
Omnicarbon *Single tilting disk*	21	37.4 ± 12.8	20.4 ± 5.4	1.3 ± 0.5
	23	28.8 ± 9.1	17.4 ± 4.9	1.5 ± 0.3
	25	23.7 ± 8.1	13.2 ± 4.6	1.9 ± 0.5
	27	20.1 ± 4.2	12.4 ± 2.9	2.1 ± 0.4
Omniscience *Single tilting disk*	21	50.8 ± 2.8	28.2 ± 2.2	0.9 ± 0.1
	23	39.8 ± 8.7	20.1 ± 5.1	1.0 ± 0.1
Starr-Edwards *Caged ball*	23	32.6 ± 12.8	22.0 ± 9.0	1.1 ± 0.2
	24	34.1 ± 10.3	22.1 ± 7.5	1.1 ± 0.3
	26	31.8 ± 9.0	19.7 ± 6.1	
	27	30.8 ± 6.3	18.5 ± 3.7	
	29	29.0 ± 9.3	16.3 ± 5.5	
Sorin Bicarbon *Bileaflet*	19	30.1 ± 4.5	16.7 ± 2.0	1.4 ± 0.1
	21	22.0 ± 7.1	10.0 ± 3.3	1.2 ± 0.4
	23	16.8 ± 6.1	7.7 ± 3.3	1.5 ± 0.2
	25	11.2 ± 3.1	5.6 ± 1.6	2.4 ± 0.3
Sorin Pericarbon *Stentless*	19	36.5 ± 9.0	28.9 ± 7.3	1.2 ± 0.5
	21	28.0 ± 13.3	23.8 ± 11.1	1.3 ± 0.6
	23	27.5 ± 11.5	23.2 ± 7.6	1.5 ± 0.5
Sorin Perceval *Sutureless*	S (21)		10.1 ± 4.2	1.3 ± 0.3
	M (23)		9.4 ± 5.5	1.5 ± 0.4
	L (25)		8.5 ± 4.6	1.5 ± 0.4
	XL (27)		9.7 ± 4.7	1.6 ± 0.4
St. Jude Medical Haem Plus *Bileaflet*	19	28.5 ± 10.7	17.0 ± 7.8	1.9 ± 0.1
	21	16.3 ± 17.0	10.6 ± 5.1)	1.8 ± 0.5
	23	16.8 ± 7.3	12.1 ± 4.2	1.7 ± 0.5
St. Jude Medical Regent *Bileaflet*	19	20.6 ± 12	11.0 ± 4.9	1.6 ± 0.4
	21	15.6 ± 9.4	8.0 ± 4.8	2.0 ± 0.7
	23	12.8 ± 6.8	6.9 ± 3.5	2.3 ± 0.9
	25	11.7 ± 6.8	5.6 ± 3.2	2.5 ± 0.8
	27	7.9 ± 5.5	3.5 ± 1.7	3.6 ± 0.5

(*Continued*)

Table A4 (*Continued*)

Valve	Size, mm	Peak gradient, mm Hg	Mean gradient, mm Hg	EOA, cm^2
St. Jude Medical Standard *Bileaflet*	19	42.0 ± 10.0	24.5 ± 5.8	1.5 ± 0.1
	21	25.7 ± 9.5	15.2 ± 5.0	1.4 ± 0.4
	23	21.8 ± 7.5	13.4 ± 5.6	1.6 ± 0.4
	25	18.9 ± 7.3	11.0 ± 5.3	1.9 ± 0.5
	27	13.7 ± 4.2	8.4 ± 3.4	2.5 ± 0.4
	29	13.5 ± 5.8	7.0 ± 1.7	2.8 ± 0.5
St. Jude Medical *Stentless*	21	22.6 ± 14.5	10.7 ± 7.2	1.3 ± 0.6
	23	16.2 ± 9.0	8.2 ± 4.7	1.6 ± 0.6
	25	12.7 ± 8.2	6.3 ± 4.1	1.8 ± 0.5
	27	10.1 ± 5.8	5.0 ± 2.9	2.0 ± 0.3
	29	7.7 ± 4.4	4.1 ± 2.4	2.4 ± 0.6

Data are expressed as mean ± SD.
Modified from Rajani *et al*.[231]

Table A5 Normal Doppler echocardiographic values for surgical prosthetic mitral valves

Valve	Size, mm	Peak gradient, mm Hg	Mean gradient, mm Hg	Peak velocity, m/sec	PHT, msec	EOA, cm^2
Abbott *Epic*	27		6.1 ± 2.9			1.4 ± 0.7
	29		5.5 ± 1.7			1.5 ± 0.5
	31		4.8 ± 1.4			1.6 ± 0.3
	33		4.1 ± 1.6			1.5 ± 0.3
Biocor *Stentless bioprosthesis*	27	13 ± 1				
	29	14 ± 2.5				
	31	11.5 ± 0.5				
	33	12 ± 0.5				
Bioflo pericardial *Stented bioprosthesis*	25	10 ± 2	6.3 ± 1.5			2 ± 0.1
	27	9.5 ± 2.6	5.4 ± 1.2			2 ± 0.3
	29	5 ± 2.8	3.6 ± 1			2.4 ± 0.2
	31	4.0	2.0			2.3
Bjork-Shiley *Tilting disk*	23			1.7	115	
	25	12 ± 4	6 ± 2	1.75 ± 0.38	99 ± 27	1.72 ± 0.6
	27	10 ± 4	5 ± 2	1.6 ± 0.49	89 ± 28	1.81 ± 0.54
	29	7.83 ± 2.93	2.83 ± 1.27	1.37 ± 0.25	79 ± 17	2.1 ± 0.43
	31	6 ± 3	2 ± 1.9	1.41 ± 0.26	70 ± 14	2.2 ± 0.3
Bjork-Shiley monostrut *Tilting disk*	23		5.0	1.9		
	25	13 ± 2.5	5.57 ± 2.3	1.8 ± 0.3		
	27	12 ± 2.5	4.53 ± 2.2	1.7 ±0.4		
	29	13 ± 3	4.26 ± 1.6	1.6 ± 0.3		
	31	14 ± 4.5	4.9 ± 1.6	1.7 ± 0.3		
Carbomedics *Bileaflet*	23			1.9 ± 0.1	126 ± 7	
	25	10.3 ± 2.3	3.6 ± 0.6	1.3 ± 0.1	93 ± 8	2.9 ± 0.8

(*Continued*)

Table A5 (*Continued*)

Valve	Size, mm	Peak gradient, mm Hg	Mean gradient, mm Hg	Peak velocity, m/sec	PHT, msec	EOA, cm^2
	27	8.79 ± 3.46	3.46 ± 1.03	1.61 ± 0.3	89 ± 20	2.9 ± 0.75
	29	8.78 ± 2.9	3.39 ± 0.97	1.52 ± 0.3	88 ± 17	2.3 ± 0.4
	31	8.87 ± 2.34	3.32 ± 0.87	1.61 ± 0.29	92 ± 24	2.8 ± 1.14
	33	8.8 ± 2.2	4.8 ± 2.5	1.5 ± 0.2	93 ± 12	
Carpentier-Edwards *Stented bioprosthesis*	27		6 ± 2	1.7 ± 0.3	98 ± 28	
	29		4.7 ± 2	1.76 ± 0.27	92 ±14	
	31		4.4 ± 2	1.54 ± 0.15	92 ± 19	
	33		6 ± 3		93 ± 12	
Carpentier-Edwards pericardial *Stented Bioprosthesis*	27		3.6	1.6	100	
	29		5.25 ± 2.36	1.67 ± 0.3	110 ± 15	
	31		4.05 ± 0.83	1.53 ± 0.1	90 ± 11	
	33		1.0	0.8	80	
Carpentier-Edwards Perimount *Stented pericardial*	25		4.0 ± 1.0	1.7 ± 0.10	67 ± 21.5	1.75 ± 0.53
	27		6.3 ± 1.65	1.7 ± 0.27	74 ± 20.6	1.88 ± 0.52
	29		6.0 ± 1.41	1.8 ± 0.19	76 ± 17.9	2.02 ± 0.57
	31		5.5 ± 1.06	1.8 ± 0.20	80 ± 21.8	2.09 ± 0.48
	33		6.1 ± 1.86	1.7 ± 0.23	77 ± 13.2	2.24 ± 0.97
Duromedics *Bileaflet*	27	13 ± 6	5 ± 3	1.61 ± 0.4	75 ± 12	
	29	10 ± 4	3 ± 1	1.40 ± 0.25	85 ± 22	
	31	10.5 ± 4.33	3.3 ± 1.36	1.38 ± 0.27	81 ± 12	
	33	11.2	2.5		85	
Edwards *Mitris*	25		4.9 ± 1.2			1.1 ± 0.4
	27		4.1 ± 1.4			1.2 ± 0.3
	29		4.1 ± 1.5			1.5 ± 0.6
	31		3.9 ± 2.0			1.4 ± 0.5
	33		3.3 ± 1.4			1.5 ± 0.7
Hancock I or not specified *Stented bioprosthesis*	27	10 ± 4	5 ± 2			1.3 ± 0.8
	29	7 ± 3	2.46 ± 0.79		115 ± 20	1.5 ± 0.2
	31	4 ± 0.86	4.86 ± 1.69		95 ± 17	1.6 ± 0.2
	33	3 ± 2	3.87 ± 2		90 ± 12	1.9 ± 0.2
Hancock II *Stented bioprosthesis*	25		8.3 ± 1.71	2.1 ± 0.28	76 ± 19.8	1.42 ± 0.29
	27		6.1 ± 1.33	2 ± 0.28	81 ± 18.9	1.62 ± 0.47
	29		6.7 ± 2.20	2.0 ± 0.31	77 ± 15.1	1.83 ± 0.68
	31		6.0 ± 1.58	2.0 ± 0.32	76 ± 12.1	1.70 ± 0.41
	33		5.5 ± 1.64	1.9 ± 0.50	65 ± 8.7	2.71 ± 0.77
Hancock pericardial *Stented bioprosthesis*	29		2.61 ± 1.39	1.42 ± 0.14	105 ± 36	
	31		3.57 ± 1.02	1.51 ± 0.27	81 ± 23	
Ionescu-Shiley *Stented bioprosthesis*	25		4.87 ± 1.08	1.43 ± 0.15	93 ± 11	
	27		3.21 ± 0.82	1.31 ± 0.24	100 ± 28	

(*Continued*)

Table A5 (*Continued*)

Valve	Size, mm	Peak gradient, mm Hg	Mean gradient, mm Hg	Peak velocity, m/sec	PHT, msec	EOA, cm^2
	29		3.22 ± 0.57	1.38 ± 0.2	85 ± 8	
	31		3.63 ± 0.9	1.45 ± 0.06	100 ± 36	
Ionescu-Shiley low profile *Stented bioprosthesis*	29		3.31 ± 0.96	1.36 ± 0.25	80 ± 30	
	31		2.74 ± 0.37	1.33 ± 0.14	79 ± 15	
Labcor-Santiago pericardial *Stented bioprosthesis*	25	8.7	4.5		97	2.2
	27	5.6 ± 2.3	2.8 ± 1.5		85 ± 18	2.12 ± 0.48
	29	6.2 ± 2.1	3 ± 1.3		80 ± 34	2.11 ± 0.73
Lillehei-Kaster *Tilting disk*	18			1.7	140	
	20			1.7	67	
	22			1.56 ± 0.09	94 ± 22	
	25			1.38 ± 0.27	124 ± 46	
Medtronic-Hall *Tilting disk*	27			1.4	78	
	29			1.57 ± 0.1	69 ± 15	
	31			1.45 ± 0.12	77 ± 17	
Medtronic Intact Porcine *Stented bioprosthesis*	29		3.5 ± 0.51	1.6 ± 0.22		
	31		4.2 ± 1.44	1.6 ± 0.26		
	33		4 ± 1.3	1.4 ± 0.24		
	35		3.2 ± 1.77	1.3 ± 0.5		
Medtronic *Mosaic*	25		8.3 ± 1.71	2.1 ± 0.28	76 ± 19.8	1.42 ± 0.29
	27		6.1 ± 1.33	2 ± 0.28	81 ± 18.9	1.62 ± 0.47
	29		6.7 ± 2.20	2.0 ± 0.31	77 ± 15.1	1.83 ± 0.68
	31		6.0 ± 1.58	2.0 ± 0.32	76 ± 12.1	1.70 ± 0.41
	33		5.5 ± 1.64	1.9 ± 0.50	65 ± 8.7	2.71 ± 0.77
Mitroflow *Stented bioprosthesis*	25		6.9	2.0	90	
	27		3.07 ± 0.91	1.5	90 ± 20	
	29		3.5 ± 1.65	1.43 ± 0.29	102 ± 21	
	31		3.85 ± 0.81	1.32 ± 0.26	91 ± 22	
Omnicarbon *Tilting disk*	23		8.0			
	25		6.05 ± 1.81	1.77 ± 0.24	102 ± 16	
	27		4.89 ± 2.05	1.63 ± 0.36	105 ± 33	
	29		4.93 ± 2.16	1.56 ± 0.27	120 ± 40	
	31		4.18 ± 1.4	1.3 ± 0.23	134 ± 31	
	33		4 ± 2			
On-X *Bileaflet*	25	11.5 ± 3.2	5.3 ± 2.1			1.9 ± 1.1
	27-29	10.3 ± 4.5	4.5 ± 1.6			2.2 ± 0.5
	31-33	9.8 ± 3.8	4.8 ± 2.4			2.5 ± 1.1
Sorin Allcarbon *Tilting disk*	25	15 ± 3	5 ± 1	2 ± 0.2	105 ± 29	2.2 ± 0.6
	27	13 ± 2	4 ± 1	1.8 ± 0.1	89 ± 14	2.5 ± 0.5
	29	10 ± 2	4 ± 1	1.6 ± 0.2	85 ± 23	2.8 ± 0.7

(*Continued*)

Table A5 (*Continued*)

Valve	Size, mm	Peak gradient, mm Hg	Mean gradient, mm Hg	Peak velocity, m/sec	PHT, msec	EOA, cm^2
	31	9 ± 1	4 ± 1	1.6 ± 0.1	88 ± 27	2.8 ± 0.9
Sorin Bicarbon *Bileaflet*	25	15 ± 0.25	4 ± 0.5	1.95 ± 0.02	70 ± 1	
	27	11 ± 2.75	4 ± 0.5	1.65 ± 0.21	82 ± 20	
	29	12 ± 3	4 ± 1.25	1.73 ± 0.22	80 ± 14	
	31	10 ± 1.5	4 ± 1	1.66 ± 0.11	83 ± 14	
St. Jude Medical *Bileaflet*	23		4.0	1.5	160	1.0
	25		2.5 ± 1	1.34 ± 1.12	75 ± 4	1.35 ± 0.17
	27	11 ± 4	5 ± 1.82	1.61 ± 0.29	75 ± 10	1.67 ± 0.17
	29	10 ± 3	4.15 ± 1.8	1.57 ± 0.29	85 ± 10	1.75 ± 0.24
	31	12 ± 6	4.46 ± 2.22	1.59 ± 0.33	74 ± 13	2.03 ± 0.32
Starr-Edwards *Caged ball*	26		10.0			1.4
	28		7 ± 2.75			1.9 ± 0.57
	30	12.2 ± 4.6	6.99 ± 2.5	1.7 ± 0.3	125 ± 25	1.65 ± 0.4
	32	11.5 ± 4.2	5.08 ± 2.5	1.7 ± 0.3	110 ± 25	1.98 ± 0.4
	34		5.0			2.6
Stentless quadrileaflet bovine pericardial *Stentless bioprosthesis*	26		2.2 ± 1.7	1.6	103 ± 31	1.7
	28			1.58 ± 0.25		1.7 ± 0.6
	30			1.42 ± 0.32		2.3 ± 0.4
Wessex *Stented bioprosthesis*	29		3.69 ± 0.61	1.66 ± 0.17	83 ± 19	
	31		3.31 ± 0.83	1.41 ± 0.25	80 ± 21	

Data are expressed as mean ± SD.
Modified from Rosenhek *et al*.[232]

Table A6 Mean Doppler echocardiographic gradients for normal SAPIEN Valves placed percutaneously in the mitral position

Reference and valve size	ViV	ViR	ViMAC	All
Guerrero *et al*.[139]	7 (6-9)	7 (6-9)	6 (4-8)	7 (5-9)
Whisenant *et al*.[138]	7.3 ± 2.73	NA	NA	NA
Eleid *et al*.[140]	5.7 ± 2.5	5.7 ± 2.2	4.3 ± 2.3	5.5 ± 2.4
23 mm	6.4 ± 2.4	5 ± 2	8*	6.25 ± 2.2
26 mm	7.0 ± 2.6	6 ± 1.4	4*	6.5 ± 2.4
29 mm	4.9 ± 2.1	6 ± 3	2.5 ± 0.5	4.8 ± 2.3

NA, Not applicable; *ViMAC*, valve–in–mitral annular calcification.
Data are expressed as median (IQR) or as mean ± SD. Data are in millimeters of mercury from each publication. Data for individual valve size are computed from Eleid *et al*.[140] None of the SAPIEN valves had >2+ MR.
*Limited data, no SD reported.

Table A7 Normal Doppler echocardiographic values for prosthetic pulmonary valves

Valve	Size, mm	Peak gradient, mm Hg	Mean gradient, mm Hg	Peak velocity, m/sec	AT, msec	EOA, cm^2
Homograft[233]		<25	<15	<2.5		
Valved conduits[233]						
Contegra	12-22					
Shelhigh	10-24		<15	<2.2		
Medtronic	19-29					
Bioprosthetic valves[233]			<15	<2.2		
Percutaneous pulmonary valves (Melody)[234]	16 (≤20)			<2.4		
	18 (≤22)			<2.4		
Percutaneous pulmonary valves (SAPIEN)[11]	20		16 ± 5			1.22 ± 0.2
	23		11 (8-17)			1.47 (1.1-2)
	26		9.5 (4.9-14.5)			1.77 (1.3-2.4)
	29		10.4 (5.9-15.5)			2 (1.5-2.6)
Percutaneous pulmonary valve native outflow (Alterra Stent with SAPIEN)		No data				
Percutaneous pulmonary valve native outflow (Harmony)		No data				
Mechanical valves (St. Jude)[235]	21	20 (19-21)	12 (11-13)	2.2	98 (85-110)	1.73
	23	20 (7-35)	11 (4-20)	2 (1.2-2.9)	87 (52-118)	2.5 (1-3.8)
	25	18 ± 7.5	11 ± 6	2	83 ± 11	2.9 ± 1
	27	15 (6-30)	6 (3-18)	1.8 (1.2-2.7)	90 (72-116)	4.2 (3-4.8)
	31	14	7	1.6	93	5.73
Mechanical valves (Carbomedics)[235]	23	19 (17-20)	12	2 (1.8-2.2)	78 (70-85)	1.7 (1.3-2.1)
	25	20 (11-30)	11 (5-33)	2 (1.6-2.7)	89 (64-108)	3.3 (1.5-4.4)
	27	19 (10-28)	10 (6-14)	1.9 (1.4-2.4)	78 (75-80)	4.1 (4-4.1)
	29	14	7	1.7	76	2.6
Mechanical valve On-X[235]	23	20 (7-36)	12 (4-22)	2.2 (1.1-2.7)	112 (106-118)	2.4 (1.9-2.9)
	25	17 (7-24)	10 (3-13)	1.8 (1.3-2.4)	100 (55-118)	1.5 (0.9-2.2)
	27	23	13	2.2	113	1.9
	29	20 (18-22)	12 ± 1	2.1 (1.9-2.3)	103 (95-110)	2.02 (1.8-2.2)

AT, Acceleration time of the prosthetic valve.
Data are expressed as mean ± SD or as median (IQR).

Table A8 Transcatheter tricuspid ViV and ViR

	n	ViV/ViR	Age, y	Mean gradient, mm Hg (mean ± SD)	EOA, cm^2	Peak velocity, m/sec	PVL
McElhinney *et al*.[203]	306	ViV, *n* = 284 (93%) ViR, n = 22 (7%)	40 (1-86)	3.8 ± 2.0	NR	NR	Trivial or none in 83%
				≥29 mm, 3.6 ± 1.8			
				<29 mm, 4.2 ± 2.3			

NR, Not reported.

Table A9 Normal Doppler echocardiographic values for prosthetic TVs

Mechanical	St. Jude Medical Standard				Carbomedics Standard			Starr-Edwards	
Size, mm	27	29	31	33	31	33	30	32	34
PHT, msec	77 ± 14.6	100 ± 35.2	81 ± 13.5	82 ± 18.8	78	98 ± 9.7	132	NA	118 ± 32.9
MG, mm Hg	2.4 ± 1.27	2.6 ± 1.13	3.3 ± 1.21	3.2 ± 1.24	4.0 ± 1.63	3.4 ± 1.19	5	4.0 ± 1.0	5.7 ± 1.63
E velocity, m/sec	1.1 ± 0.32	1.2 ± 0.21	1.4 ± 0.31	1.3 ± 0.22	1.4 ± 0.19	1.2 ± 0.16	1.5	1.5 ± 0.44	1.8 ± 0.28
VTI_{TVP}, cm	25 ± 7.0	31 ± 6.5	30 ± 5.1	30 ± 7.8	40 ± 11.4	34 ± 7.3	41	39 ± 14.2	44 ± 7.8
VTI_{TVP}/VTI_{LVOT}	1.2 ± 0.33	1.4 ± 0.30	1.4 ± 0.23	1.5 ± 0.33	1.9 ± 0.53	1.6 ± 0.33	1.5	2.0 ± 0.68	1.9 ± 0.32
EOA CON, cm^2	2.54 ± 0.64	2.20 ± 0.33	2.49 ± 0.45	2.46 ± 0.59	2.01 ± 0.51	2.33 ± 0.43	2.07	1.87 ± 0.33	1.81 ± 0.48
iEOA CON, cm^2/m^2	1.52 ± 0.34	1.21 ± 0.13	1.38 ± 0.29	1.36 ± 0.36	1.04 ± 0.18	1.25 ± 0.35	1.51	0.96 ± 0.18	1.08 ± 0.29

Bioprosthesis	Medtronic Mosaic					Carpentier Edwards Perimount		
Size, mm	25	27	29	31	33	29	31	33
PHT, msec	80	NA	115 ± 13.4	144 ± 28.6	139 ± 56.5	94 ± 2.8	74 ± 26.2	137 ±53
MG, mm Hg	4.0	5.5 ± 0.53	6.0 ± 2.0	5.2 ± 1.43	4.3 ± 1.3	2.0 ± 1.41	3.7 ± 1.53	3.9 ± 1.07
E velocity, m/sec	1.6	1.6 ± 0.17	1.5 ± 0.26	1.5 ± 0.21	1.4 ± 0.19	1.1 ± 0.21	1.2 ± 0.20	1.4 ± 0.21
VTI_{TVP}, cm	35	51 ± 6.8	37 ± 0.97	46 ± 9.5	40 ± 8.6	29 ± 7.1	37 ± 9.1	38 ± 7.9
VTI_{TVP}/VTI_{LVOT}	3.2	2.2 ± 0.4	1.8 ± 0.39	2.2 ± 0.6	2.1 ± 0.3	1.6 ± 0.20	1.7 ± 0.35	1.9 ± 0.28
EOA CON, cm^2	1.37	1.53 ± 0.16	1.96 ± 0.39	1.74 ± 0.52	2.0 ± 0.53	2.16 ± 0.43	2.12 ± 0.53	1.93 ± 0.43
iEOA CON, cm^2/m^2	0.93	0.86 ± 0.18	1.12 ± 0.21	0.95 ± 0.29	1.01 ± 0.26	1.39 ± 0.42	1.20 ± 0.29	1.03 ± 0.19

Bioprosthesis	Carpentier Edwards Duraflex					St. Jude Biocor		
Size, mm	27	29	31	33	35	29	31	33
PHT, msec	130 ± 45.4	102 ± 26.5	115 ± 40.8	116 ± 39.7	83 ± 26.5	NA	106 ± 48.5	125 ± 45.7
MG, mm Hg	5.2 ± 1.69	6.0 ± 1.95	5.7 ± 1.67	5.6 ± 2.10	5.3 ± 1.61	6	5.1 ± 1.36	3.9 ± 1.20
E velocity, m/sec	1.5 ± 0.26	1.7 ± 0.27	1.5 ± 0.27	1.5 ± 0.26	1.5 ± 0.25	1.6	1.5 ± 0.34	1.3 ± 0.23
VTI_{TVP}, cm	46 ± 8.0	47 ± 9.6	48 ± 9.0	47 ± 10.2	46 ± 10.5	43	46 ± 12.5	39 ± 10
VTI_{TVP}/VTI_{LVOT}	2.4 ± 0.40	2.3 ± 0.60	2.3 ± 0.53	2.3 ± 0.54	2.3 ± 0.54	1.7	2.2 ± 0.57	1.9 ± 0.56
EOA CON, cm^2	1.34 ± 0.22	1.54 ± 0.38	1.57 ± 0.39	1.69 ± 0.44	1.63 ± 0.38	2.84	1.92 ± 0.53	1.88 ± 0.49
iEOA CON, cm^2/m^2	0.78 ± 0.15	0.88 ± 0.19	0.88 ± 0.22	0.92 ± 0.24	0.88 ± 0.22	1.54	0.99 ± 0.19	1.07 ± 0.29

Bioprosthesis	Medtronic Hancock II		
Size, mm	31	33	35
PHT, msec	NA	NA	NA
MG, mm Hg	5.7 ± 1.37	5.5 ± 3.54	5.3 ± 0.58
E velocity, m/sec	1.6 ± 0.19	1.4 ± 0.28	1.3 ± 0.32
VTI_{TVP}, cm	49 ± 8.7	50 ± 16.3	41 ± 2.5
VTI_{TVP}/VTI_{LVOT}	2.3 ± 0.36	2.9 ± 0.48	1.8 ± 0.12
EOA CON, cm^2	1.4 ± 0.21	1.4 ± 0.59	2.11 ± 0.23
iEOA CON, cm^2/m^2	0.77 ± 0.19	0.71 ± 0.24	1.01 ± 0.22

CON, Continuity equation; *iEOA*, indexed EOA; *MG*, mean gradient; *VTI*, velocity-time integral; *TVP*, TV prosthesis.
Data are mean ± SD. Data for mechanical and bioprosthetic TVs are from Blauwet *et al*.[192,202]